C. 4

PNE - 1104
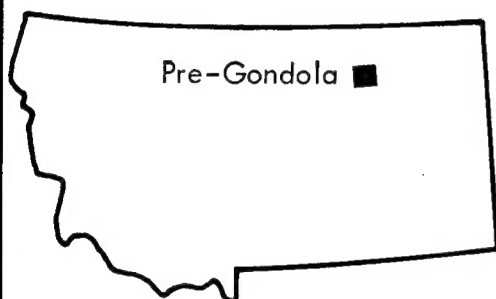
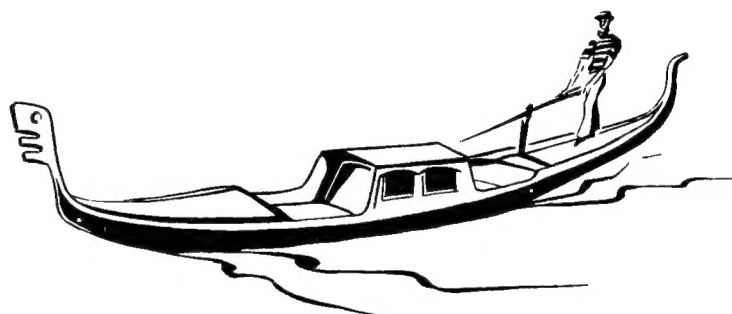Plowsbare civil, industrial and scientific uses for nuclear explosives

UNITED STATES ARMY CORPS OF ENGINEERS

FORT PECK RESERVOIR
MONTANA

Pre-Gondola ■

PROJECT
PRE-GONDOLA I

CLOSE-IN GROUND MOTION, EARTH STRESS,
AND PORE PRESURE MEASUREMENTS

J. D. Day, D. W. Murrell and W. C. Sherman
U. S. Army Engineer Waterways Experiment Station
Vicksburg, Misissippi 39180

U. S. Army Engineer Nuclear Cratering Group
Livermore, California

ISSUED: September 1967

LEGAL NOTICE

PROJECT PRE-GONDOLA I

CRATERING SITE CALIBRATION SERIES

CLOSE-IN GROUND MOTION, EARTH STRESS,
AND PORE PRESSURE MEASUREMENTS

J. D. Day
D. W. Murrell
W. C. Sherman

U. S. Army Engineer
    Waterways Experiment Station
Vicksburg, Mississippi   39180

20011105 091

July 1967

ABSTRACT

The objectives of this project were to measure and analyze the particle velocities, soil stresses, and pore water pressures produced by detonation of 20 tons of nitromethane in saturated clay-shale. The ground range of primary interest was 85 to 375 feet from surface ground zero with most instruments placed at shot depth (46.3 feet).

Peak stresses were greater than estimated at the close-in locations (8,000 to 12,000 psi measured vs 5,000 psi predicted) and attenuated as the -2 power with distance. Particle velocities were consistently higher than predictions based on experience in other media.

High amplitude transient pore pressures were produced by the explosion. Residual excess pore water pressures tended to drop off slowly with time.

CONTENTS

TABLES

FIGURES

4

Missouri R.

MONTANA

Great Northern RR

Glasgow

Milk River

Nashua

2

24

Willow Creek

Missouri River

Spillway

Fort Peck

Fort Peck Dam

Duck Creek Inlet

Pre-Gondola

Fort Peck Reservoir

Fort Peck Reservoir

Youth Camp

Pines Recreation Camp

Airport   Paved Road   Scale in Miles

Landing Strip   Graded Road   0   5

N

SITE LOCATION MAP

5

ALFA

SC-2

CHARLIE

SC-4

SC-1

BRAVO

DELTA

SC-3

FRONTISPIECE

6

CLOSE-IN GROUND MOTION, EARTH
STRESS, AND PORE PRESSURE MEASUREMENTS

CHAPTER 1

INTRODUCTION

1.1 DESCRIPTION

Project Pre-GONDOLA I was a series of chemical explosive single-charge cratering experiments in weak, wet clay-shale conducted by the U. S. Army Engineer Nuclear Cratering Group (NCG) as a part of the joint Atomic Energy Commission-Corps of Engineers nuclear excavation research program. The purpose of the Pre-GONDOLA I Cratering Calibration Series was to calibrate the project site with respect to its cratering characteristics and to provide a basis for design of the proposed 140-ton Pre-GONDOLA II and the Pre-GONDOLA III row-charge cratering detonations in the same medium.

The Pre-GONDOLA I detonations occurred in Valley County, near the edge of the Fort Peck Reservoir approximately 18 miles south of Glasgow, Montana, as follows:

Event	Date	Time (MST)	Longitude	Latitude
Bravo	25 October 1966	1000:00.760	W106°38'24.894"	N47°55'46.154"
Charlie	28 October 1966	1200:00.654	W106°38'29.974"	N47°55'53.294"
Alfa	1 November 1966	1000:00.275	W106°38'15.325"	N47°55'46.570"
Delta	4 November 1966	1000:00.032	W106°38'38.134"	N47°55'48.077"

The four 20-ton (nominal) spherical charges of liquid explosive nitromethane (CH_3NO_2) resulted in the following craters:

Event	Tons	Depth of Burst		Apparent Crater Radius		Apparent Crater Depth	
		(ft)	(m)	(ft)	(m)	(ft)	(m)
Charlie	19.62	42.49	12.95	80.4	24.50	32.6	9.94
Bravo	19.36	46.25	14.10	78.5	23.93	29.5	8.99
Alfa	20.35	52.71	16.07	76.1	23.19	32.1	9.78
Delta	20.24	56.87	17.34	65.1	19.84	25.2	7.68

To assist in seismic site calibration and to provide preliminary information for the design of the Pre-GONDOLA I experiment, NCG had earlier conducted the following Pre-GONDOLA Seismic Site Calibration Series at the Pre-GONDOLA I site:

Event	Date	Time (MST)	Longitude	Latitude
SC-1	20 June 1966	0845	W106°38'30.573"	N47°55'48.383"
SC-4	21 June 1966	0811	W106°38'35.059"	N47°55'53.380"
SC-2	22 June 1966	0805	W106°38'20.792"	N47°55'48.181"
SC-3	23 June 1966	0837	W106°38'29.495"	N47°55'44.579"

1.2 OBJECTIVES

The objectives of this study were to measure and analyze the close-in ground motion, total soil stress, and pore water pressure produced by a detonation of 20 tons of nitromethane (in a weak, wet clay-shale). The ground motion and total stress measurements were expected to serve a dual purpose - to provide input information for the assessment of shock wave effects on the in-situ medium, and to add important information to the collection of empirical ground motion data by making such measurements in a relatively unexplored medium. Measurements of pore water pressure were needed to evaluate the engineering properties of the cratered medium and, in particular, to assess the stability of crater slopes.

8

1.3 BACKGROUND

The Pre-Gondola I Series provided an excellent opportunity to study ground shock propagation and attenuation with distance in a saturated clay-shale, a geologic environment significantly different from any encountered on previous nuclear or HE detonations. It has been determined from previous detonations in various media such as desert alluvium, welded tuff, halite, and granite that particle motions and stresses are dependent on soil and rock properties. For instance, particle velocities in granite will be roughly four times those in tuff at comparable scaled ranges.[1] Consequently, it is desirable to obtain such measurements in as many different media as possible in order to (1) establish adequate public safety and damage criteria, (2) provide information for the design of protective structures, and (3) aid in studying the relevant mechanisms and media-dependency of crater formation.

1.4 PREDICTIONS

In order to make good measurements it is necessary to make adequate predictions of the parameters to be measured. These predictions are used in the selection of gage ranges and amplifier gain settings. Since no proven theory is

available which can adequately predict motions and stresses, predictions must be based on empirical data obtained from tests in the same or a similar medium. In the case of Pre-Gondola I, the limited amount of data gathered on the Seismic Site Calibration (SC) Series in June 1966 served as the basis for these predictions. A description of this series as well as the results obtained on SC-2 are given in Appendix B. The measurements made on that series indicated that pressure magnitudes were only slightly less than would have occurred in free water at a similar scaled distance. Consequently, a stress prediction curve of two-thirds the magnitude and equal slope of a free water pressure-distance curve was used for Pre-Gondola I. The pressure-distance curve for TNT explosions in free water is described by the following relation:

$$P = 21.6 \times 10^3 \ (\frac{R}{W^{1/3}})^{-1.13}$$

where
P = Peak pressure, psi

R = Slant range, feet

W = Charge weight, pounts of TNT

No adjustments were made for the energy equivalence of nitromethane. This prediction method was expected to be conservative at the larger distances since the dissipative

10

action of the clay-shale would produce a more rapid attenuation rate than would water with its nearly elastic behavior. Moreover, reflected rarefactions from the ground surface were expected to further reduce amplitudes at large distances.

For purposes of selecting gage ranges for the pore pressure measurements, it was assumed that pore water pressures would not vary greatly from anticipated total soil stresses. Predictions of particle velocity were also made by cube root scaling data from SC-2 up to a 20-ton yield. In this case the two data points from SC-2 were assumed to be definitive of both magnitude and attenuation, and no alternate source of information, such as the free water curve for stresses, was used. Predicted stress and particle velocity values are listed in Table 2.1.

CHAPTER 2

PROCEDURE

2.1 EXPERIMENTAL PLAN

The primary gage layout for Event Bravo is shown in
profile in Figure 2.1. A total of 13 locations was instru-
mented along this line with an additional pore pressure gage
installed after the shot at a distance of 150 feet and a depth
of 20 feet. In addition, it was desired to assess the effects,
if any, of the Bravo detonation on the three remaining shot
cavities, Alfa, Charlie, and Delta, which were filled with
water to decrease chances of cavity failure. For this
purpose, a soil stress gage was installed adjacent to, and
a water shock gage placed in, each remaining cavity. The
gages at the Alfa and Delta sites were also operated for
Shot Charlie, and the gages at Delta were operated for Shot
Alfa. Tables 2.1 and 2.2 list all gages by gage type and
location and also give predicted motions and total stresses.

2.2 INSTRUMENTATION

2.2.1 Gages. The horizontal (radial) particle velocity
measurements were made with Sandia Model DX-B velocity gages.
These gages are essentially highly overdamped (integrating)
accelerometers and have proved to be reliable and rugged on
many previous field experiments.

12

Three different types of total stress gages were used. Since no available soil stress gages were expected to be usable at pressures above 3,000 to 3,500 psi, water shock gages were used at higher stress levels. These gages (which utilize tourmaline crystals) have proved highly reliable in making water shock measurements and it was thought they would perform adequately in the saturated, high stress environment expected on Pre-Gondola. For expected stresses between about 2,000 psi and 3,500 psi piezoelectric gages manufactured by the Road Research Laboratory of England were used. These use a stack of four quartz crystals to sense the pressure on aluminum diaphragms. SE-type soil stress gages were used to measure stresses lower than about 2,000 psi. These gages were developed in-house and have a four-arm strain gage bridge bonded to stainless steel diaphragms as the sensing element. The SE gages had been used routinely on laboratory and field tests at stress levels below approximately 1,000 psi. Figure B.2 shows typical transducers used.

Eight electronic piezometers (also called transducer piezometers) were installed prior to the Bravo Event to measure the residual pore pressures induced as a result of the explosion. A single U. S. Bureau of Reclamation (USBR) type twin-tube, hydraulic piezometer was also installed to measure static pore pressures at various times prior to and

13

after the shot. The electronic piezometers, designated PR-1 through PR-8, utilized Norwood pressure transducers with capacities ranging from 500 to 5,000 psi. Piezometer PR-9, which was installed two days after Event Bravo, utilized a CEC transducer with a capacity of 50 psi. All piezometers, with the exception of PR-2, were designed to filter out the peak dynamic pore pressure and to record residual pore pressures only.

On the basis of dynamic pore pressure measurements during the seismic calibration shots for the Pre-Gondola Series,it was considered that negative pore pressures less than zero psi (absolute) might develop, and it was intended that transducers capable of measuring these negative pressures would be utilized. However, it was not possible to secure delivery of such devices in time for the event. Furthermore, the capacity of the Norwood devices, except for the 5,000 psi transducer in PR-2, was much more than had been planned. Because of the inability to secure delivery of transducers of desired capacity, available devices with a higher capacity had to be used.

A detail of the transducer-type piezometer is shown in Figure 2.2; a photograph of the device is shown in Figure 2.3. The porous tips consisted of 10-micron pore size, porous

14

stainless steel with a length of one inch (except for PR-2 which contained a similar tip with 100-micron pore size). All transducer piezometers were leak-tested and calibrated in the laboratory before shipment to the field. Peak pore pressures were measured at three locations (Gages 6-Pa-1, 15-Pa-2, and 21-Pa-3) using a tourmaline crystal gage suspended in a stainless steel canister which was open at one end. A porous bronze plug one-eighth inch thick was then inserted in the opening to seal off grain pressure, but which was expected to admit the pore water pressure without appreciable attenuation or distortion of wave amplitude or shape.

2.2.2 Gage Installation. The particle velocity gages were mounted in four-inch diameter aluminum canisters, which were then potted with paraffin to provide a high degree of water protection and to attenuate any structural vibration of the housing. The electrical cable was led to the ground surface through a one-half inch diameter aluminum pipe attached to the canister; the pipe also served as the placement and orientation device. Approximately three feet of grout was placed above the canister and the remainder of the placement hole was filled with sand. The total stress gages were not grouted into place, but were placed directly in the sand backfill.

15

The peak and residual pore pressure gages were installed as shown in Figure 2.2. Piezometer tips were surrounded with a well-graded medium sand filter extending two feet above and one foot below the tip. The hole was sealed with a two-foot grout plug and then backfilled to the surface with a clay silt slurry. Peak pore pressure gages were installed in three holes as shown in Figure 2.1 to measure explosion-induced peak pore water pressures.

The USBR-type piezometer was installed at a 25-foot depth. The tip was attached to a steel pipe with plastic tubing inside the pipe. The tip was boiled in water for thirty minutes prior to installation in the water-filled hole in order to expel as much air as possible from the porous tip. Readings from this piezometer were obtained after insertion by using Bourdon gages. The piezometer was connected to a 120 psi pressure gage and also to a compound gage of 30-inch vacuum and 150 psi capacity. Also included was a pressure gage with a maximum range of 3,000 psi, capable of recording the peak dynamic pressure. A photograph of the gage board is shown in Figure 2.3.

All electric cables extending from the instruments were protected in the drill holes by placing the cables in one- to one-half inch diameter steel pipe to provide protection from shear deformations. From the drill holes, cables were placed

16

in trenches approximately four feet deep, extending from the holes to a point beyond which damage from falling debris was not anticipated. The cables were placed loosely in the trenches and then protected by corrugated-metal half pipe, approximately eight to twelve inches in diameter. The trenches were then backfilled with sand overlain by native material. At a distance of 400 feet from surface ground zero (SGZ), the cables in the trenches were protected by wooden planks laid over the cables in the bottoms of the trenches in lieu of the corrugated-metal half pipe, and the trenches were backfilled as described above.

2.2.3 Recording System. All instrument outputs except from the residual pore pressure gages were recorded on both FM magnetic tape recorders and light-beam galvanometer oscillographs. The low frequency residual pore pressure data were recorded only on the oscillograph. Signal conditioning equipment varied with the type of instrument; velocity gages and residual pore pressure gages used a 3 kcps carrier-demodulator system; SE-type stress gages used a DC amplifier system, and the tourmaline and Road Research Laboratory stress gages used a charge amplifier system. After completion of the electronic recording phase, which lasted for approximately ten seconds, the pore pressure gage outputs were read manually

17

with a strain indicator for a period of ten days after the
Bravo Event. These readings were used to determine the rate
of pore pressure dissipation following the Bravo detonation and
to determine the effects of the subsequent detonations on the
residual pore pressures.

All electronic recording equipment was housed in the
WES recording van located approximately 2,500 feet south of
Bravo ground zero.

TABLE 2.1 GAGE TYPE, LOCATION AND PEAK PREDICTIONS

Gage	Distance	Depth	Placement Hole No.	Gage Type	Predicted Peak
1-σ-1	85	25	1-24	Stress - Tourmaline	5,400 psi
2-σ-2	85	46	1-24	Stress - Tourmaline	5,400 psi
3-u-1	85	46	1-24	Velocity	40 ft/sec
6-Pa-1	85	46	1-25	Peak Pore Pressure	5,400 psi
7-σ-3	100	10	1-26	Stress - Tourmaline	4,200 psi
8-u-2	100	10	1-26	Velocity	26 ft/sec
9-σ-4	100	25	1-26	Stress - Tourmaline	4,300 psi
10-σ-5	125	25	1-14	Stress - Tourmaline	3,400 psi
11-σ-6	125	46	1-14	Stress - Tourmaline	3,500 psi
12-u-3	125	46	1-14	Velocity	17 ft/sec
15-Pa-2	125	46	1-27	Peak Pore Pressure	3,500 psi
16-σ-7	175	25	1-15	Stress - RRL Gage	2,300 psi
17-σ-8	175	46	1-15	Stress - RRL Gage	2,400 psi
18-u-4	175	46	1-15	Velocity	8 ft/sec
21-Pa-3	175	46	1-28	Peak Pore Pressure	2,400 psi
22-σ-9	225	46	1-16	Stress - SE Gage	1,800 psi
23-u-5	225	46	1-16	Velocity	4.6 ft/sec
27-u-6	300	46	1-30	Velocity	2.5 ft/sec
28-u-7	375	46	1-17	Velocity	1.4 ft/sec
29-σ-10	930/Delta	57	—	Stress - SE Gage	350 psi
30-ω-1	800/Charlie	57	—	Cavity Pressure - Tourmaline	350 psi
31-σ-11		42	—	Stress - SE Gage	430 psi
32-ω-2		42	—	Cavity Pressure - Tourmaline	430 psi
33-σ-12	660/Alfa	52	—	Stress - SE Gage	540 psi
34-ω-3		52	—	Cavity Pressure - Tourmaline	540 psi
29-σ-10	770/Delta	57	—	Stress - SE Gage	450 psi
30-ω-1	770/Delta	57	—	Cavity Pressure - Tourmaline	450 psi
33-σ-12	1210/Alfa	52	—	Stress - SE Gage	300 psi
34-ω-3	1210/Alfa	52	—	Cavity Pressure - Tourmaline	300 psi
29-σ-10	1570/Delta	57	—	Stress - SE Gage	200 psi
30-ω-1	1570/Delta	57	—	Cavity Pressure - Tourmaline	200 psi

TABLE 2.2 PIEZOMETER TYPE AND LOCATION

All piezometers installed prior to the Bravo Event except for PR-9 which was installed two days after the event.

Piezometer No.	Type	Sensor	Nominal Capacity	Hole No.	Distance Horizontal	Slant	Tip Elev	Depth Below Surface	Depth Below GWL[a]
			psi		ft	ft	ft-msl	ft	ft
PR-1	WES Transducer	Norwood	1,000	I-38	85	87	2221.7	25.1	18.5
PR-2	WES Transducer	Norwood	5,000	I-25	85	85	2200.9	45.9	39.3
PR-3	WES Transducer	Norwood	1,000	I-39	125	126	2223.8	24.9	16.4
PR-4	WES Transducer	Norwood	1,000	I-27	125	125	2202.5	46.2	37.7
PR-5	WES Transducer	Norwood	1,000	I-40	175	176	2223.7	24.9	16.5
PR-6	WES Transducer	Norwood	1,000	I-28	175	175	2202.1	46.5	38.1
PR-7	WES Transducer	Norwood	500	I-41	225	226	2222.7	24.4	17.5
PR-8	WES Transducer	Norwood	500	I-29	225	225	2201.3	45.8	38.9
PR-9	WES Transducer	CEC	50	-	150	151	2228.6	20.0	11.6
PR-10	USBR Hydraulic	Bourdon Tube	3,000	I-30	300	299	2223.5	24.9	16.7

[a]Based on ground water level at elev 2240.2 (24 Oct 1966).

Figure 2.1 Gage layout

GROUND SURFACE

4-FOOT DEEP CABLE TRENCH

DEPTH BELOW GROUND SURFACE VARIES

CLAY-SILT PUDDLED BACKFILL TO GROUND SURFACE

GROUT SEAL

2 FEET

1-1/2-INCH STEEL PIPE

SAND FILTER

2 FEET

PIEZOELECTRIC GAGE

PORE PRESSURE CELL (SEE DETAIL)

TIP ELEVATION

1 FOOT

GROUT SEAL TO BOTTOM OF HOLE

5 INCHES

PYLE-NATIONAL FITTING

1-7/8 INCHES

4-5/8 INCHES

TRANSDUCER

POROUS DISK

3 - (6- 32, FH SCREWS)

1-7/16 INCHES

2-1/2 INCHES

PORE PRESSURE CELL DETAIL

Figure 2.2 Typical transducer piezometer installation

22
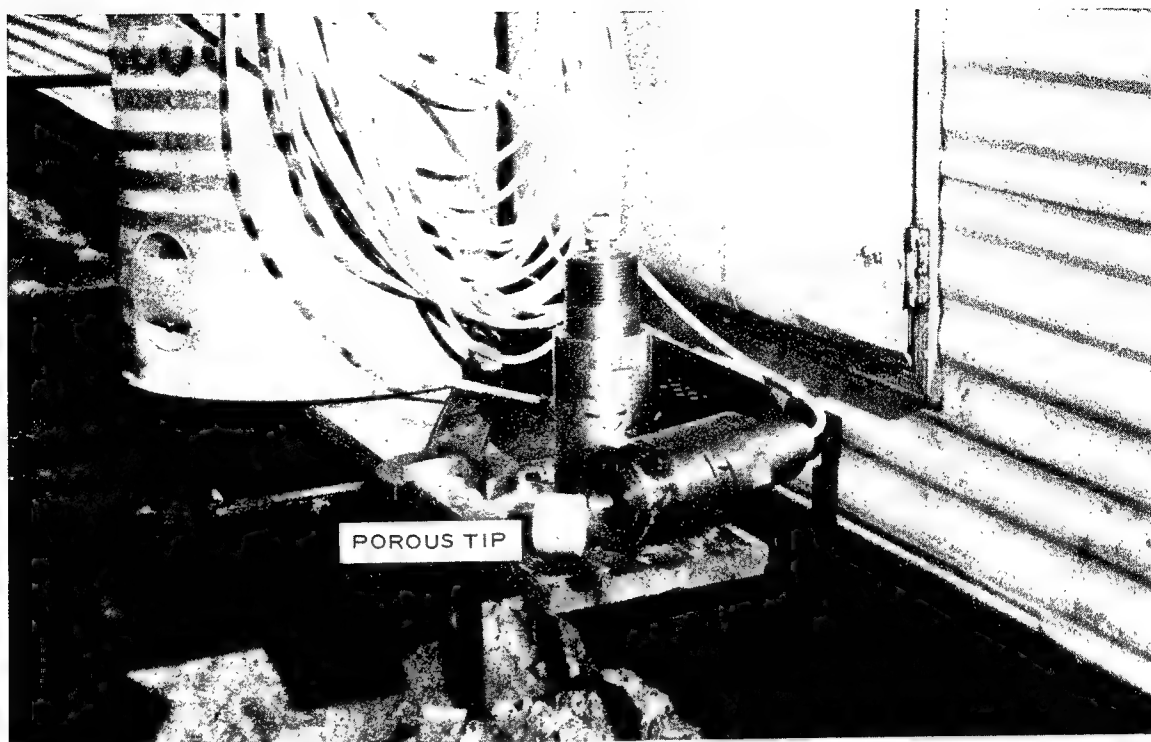
a. WES transducer piezometer with porous stainless steel tip removed
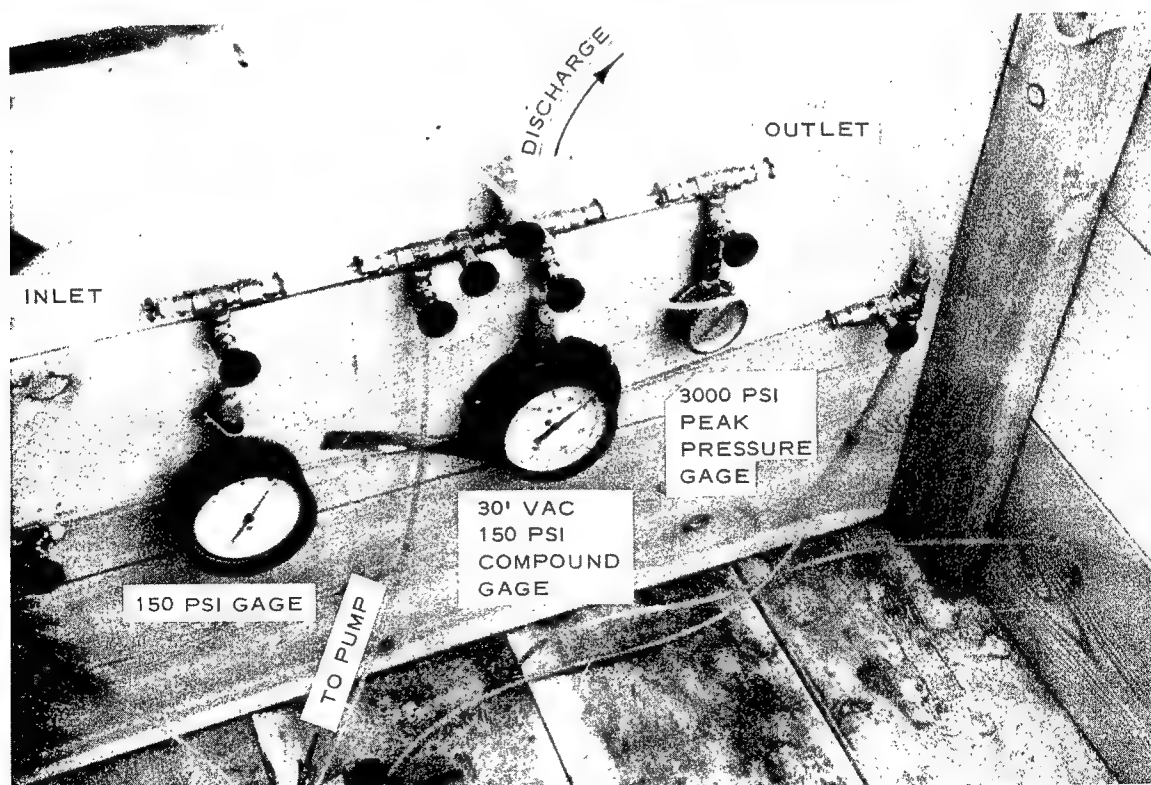
b. Gage board for USBR hydraulic piezometer

Fig. 2.3 Photographs of transducer piezometer and USBR piezometer gage boar‑

CHAPTER 3

RESULTS AND DISCUSSION

3.1 INSTRUMENT PERFORMANCE

All timing and sequence initiating signals were received
and properly translated, resulting in all recording equipment
operating as planned.

Of the thirty-three electronic gages installed prior to
the Bravo Event, thirty-two were operable at shot time. Gage
6-Pa-1 had succumbed to apparent water leakage prior to the
detonation. Seven of the remaining gages (3-u-1, 9-σ-4,
15-Pa-2, 28-u-7, 30-ω-1, 31-σ-11, and 32-ω-2) produced no
useful peak data because of severely overdriving the galvanome-
ters and saturation of the magnetic tape channels. The four
gages emplaced for the Charlie Event were recorded successfully.
Only one of the two measurements scheduled for the Alfa Event
was recorded because of a cable mix-up at the instrument van.

3.2 DATA REDUCTION

The oscillograms were read on an electromechanical digitizer,
and the data converted to card form. These were then processed
through a digital computer where an integration was performed on
the particle velocity records to yield displacements, and all
data were then automatically plotted.

24

Peak measurements of particle velocity and stress are summarized in Table 3.1. A listing of pore pressure observations is presented in Table 3.2. Time histories of particle velocities and their associated displacements, soil stresses, and cavity pressures are presented in Appendix A.

3.3 ARRIVAL TIMES

The times of arrival of the shock front at all electronic gages are plotted versus distance in Figure 3.1. A linear relationship is seen to exist which yields an average compression wave velocity of 6,800 ft/sec. This value is considerably higher than that recorded on the SC-2 shot, 6,800 ft/sec versus 5,750 ft/sec. The probable significance of this fact is that the Bravo data were obtained from a deeper strata of more competent and more saturated material. This efficient shock transmission is evidenced also by the higher stresses and particle velocities measured on Bravo than on SC-2.

It was noted that arrival times registered by the pore pressure gages were slightly longer than those reported by the remaining instruments. This was probably caused by the filtering action of the gage tip which both delayed and attenuated the shock front such that the exact arrival time was difficult to determine precisely.

25

3.4 TOTAL SOIL STRESS

The peak total soil stresses which were measured on Shots Bravo, Charlie, and Alfa are plotted versus distance in Figure 3.2. As is shown by the "best-fit" solid line on this figure, a fairly consistent pattern of stress attenuation with distance exists over the range instrumented (85 feet to 1,570 feet). The relatively good fit of most of the data points to this mean line adds confidence in the stress data, especially in view of the fact that three different gage types were used for these measurements.

As was discussed in Section 1.4, the free water pressure versus distance curve was used as an upper bound for the expected stress levels in this saturated medium. This curve is presented in Figure 3.2. Although the SC-2 data provided upper bound, the actual SC-2 data points all fell slightly under this curve and therefore the final stress prediction curve was reduced to two-thirds of the free water data. The reduced curve is presented on Figure 3.2 also.

It is interesting to note on this figure that for those Pre-Gondola I data which correspond to the scaled SC-2 data, i.e., between 100-175 feet, the agreement with

26

this reduced curve is good. The close-in data (< 100 feet)
are slightly above the free water curve, whereas the data
at large distances (>500 feet) fall below both free-water
based curves. This over-all attenuation rate (solid line)
is of the -2 power of distance, a rate one would expect in
dry soil, tuff or hard rock (granite). For comparison,
extrapolated data from Hardhat and Shoal[2,3] are dotted in
on Figure 3.2. The Pre-Gondola I data show an amazing
likeness to this granite data.

As is shown in Figure 3.2 there is considerable dif-
ference in the two close-in stress measurements at the
85-foot range station. Gage 2-σ-2 was at the same depth
as the charge (46 feet) therefore had a slant range of
85 feet, while Gage 1-σ-1 was buried only 25 feet giving
a slightly larger slant range of 87.6 feet. Gage 2-σ-2
measured 12,400 psi while Gage 1-σ-1 measured only 8,980 psi.
A check was made to see if the unloading or tensile (rare-
faction) wave which was reflected from the shallow (8 feet)
ground water level interface could have arrived back at the
shallow (25 feet) station before the peak of the incident
stress was reached. This would have lowered absolute peak.
Judging from the rise times of the two incident wave fronts,

27

this was not considered likely in that both had identically

sharp fronts of slightly less than 0.5 msec.

To compare the two waves:

	1-σ-1 (87.5 ft)	2-σ-2 (85 ft)
Incident stress wave arrival	12.0 msec	11.4 msec
Peak incident stress	12.5 msec (8,980 psi)	11.9 msec (12,400 psi)
Refraction wave arrival	13.8-14.2 msec	15.0-15.4 msec
Calculated wave arrival	13.8 msec	15.2 msec
Stress cut-off	15.3 msec	17.7 msec

It is interesting to note on Figures A.1 and A.2 in

Appendix A that the arrivals of the tensile wave are

discernible at both stations and agree well with the

calculated times. The durations at both stations were

shortened by this unloading wave. Because of dispersion

of the wave at greater distances, the influence of the

rarefaction is less pronounced and becomes progressively

more difficult to identify. The best example of this

relief or "surface cut-off" effect occurs at Gage 7-σ-3,

where the gage was very near the reflecting surface. The

gage was buried only 10 feet below the surface and was

only 2 feet below the reflecting interface, i.e., the ground

water at 8 feet. The stress waveform plotted in Figure A.3

shows a radical change from A.1 and A.2. Whereas 1-σ-1 and

2-σ-2 had rise times of 0.5 msec, peaked-out, started to

decay and then sharply fell to ambient, 7-σ-3's rise was

discontinued at 0.3 msec and the stress experienced a sharp

relief. This was the tensile wave reflected from the

interface arriving almost simultaneously with the incident

wave.

The 0.3 msec value is logical in that the reflected

wave path was approximately 2 feet longer than the incident

wave and using a travel of about 6.8 feet per msec this

yields a time for the reflected arrival of 0.3 msec. If

one assumes a stress rise similar to the previous stations

(0.5 msec) then the peak at 7-σ-3 represents about 0.6 of

the possible maximum stress, had the station been in an

infinite medium, i.e., 6,780 psi versus 10,500 psi. The

rarefaction becomes less significant with increasing

ground range because of radial divergence and dispersion.

However, the possibility of its arrival at more remote

stations before incident stress is reached is greater

because the difference between the reflected path and

29

the incident path decreases and, as the stress pulse attenuates, its rise time is slower. This is seen at 16-σ-7 (A.10) and 22-σ-9 (A.15). With the faster arrival but weaker strength of the rarefaction wave and the slower rise of the incident, this occurence is not much more than a slight inflection on the upward sweep of the trace. The peak stress was probably lessened, but only slightly.

Although this rarefaction phenomena was not observed on SC-2 because of rather meager data, it was suspected and is discussed in the Results section of Appendix B. The agreement between the two sets of data would lead one to surmise that it did exist on SC-2.

3.5 PARTICLE VELOCITY

Peak values of particle velocity were obtained at five of the seven locations instrumented. As mentioned previously, Gages 3-u-1 and 28-u-7, which were closest and farthest from the shot point, respectively, gave no reportable data other than shock arrival times. These channels were greatly overdriven and although one cannot report a peak velocity one can infer that the amplitude was significantly higher than the gage set range, viz, 40 ft/sec and 1.4 ft/sec.

30

The measured velocities are plotted versus distance in Figure 3.3. An irregular pattern of attenuation exists and all five measurements are above the predicted values, as were the measurements from the overdriven channels. This is not too surprising in that the close-in stress measurements were higher also and particle velocity is proportional to stress. The irregular pattern of amplitude with distance is brought about by the same mechanism that produced early stress relief, i.e., the reflected tensile wave. Figures A.4, A.8, A.12, A.16, and A.18 all present evidence of sudden change in form at or near the peak velocity occurrence. The times of occurrence coincides with that exhibited by the stress waveforms.

No direct comparison of other measured particle velocities can be made due to a lack of such measurements in a saturated media. However, a general comparison, which can give some insight as to the relative magnitude of velocity in saturated Bearpaw Shale, granite, and tuff, is made in Figure 3.3. Here the composite of the particle velocities measured in granite (shaded area) and tuff (cross-hatched area) are plotted. These plots were derived from the following empirical equations which best represent measured data[1]:

$$u = 0.8 \times 10^5 \ (\frac{R}{W^{1/3}})^{-1.65} \ \pm 35\% \ \text{(tuff)}$$

$$u = 3.1 \times 10^5 \left(\frac{R}{W^{1/3}}\right)^{-1.65} \pm 35\% \text{ (granite)}$$

Where u is in ft/sec, R is in feet, and W is in kt. The Bravo data points are seen to lie significantly above the granite data, which is an emphatic departure from the trend toward smaller motions for media with lower seismic impedances, i.e., ρc . Since this trend has been observed for a rather wide variety of dry rock and soil types, the answer to the Pre-Gondola I data variation would seem to be attributable to the high degree of saturation rather than failure of the ρc hypothesis. It is felt that the stress pulse transmission characteristics of the shale were enhanced to a large degree by the water.

A similar enhancement was indicated by a direct comparison of free-field acceleration measurements made in both wet and dry sand on Operation Snow Ball[4]. The particle acceleration measured in the wet sand was nearly twice that recorded in dry sand.

3.6 CAVITY PRESSURE

Water shock measurements were made in the Alfa cavity for Shot Bravo and in the Alfa and Delta cavities for Shot Charlie.

An upper bound of the stress transmission factor across the shale-water interface can be calculated by the following relationship:

$$\frac{\sigma_w}{\sigma_s} = \frac{2 \, \rho_w \, c_w}{\rho_w c_w + \rho_s c_s} \quad \text{or} \quad \sigma_w = 0.5 \, \sigma_s$$

where, σ_w = Peak stress transmitted into water, psi

σ_s = Peak incident stress in shale, psi

ρ = Density, lb/ft^3

c = Seismic velocity, ft/sec

This yields an upper bound of 0.5 since a normal reflection at a plane interface is assumed.

The measurement in Alfa for Shot Bravo gave a value of 126 psi as compared to the total soil stress of 308 psi outside the cavity. The measurement in Delta for Shot Charlie gave a value of 51 psi as compared to the total soil stress of 142 psi outside the cavity. These values yield a transmission factor of approximately 0.4 which seems reasonable. The stress outside the Alfa cavity for Shot Charlie was 48 psi (which correlates well on Figure 3.2) while the cavity pressure measured 158 psi. This unexplainably high value is considered anomalous.

3.7 PORE PRESSURE

A plot of the piezometer readings versus time is shown in Figure 3.4. Prior to the event, all piezometers indicated fairly stable conditions for a period of approximately two weeks before the event, except for Piezometer PR-6 which indicated increasing pressures from the time of installation until prior to the event, at which time it indicated a pressure of 300 psi. It is presumed that this piezometer was defective or possibly damaged during installation. The remaining piezometers prior to the event indicated pressures in the range of ± 15 psi; these are not actual pressures. The piezometers could not be expected to indicate precisely the groundwater level pressures, since these were only a small fraction of the total range of the devices. It is believed, however, that the preshot data indicate that the piezometers, excluding PR-6, were relatively stable and offer a basis for determining the difference in groundwater pressure as a result of the shot.

None of the piezometers, except PR-2, indicated the peak pore water pressure, as the traces went off the paper. Piezometer PR-2 indicated a peak pressure of 12,800 psi, which is in close agreement with values of total stresses measured at that distance of 12,375 psi and 8,980 psi.

34

The traces of piezometers PR-1, PR-2, and PR-4 were lost after arrival of the peak pressures, and no further information could be obtained from these gages which were presumably rendered inoperative by the shock wave. Damage to the cables as a result of falling debris (despite the protection provided) did not permit manual reading of the above-mentioned gages. The trace for Piezometer PR-3 indicated a negative pore pressure of -59 psi, which is not possible for this gage. Therefore, it is also presumably inoperative. Residual pore pressures at Piezometers PR-5 through PR-8 were recorded on the traces until cable damage occurred; subsequently, manual readings of these piezometers were made at the top of the instrument holes in which they were located. Manual readings could not be made at the top of the Instrument Holes PR-1 through PR-4 as the instrument holes were covered by ejecta from the crater.

It may be noted from Figure 3.4 that the pore pressures indicated by Piezometers PR-5, PR-7, and PR-8 showed an increase after the Bravo Event. During the ten days of observations after the event, these piezometers showed a steady reduction in the residual pore pressures. These

piezometers were also read immediately prior to and sub-
sequent to the Alfa, Charlie, and Delta events; however,
no significant changes in indicated pore pressure were
observed as a result of these events. In order to define
the rate of dissipation of residual pore pressures, they
have been plotted versus the logarithm of elapsed time, as
shown in Figure 3.5. This plot shows that the pore
pressures for PR-5, PR-7, and PR-8 were relatively constant
for the first twenty-four hours, and then the indicated
pressures dropped off. Additional observations of the
piezometers will be needed to establish the significance
of these relationships and to determine when equilibrium
will be reached. Piezometer PR-9, installed after the
Bravo Event, evidently had not had time to reach equilibrium
during the short period of observation. Future observa-
tions of this piezometer may give further indication of
the true pore pressures.

Contours of excess pore pressures indicated ten days
after the Bravo Event have been plotted, as shown in
Figure 3.6. At a distance of 300 feet from SGZ (approxi-
mately four crater radii), the USBR-type piezometer indi-
cated no excess pore pressures. At a distance of 225 feet

36

from SGZ (approximately three crater radii), the excess
pore pressure ranged in the vicinity of 20 to 30 psi.
The maximum excess pore pressure measured at PR-8 was
36.7 psi and exceeded the effective overburden pressure
which is approximately 25 psi at the piezometer tip.

Residual pore pressure measurements resulting from
blasting in a fine sand have been reported by Kummeneje
and Eide.[4] The pore pressures observed within a few
minutes after the blast are plotted in Figure 3.7.
Although a crater was not formed, the contours of residual
excess pore pressures provide an insight into the probable
distribution of excess pore pressures generated by the
Pre-Gondola Event and thus were used as a guide in
developing the contours shown in Figure 3.6.

TABLE 3.1 PEAK MEASUREMENTS FOR MOTION AND STRESS GAGES

Gage	Distance	Depth	Arrival Time	Peak Stress	Peak Velocity	Remarks
	(ft)	(ft)	(msec)	(psi)	(fps)	
Bravo Event						
1-σ-1	85	25	12.0	8,980		Appears low
2-σ-2	85	46	11.4	12,375		
3-u-1	85	46	11.4		70	Overdriven
6-Pa-1	85	46	--			Gage inoperable
7-σ-3	100	10	15.1	6,380		Tensile relieved
8-u-2	100	10	14.5		36.9	Tensile relieved
9-σ-4	100	25	--			No data
10-σ-5	125	25	18.7	3,250		
11-σ-6	125	46	17.7	3,205		
12-u-3	125	46	17.8		23.9	Tensile relieved
15-Pa-2	125	46	17.8			Overdriven
16-σ-7	175	25	26.4	2,550		
17-σ-8	175	46	25.2	2,105		
18-u-4	175	46	25.9		29.9	
21-Pa-3	175	46	25.4	5,305		
22-σ-9	225	46	32.6	2,550		
23-u-5	225	46	33.3		18.8	
27-u-6	300	46	45.0		5.1	
28-u-7	375	46	57.5		5	Overdriven
29-σ-10	930/Delta	57	137.4	171		
30-ω-1	930/Delta	57	--			No data
31-σ-11	800/Charlie	42	--			No data
32-ω-2	800/Charlie	42	--			No data
33-σ-12	660/Alfa	52	91.9	308		
34-ω-3	660/Alfa	52	97.6	126		

TABLE 3.1 PEAK MEASUREMENTS FOR MOTION AND STRESS GAGES (CONTINUED)

Gage	Distance	Depth	Arrival Time	Peak Stress	Peak Velocity	Remarks
	(ft)	(ft)	(msec)	(psi)	(fps)	
			Charlie Event			
29-σ-10	770/Delta	57	124	142		
30-ω-1	770/Delta	57	119	51		
33-σ-12	1210/Alfa	52	177	48		
34-ω-3	1210/Alfa	52	181	158		
			Alfa Event			
29-σ-10	1570/Delta	57	226	31		
30-ω-1	1570/Delta	57	--			Gage inoperable

39

TABLE 3.2 PIEZOMETRIC OBSERVATIONS

Date and Time	Elapsed Time	Indicated Pore Pressures in psi									
		PR-1	PR-2	PR-3	PR-4	PR-5	PR-6	PR-7	PR-8	PR-9	PR-10
28 Sep 66	-28 days					-3.7[a]	11.7[a]	-5.5[a]			
3 Oct	-22 days		18.3[a]		2.9[a]				-19.4[a]		
4 Oct	-21 days	-9.8[a]		-7.5[a]							
7 Oct	-18 days	-6.2	13.9	-6.6	-7.4	2.4	25.5	-1.0	-12.9	-	
11 Oct	-14 days	-6.4	14.4	-3.9	-6.9	2.5	131.0	-1.1	-12.9	-	
14 Oct	-11 days	-6.6	15.0	-3.7	-7.5	2.5	195.0	-1.1	-12.8	-	
18 Oct	- 7 days	-6.9	15.4	-3.4	-7.4	3.1	254.0	-1.1	-12.7	-	-2.5
21 Oct	- 4 days	-5.9	13.9	-2.4	-8.7	3.5	285.0	-1.2	-12.6	-	
24 Oct	- 1 day	-6.5	14.4	0.5	-2.2	4.1	300.0	-1.1	-12.3	-	-2.5
Bravo Event (1000)											
25 Oct	0.5 sec	-	b	-59.0	-	43.6	346.0	27.3	41.2	-	
25 Oct	30 min	-	-	-	-	30.7	228.0	16.0	29.6	-	-2.5
25 Oct	2.5 hr	-	-	-	-	30.5	226.0	15.0	28.6	-	
25 Oct	6 hr	-	-	-	-	30.8	227.0	14.8	28.3	-	-2.5
26 Oct	24 hr	-	-	-	-	30.8	234.0	14.9	27.7	-	-2.5
Charlie Event (1200)											
27 Oct	2 days	-	-	-	-	30.1	244.0	14.8	27.8	4.5[a]	0
28 Oct (0830)	3 days	-	-	-	-	31.4	248.0	15.1	27.6	-1.6	
28 Oct (1223)	3 days	-	-	-	-	30.4	249.0	14.2	27.0	-1.8	
28 Oct (1500)	3 days	-	-	-	-	30.1	251.0	14.4	27.2	-1.9	
29 Oct	4 days	-	-	-	-	30.4	255.0	14.7	27.0	-1.7	
Alfa Event (1000)											
1 Nov (0820)	7 days	-	-	-	-	25.8	274.0	12.8	25.4	-1.3	
1 Nov (1020)	7 days	-	-	-	-	25.8	276.0	12.6	24.8	-1.3	
1 Nov (1410)	7 days	-	-	-	-	25.4	276.0	12.6	25.1	-1.3	
3 Nov	9 days	-	-	-	-	25.7	284.0	12.8	24.9	-1.5	
Delta Event (1000)											
4 Nov (0840)	10 days	-	-	-	-	25.7	288.0	12.7	24.9	-1.4	
4 Nov (1020)	10 days	-	-	-	-	25.8	288.0	12.6	24.4	-1.4	
4 Nov (1415)	10 days	-	-	-	-	25.5	289.0	12.6	24.4	-1.5	

[a] Initial reading after installation. Zero reading made with transducer in a container of water before installation in drill hole.

[b] Peak pore pressures were not recorded except at Piezometer PR-2 which indicated a peak pressure of 12,800 psi at 11.9 msec.
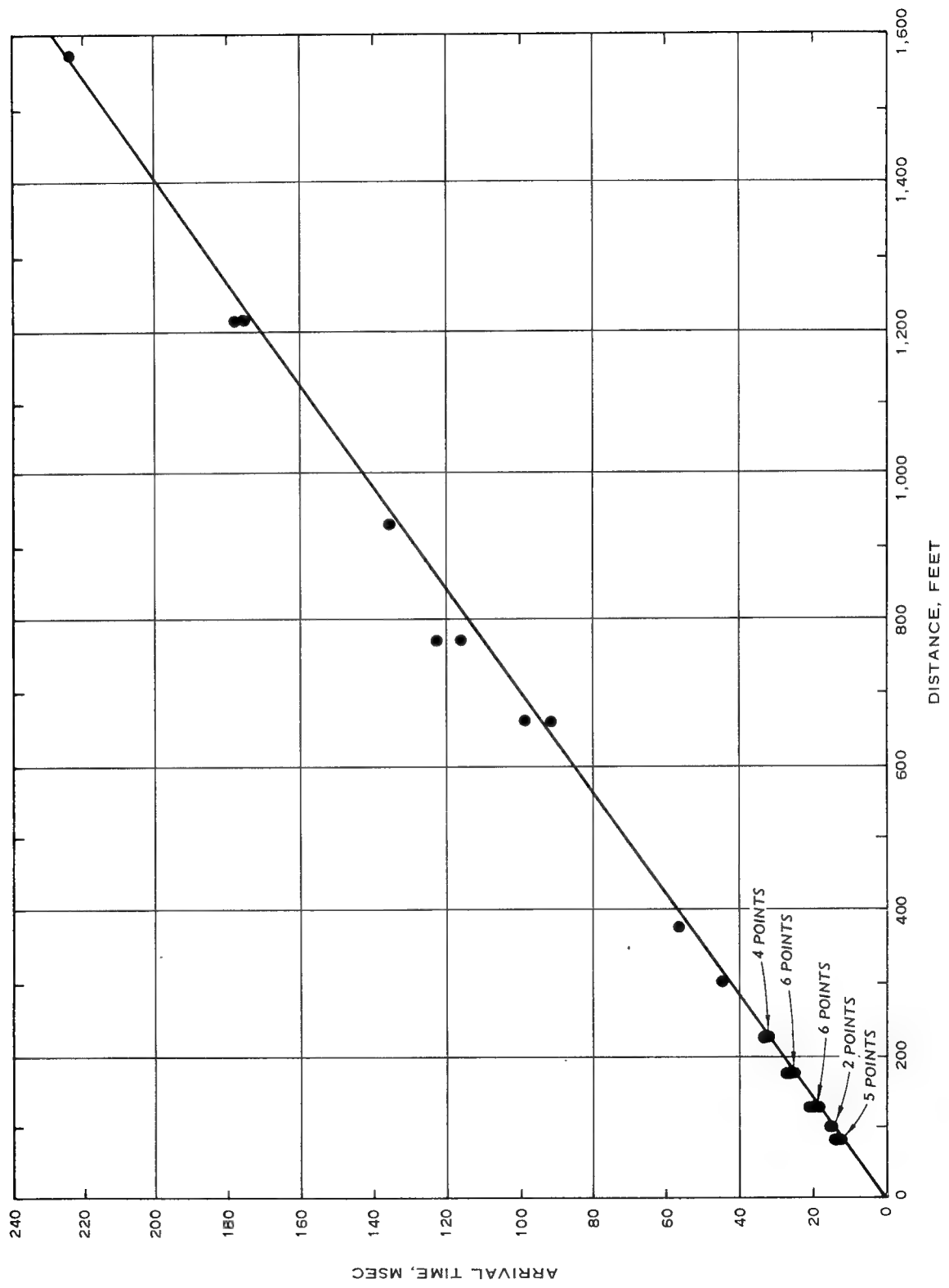
40

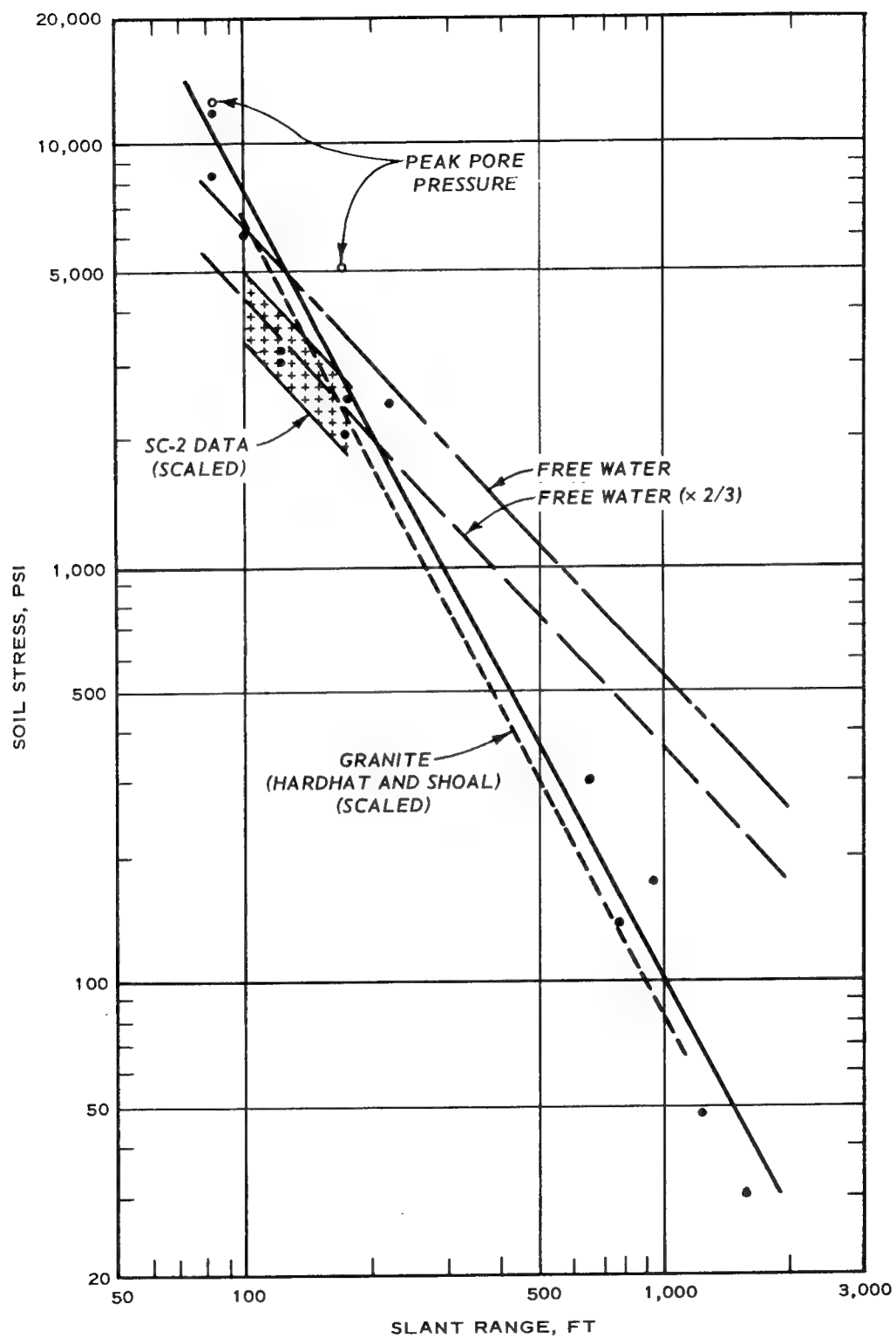Figure 3.1 Arrival time versus distance

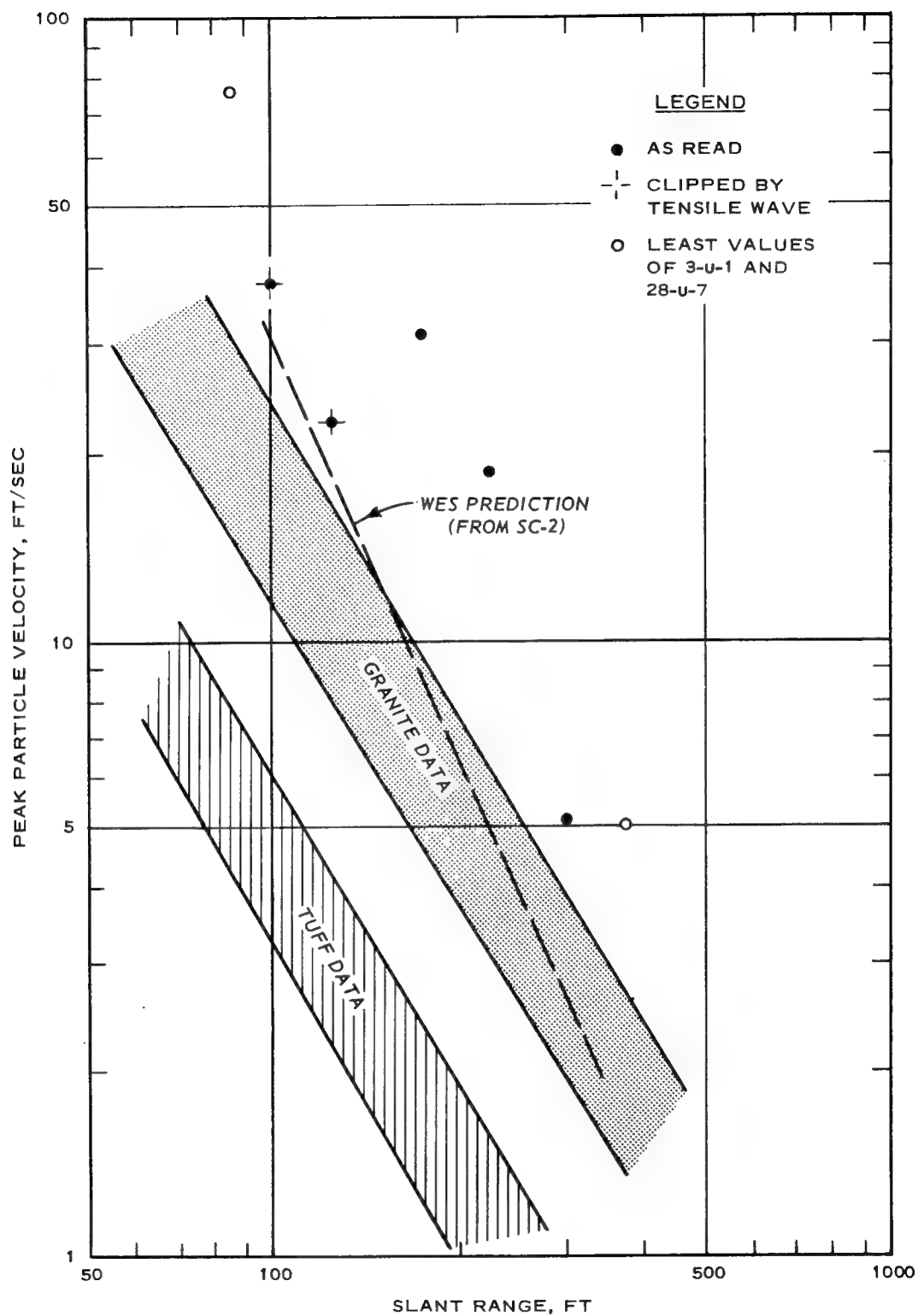41

Figure 3.2   Soil stress versus slant range

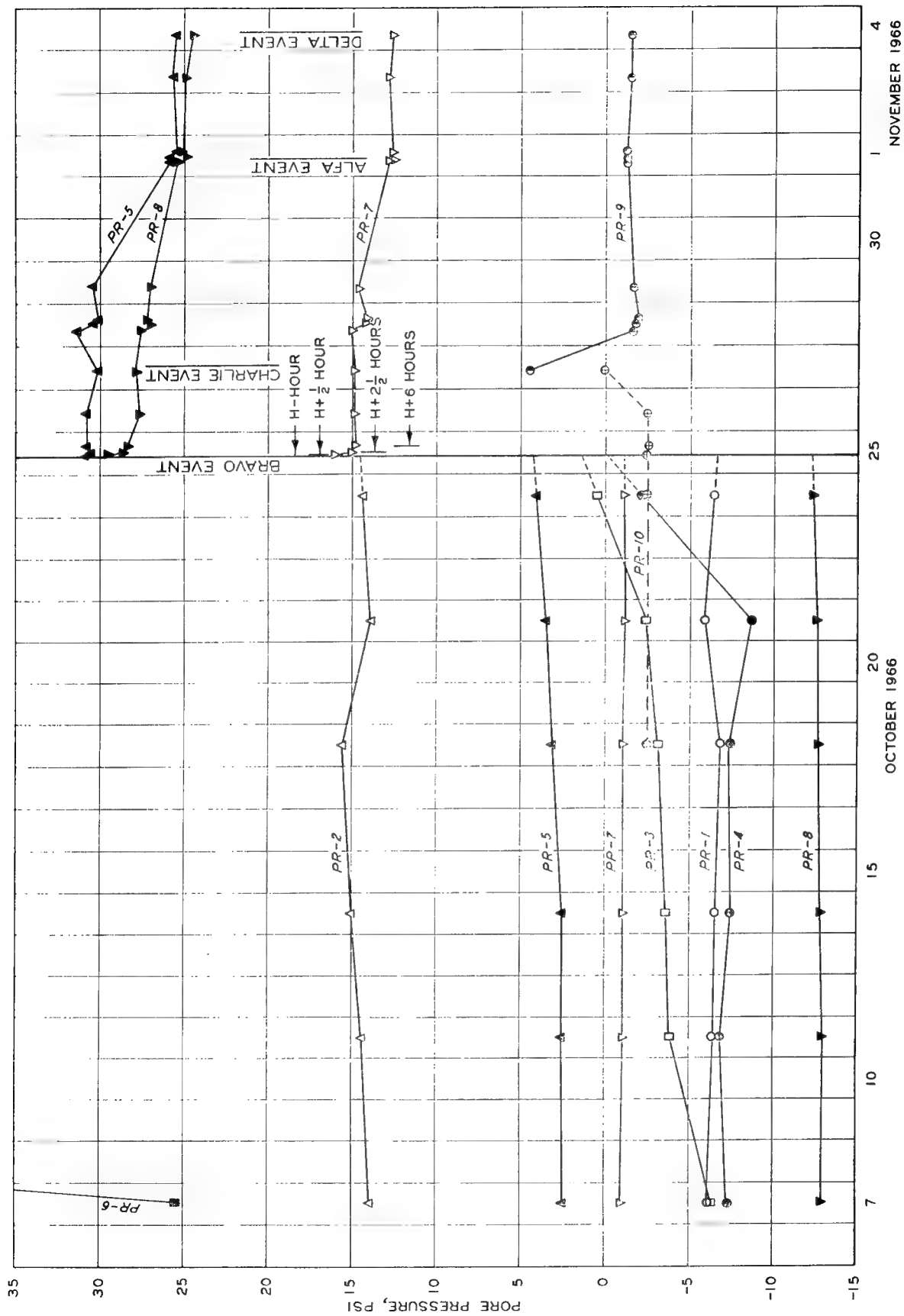Figure 3.3 Particle velocity versus slant range

43

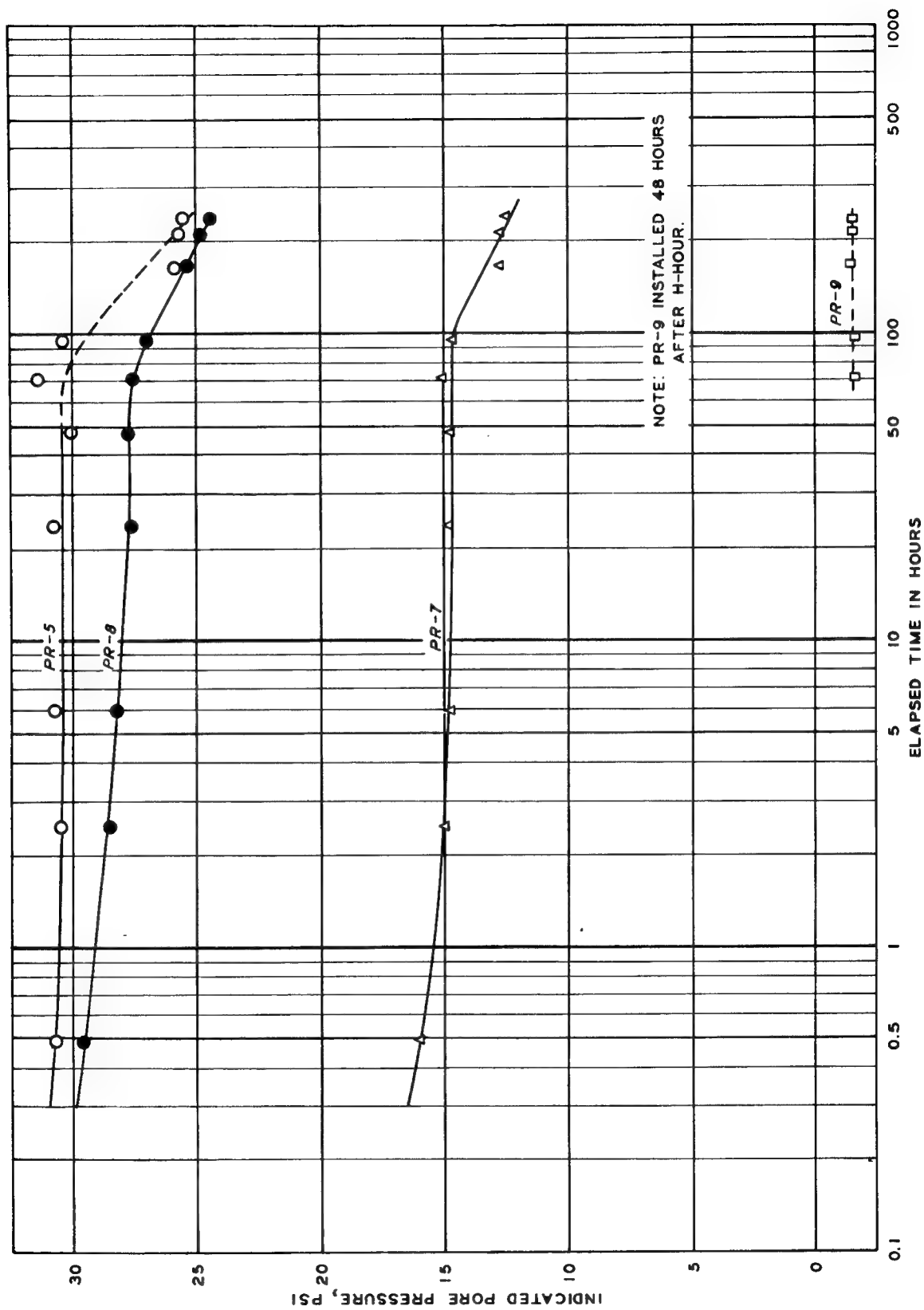Figure 3.4 Indicated pore pressures versus time

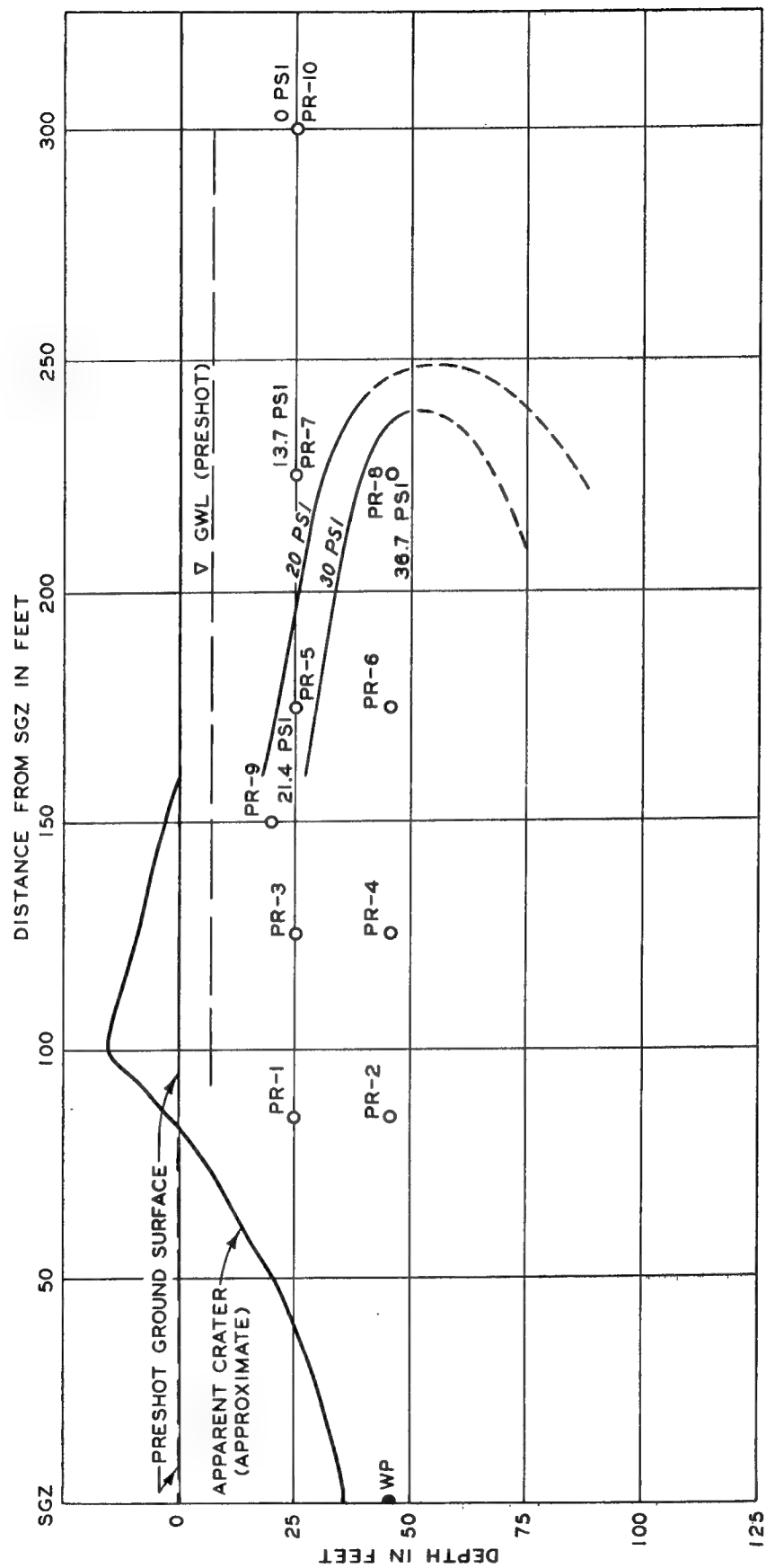Figure 3.5   Residual pore pressures versus elapsed time

45

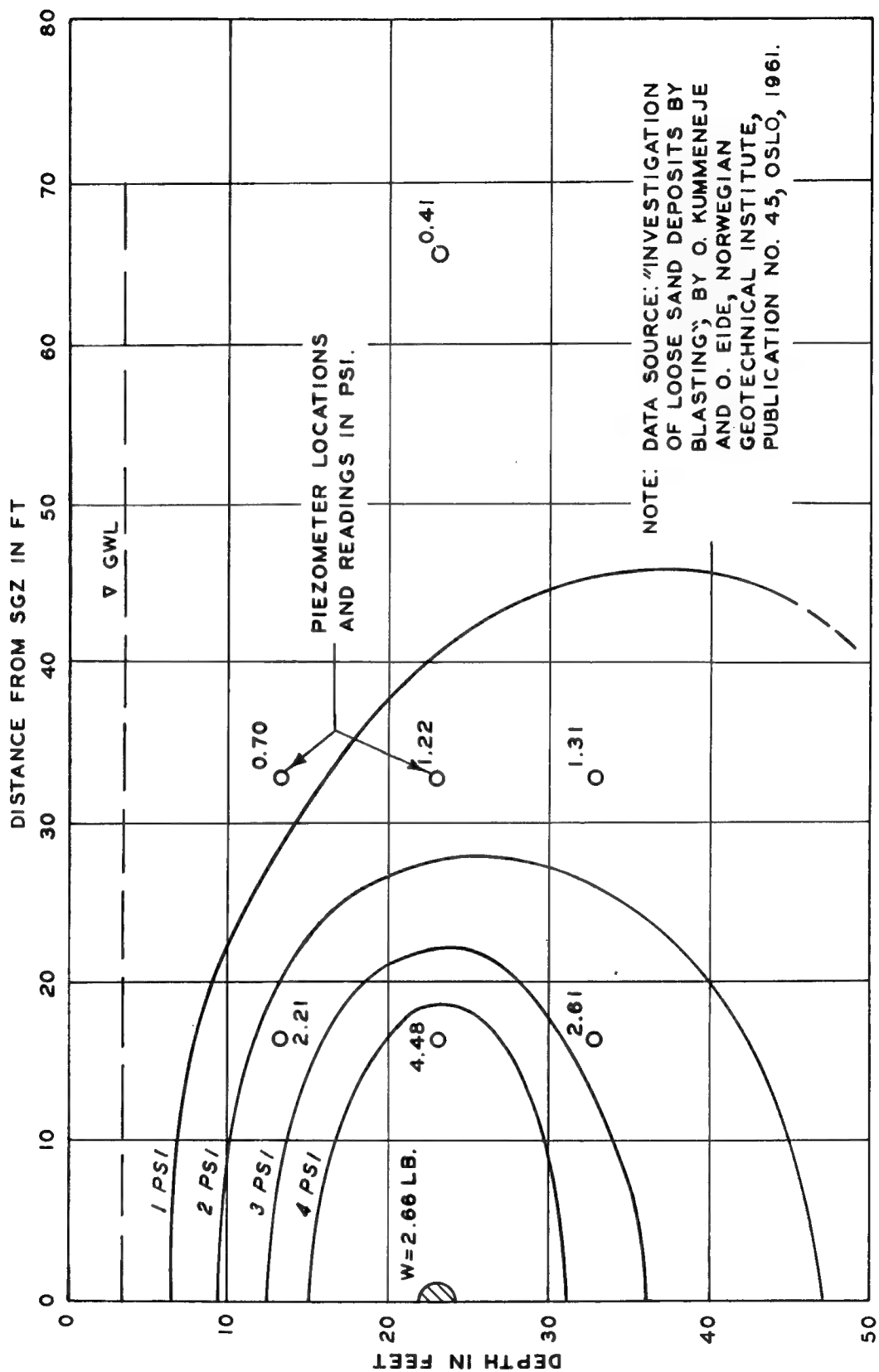Figure 3.6 Contours of indicated excess pore pressures (D + 10)

Figure 3.7 Contours of residual excess pore pressure due to blasting in a fine sand

47

CHAPTER 4

CONCLUSIONS

As was first observed during the Calibration Series,
a high amplitude, short period stress pulse was measured
at the close-in stations on Shot Bravo. Propagation
velocities measured on Bravo, Charlie, and Alfa averaged
6,800 ft/sec, significantly faster than that of the shallow
SC-2. It is concluded that the stresses were propagated
more efficiently at the deeper (more competent shale) levels.

The amplitude of peak stress varied from 12,375 psi
at 85 feet on Bravo to 31 psi at 1,570 feet on Alfa, and
attenuated as the -2 power of distance over this interval.
The higher stress value was greater than predicted by the
scaling up of the SC-2 data. The attenuation was more
rapid than that postulated by the free water analogy.
Both the amplitude and attenuation rate closely resembles
data gathered from a much more competent medium, such as
granite..

Much the same conclusion is reached concerning particle
velocity. The measured data from Bravo exceeded that pre-
dicted by using the SC-2 data, scaled to the Bravo conditions.

48

When compared to tuff and granite, albeit dry, the data from the saturated shale is higher than one would expect from a material with a much higher ρc, i.e., granite.

The scatter in the stress and particle motion data at the close-in stations is attributed to the unique shot-gage geometry. A strong rarefaction (tensile) wave traveling down from the surface essentially prematurely relieved the incident stress wave before it peaked at the close-in stations. This rarefaction wave became less pronounced with distance. In an infinite medium one would expect the data to be more consistent.

The two successful water pressure measurements made inside the flooded Alfa and Delta cavities gave a stress transmission factor of about 0.4 which compares well with the theoretical factor of 0.5 (the theoretical factor assumes normal incidence at the rock-water interface). Postshot inspection of these cavities showed no damage sustained, with the Alfa cavity on Shot Bravo being at the 310 psi level.

The passage of the shock wave induced a peak pore water pressure which was in close agreement with the peak total stress. Residual excess pore water pressures as high as 37 psi were recorded. These residual pressures tended to drop slowly with time.

49

CHAPTER 5

RECOMMENDATIONS

The following recommendations are made as a result of this test:

With large charges, i.e., 20 tons or greater, stress propagation of at least 6,800 ft/sec should be expected in this medium. The total peak stresses should be predicted on the basis of the Pre-Gondola I series.

For the Pre-Gondola II row shot the geometry of the charge row should be examined closely. With extremely strong shocks possible from single charges, depending on how fast the surface relief wave arrives, the multiple shocks from a row could arrive at close-in stations almost simultaneously. These pulses would add and could over-range the gages significantly.

Waterproofing and shockproofing of gages and cables must be improved.

More tests in various media, especially in saturated media, are deemed necessary in order to determine the influence of water on the shock propagation characteristics.

APPENDIX A

MOTION AND STRESS-TIME HISTORIES
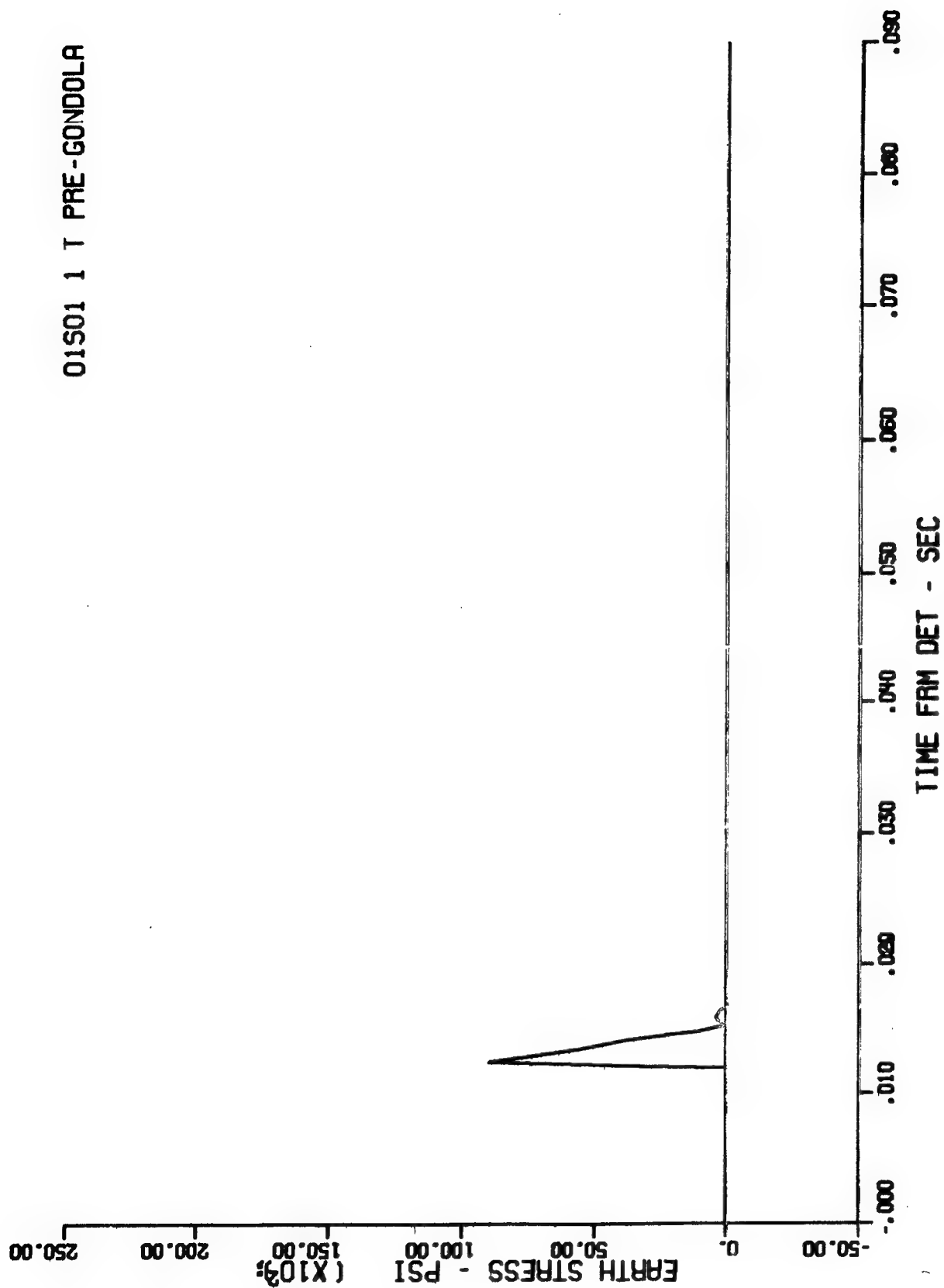
Figure A.1 Gage 1-g-1, range 35 ft, depth 25 ft, Event Bravo
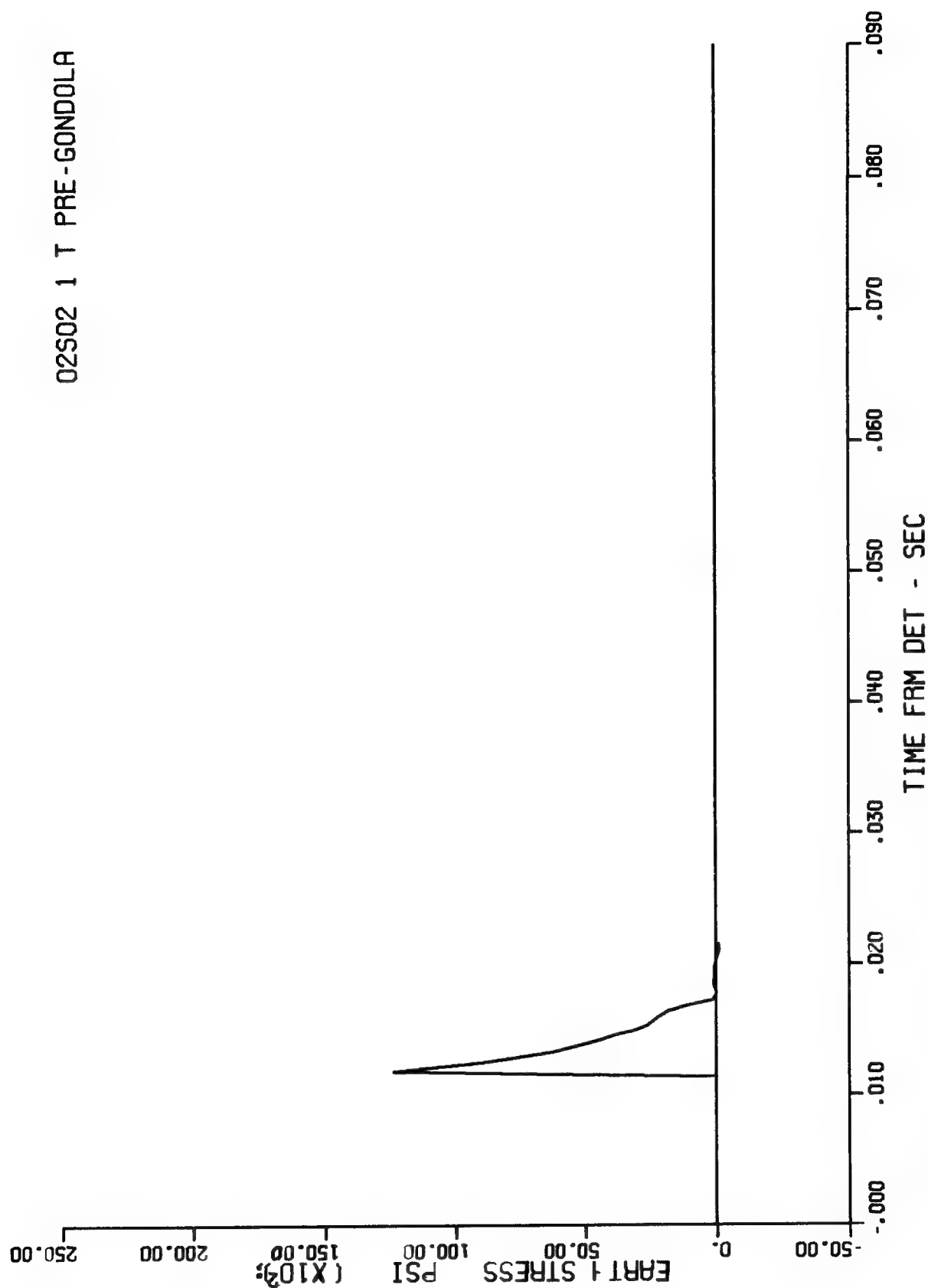
Figure A.2   Gage 2-σ-2, range 85 ft, depth 46 ft, Event Bravo

53

07S03 1 B PRE-GONDOLA

EARTH STRESS - PSI (X10³)

TIME FRM DET - SEC
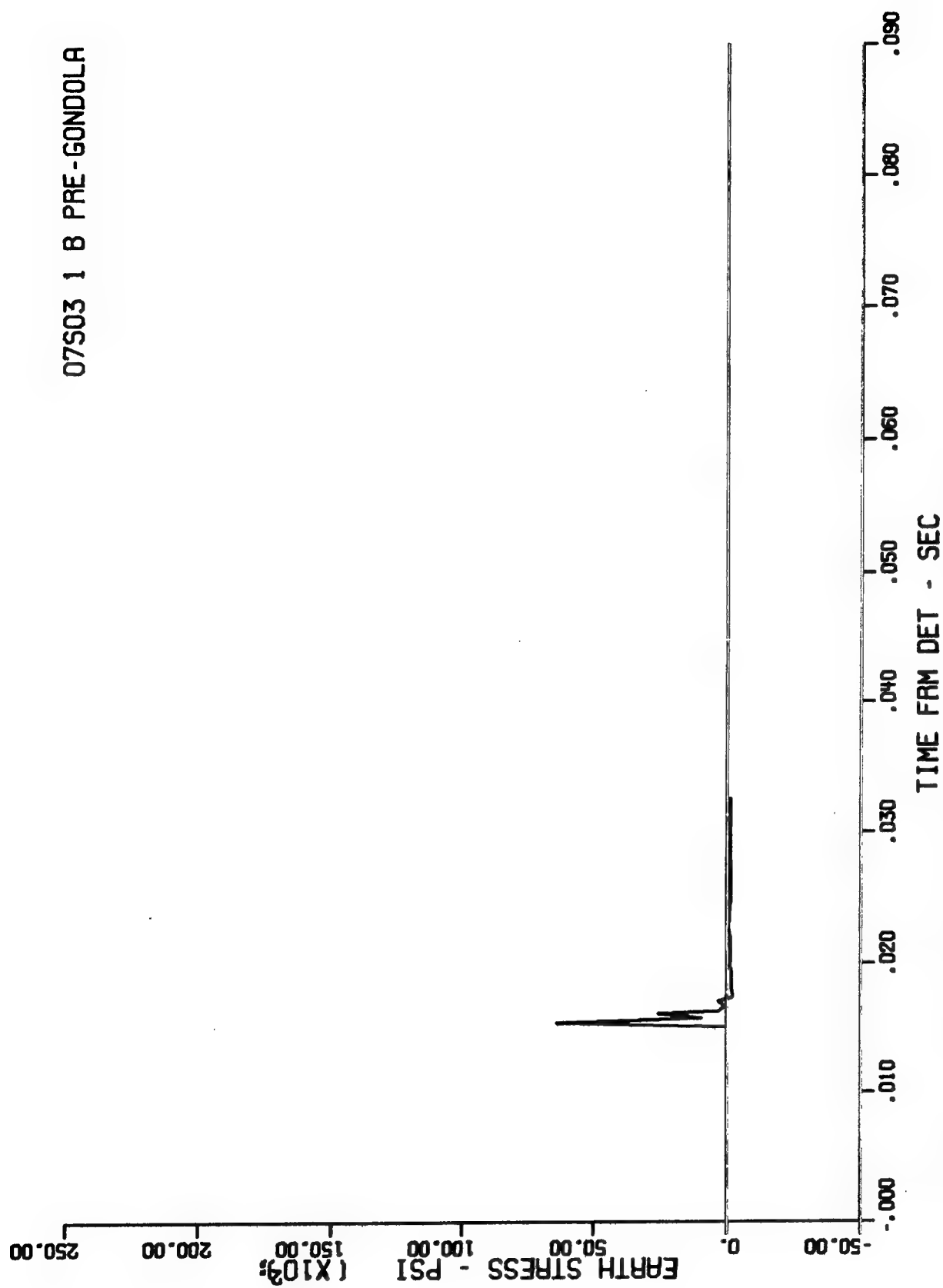
Figure A.3 Gage 7-σ-3, range 100 ft, depth 10 ft, Event Bravo

54

Figure A.4 Gage 8-u-2, range 100 ft, depth 10 ft, Event Bravo

55
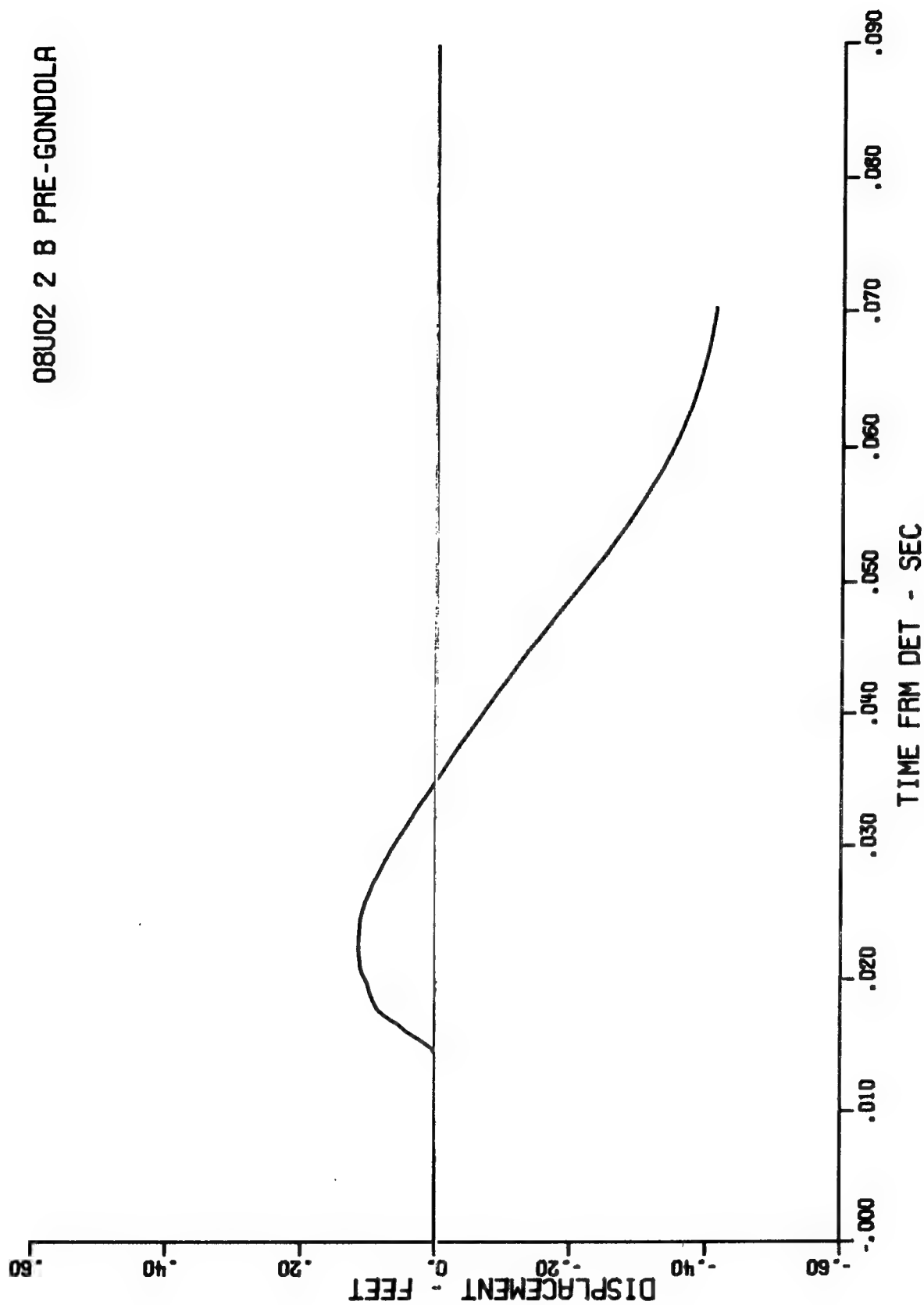
Figure A.5   First integral of Gage 8-u-2, range 400 ft, depth 10 ft, Event Bravo

56

10505 2 B PRE-GONDOLA

TIME FRM DET - SEC

EARTH STRESS - PSI (X10³)
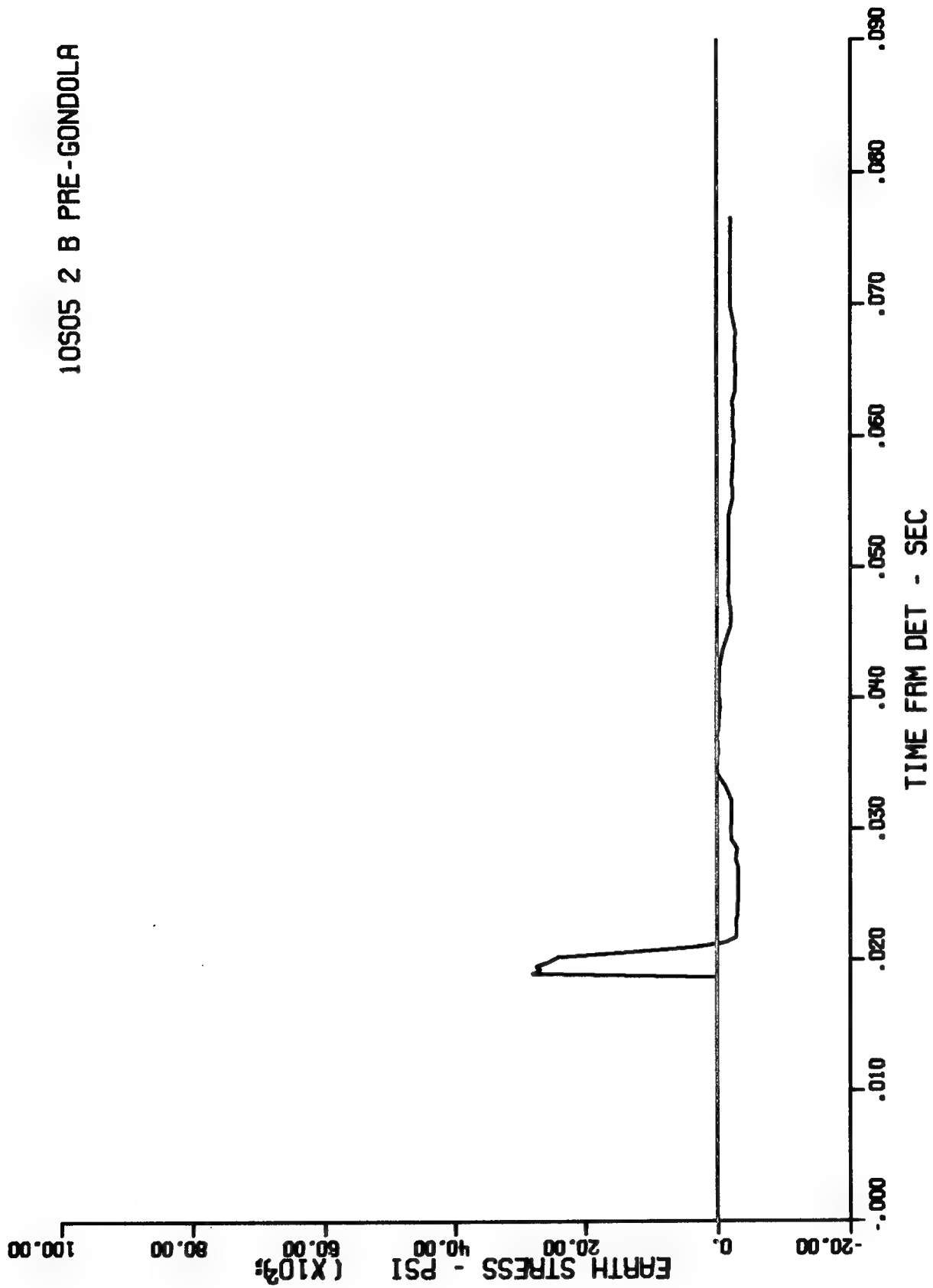
Figure A.6 Gage 10-σ-5, range 125 ft, depth 25 ft, Event Bravo

57
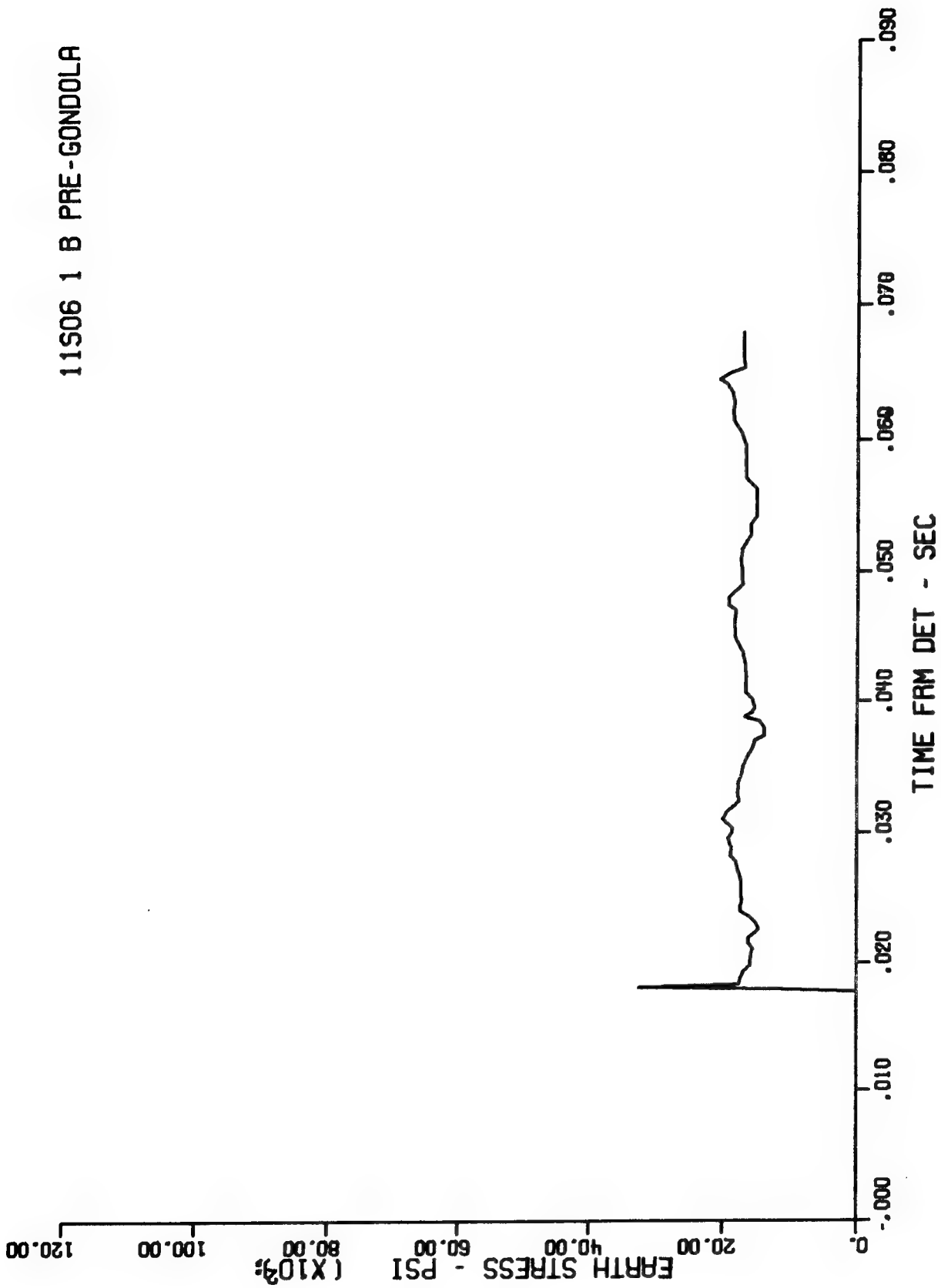
Figure A.7 Gage 11-σ-6, range 125 ft, depth 46 ft, Event Bravo
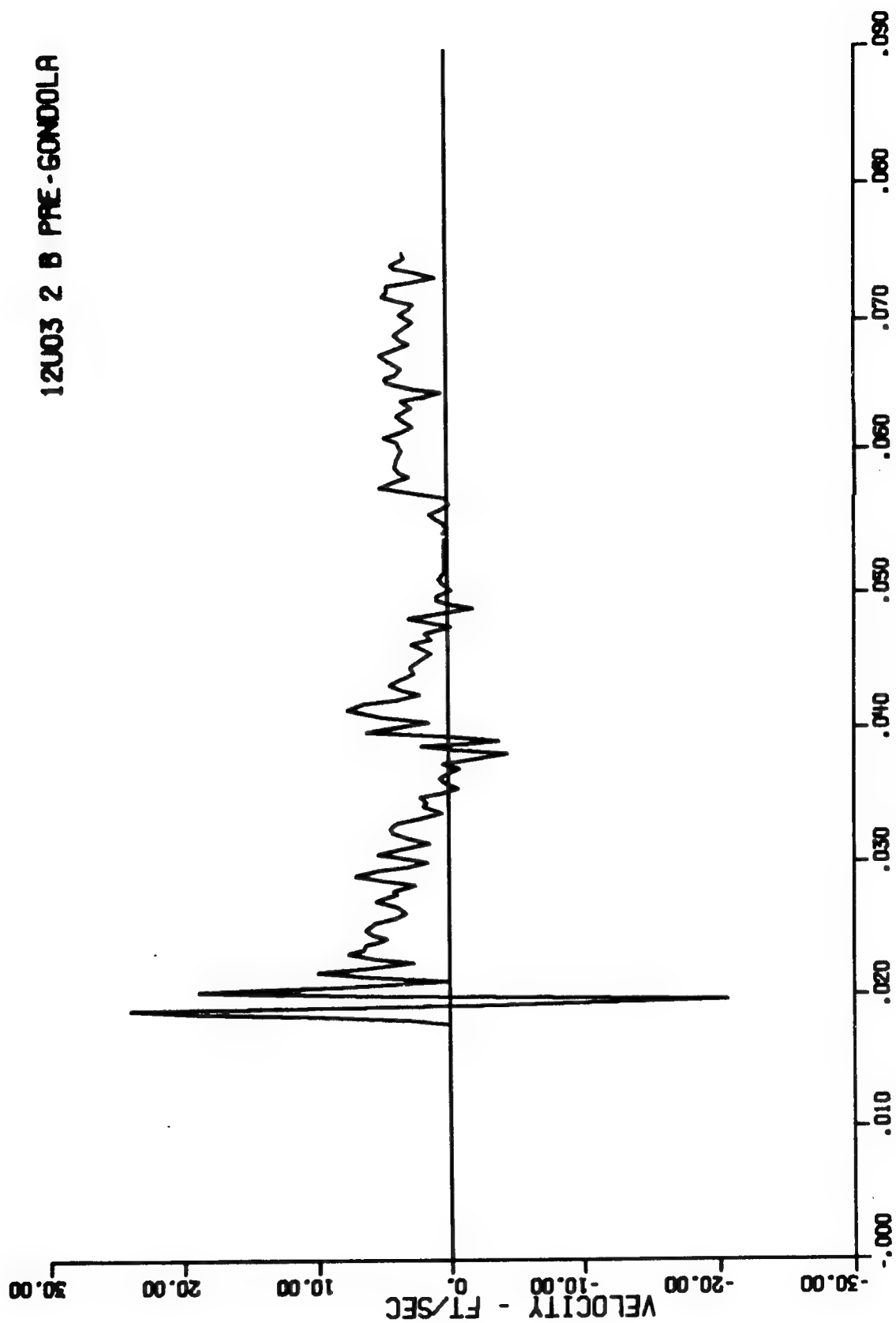
Figure A.8 Gage 12-u-3, range 125 ft, depth 46 ft, Event Bravo
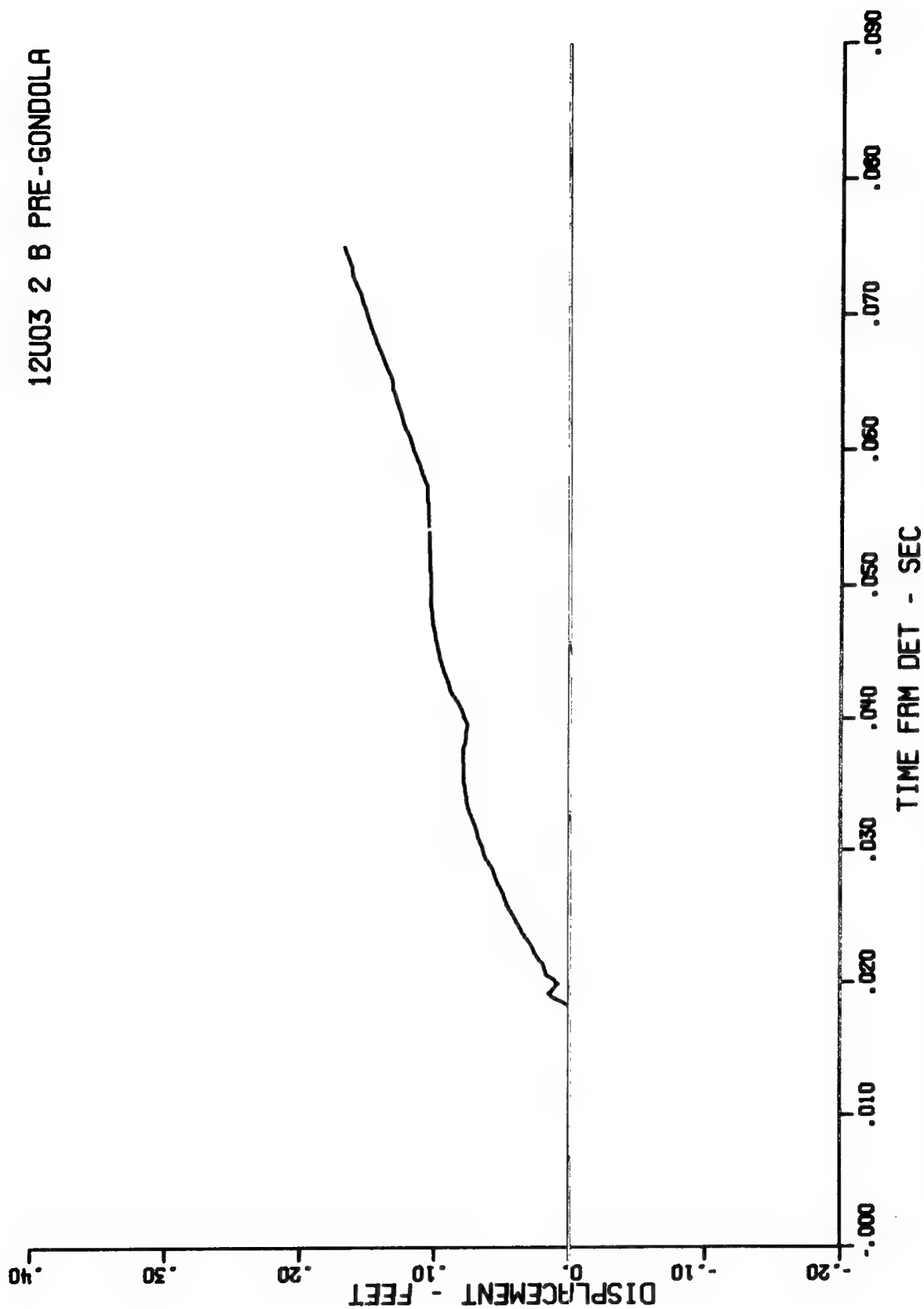
Figure A.9 First integral of Gage 12-u-3, range 125 ft, depth 46 ft, Event Bravo
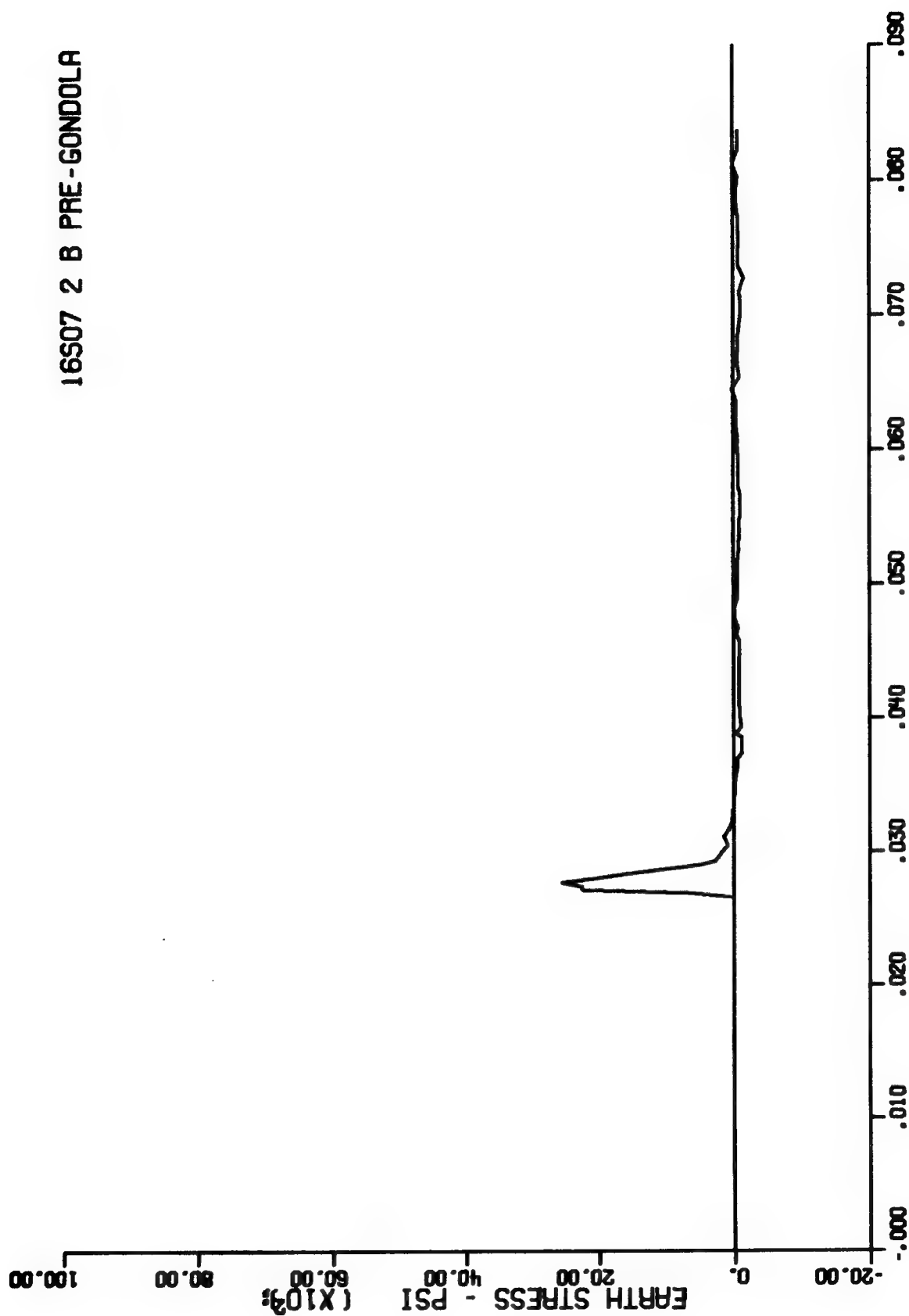
Figure A.10 Gage 16-σ-7, range 175 ft, depth 25 ft, Event Bravo

61
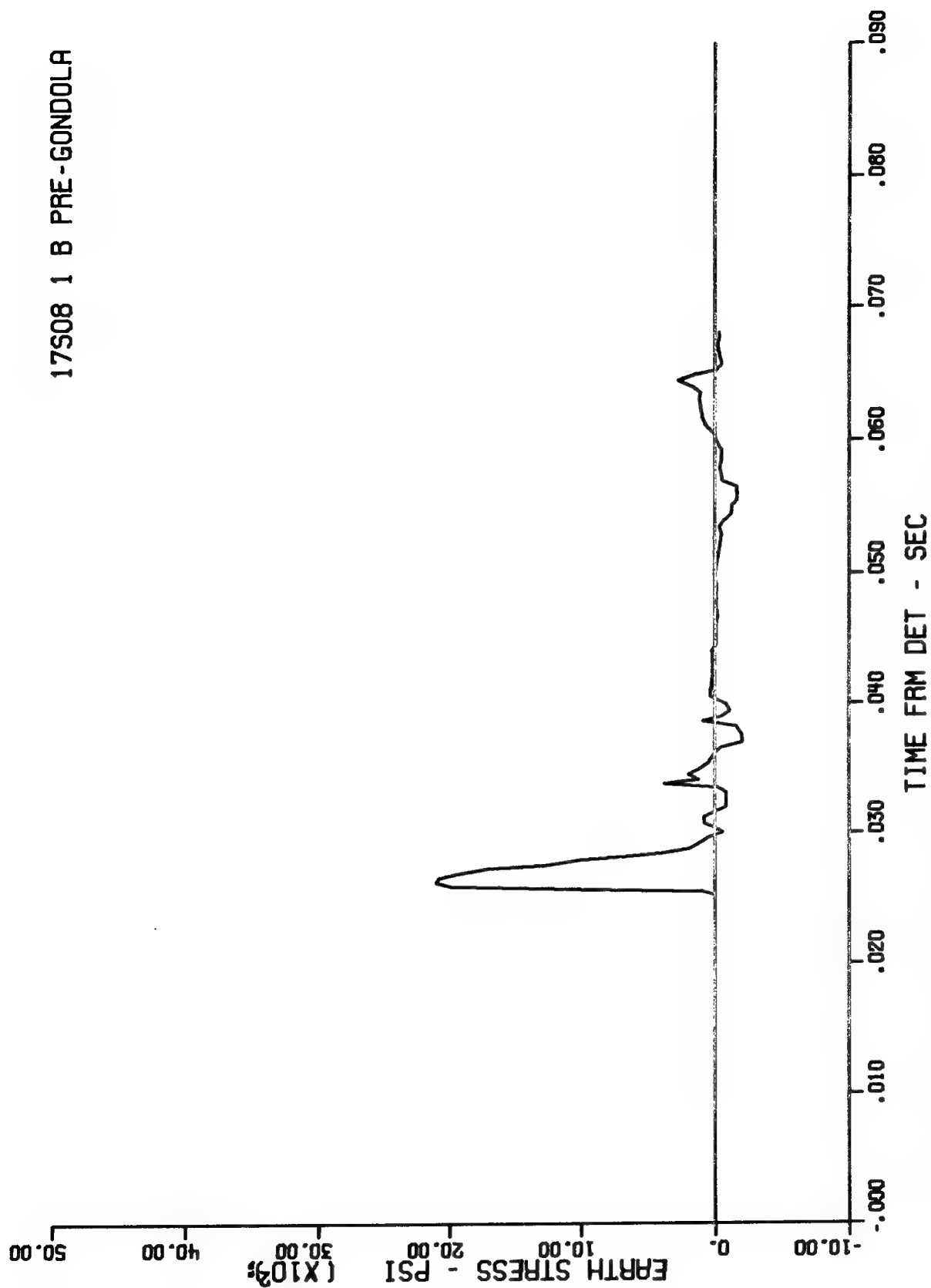
Figure A.11 Gage 17-σ-8, range 175 ft, depth 46 ft, Event Bravo

18U04 2 B PRE-GONDOLA

VELOCITY - FT/SEC
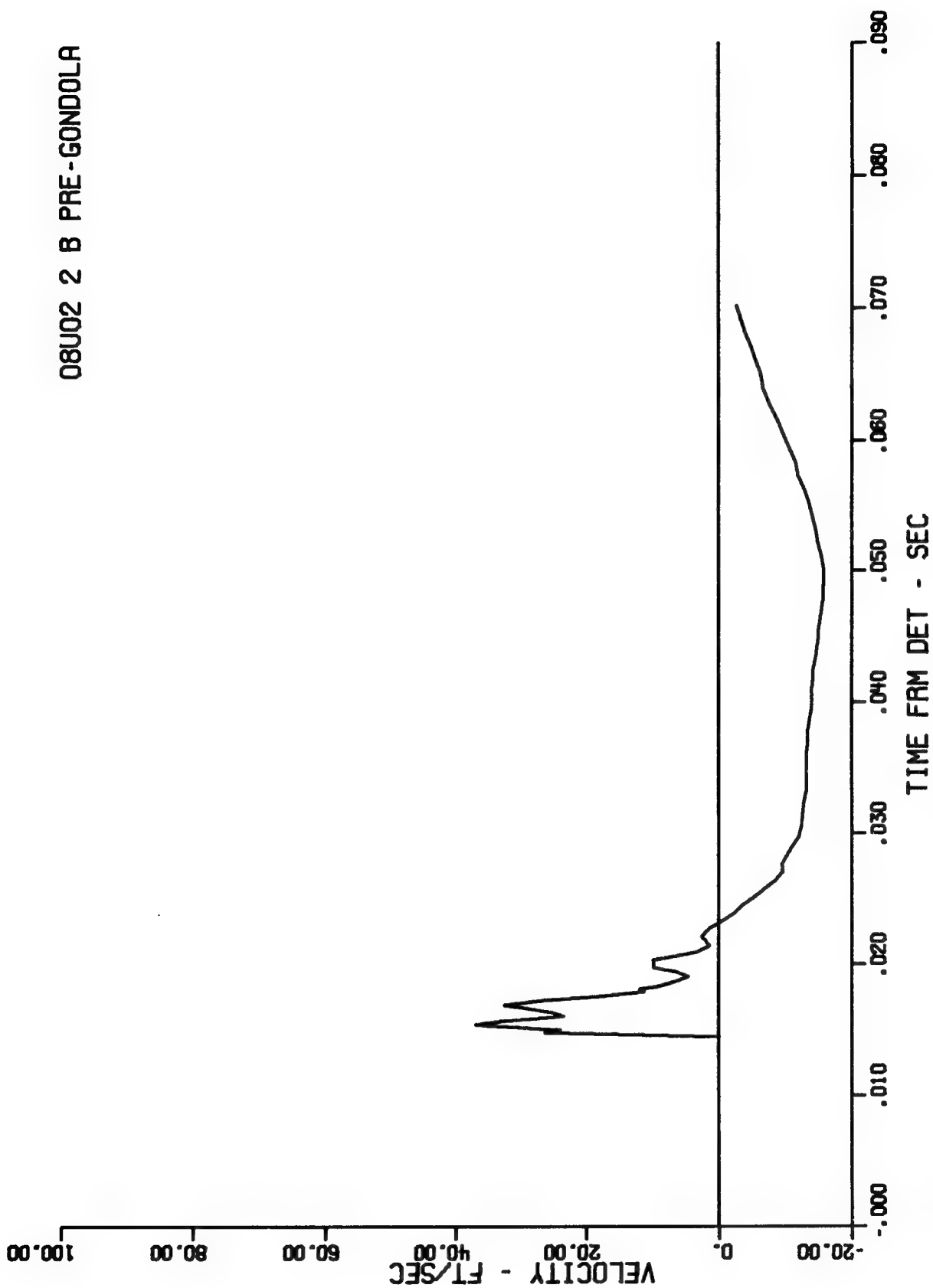
TIME FRM DET - SEC
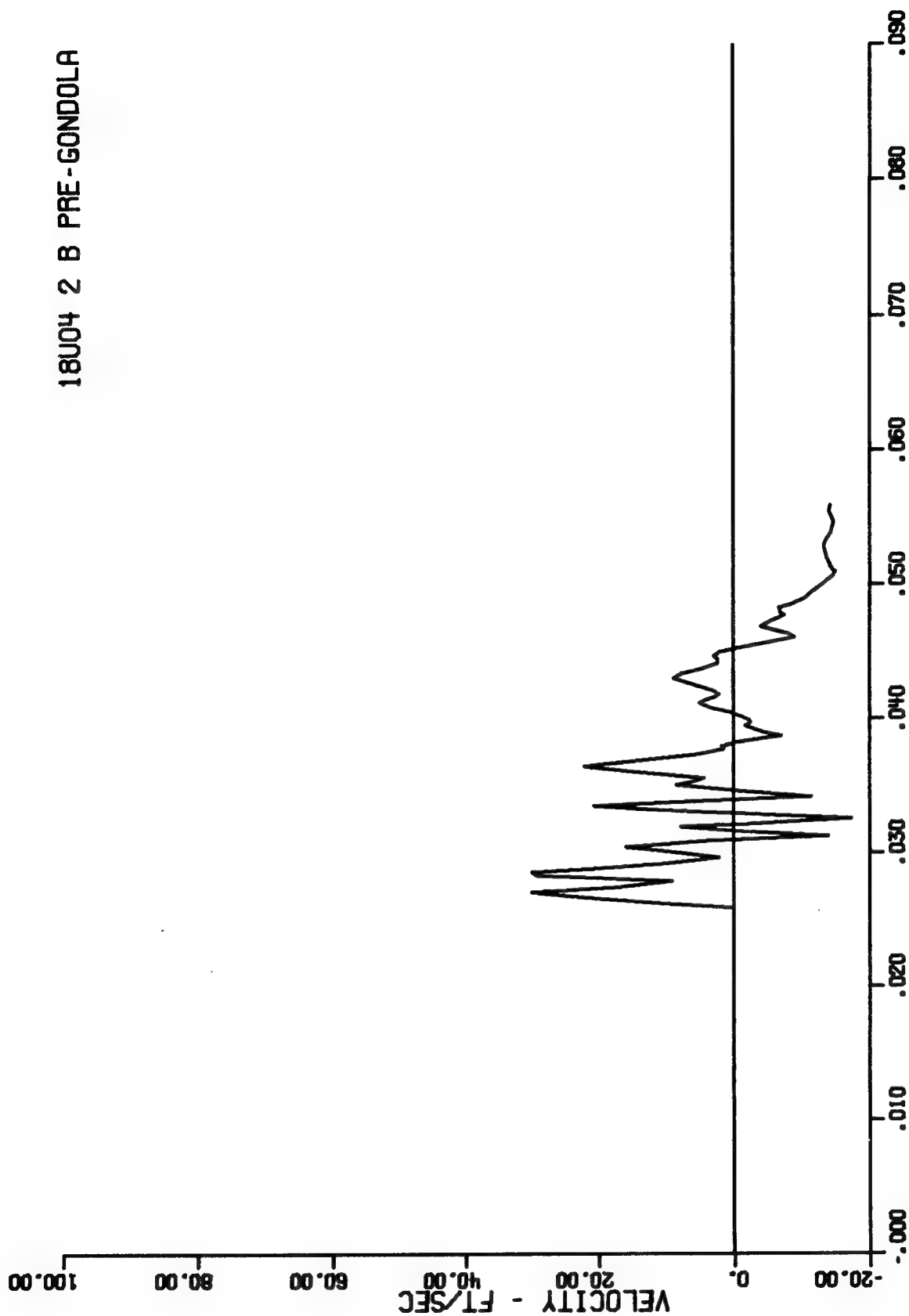
Figure A.12 Gage 18-u-4, range 175 ft, depth 46 ft, Event Bravo

63

18U04 2 B PRE-GONDOLA
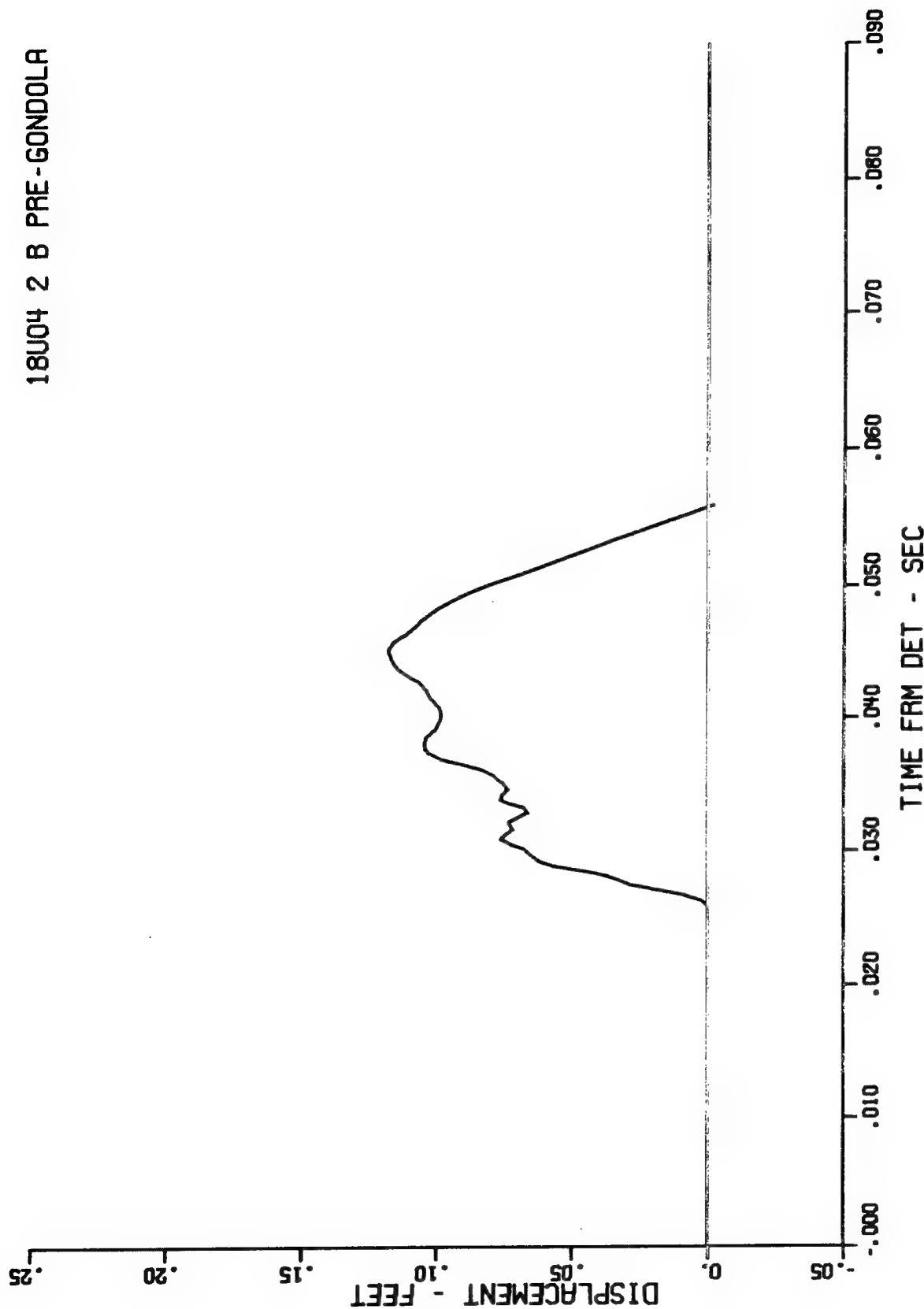
Figure A.13 First integral of Gage 18-u-4, range 175 ft, depth 46 ft, Event Bravo

TIME FRM DET - SEC

DISPLACEMENT - FEET

64
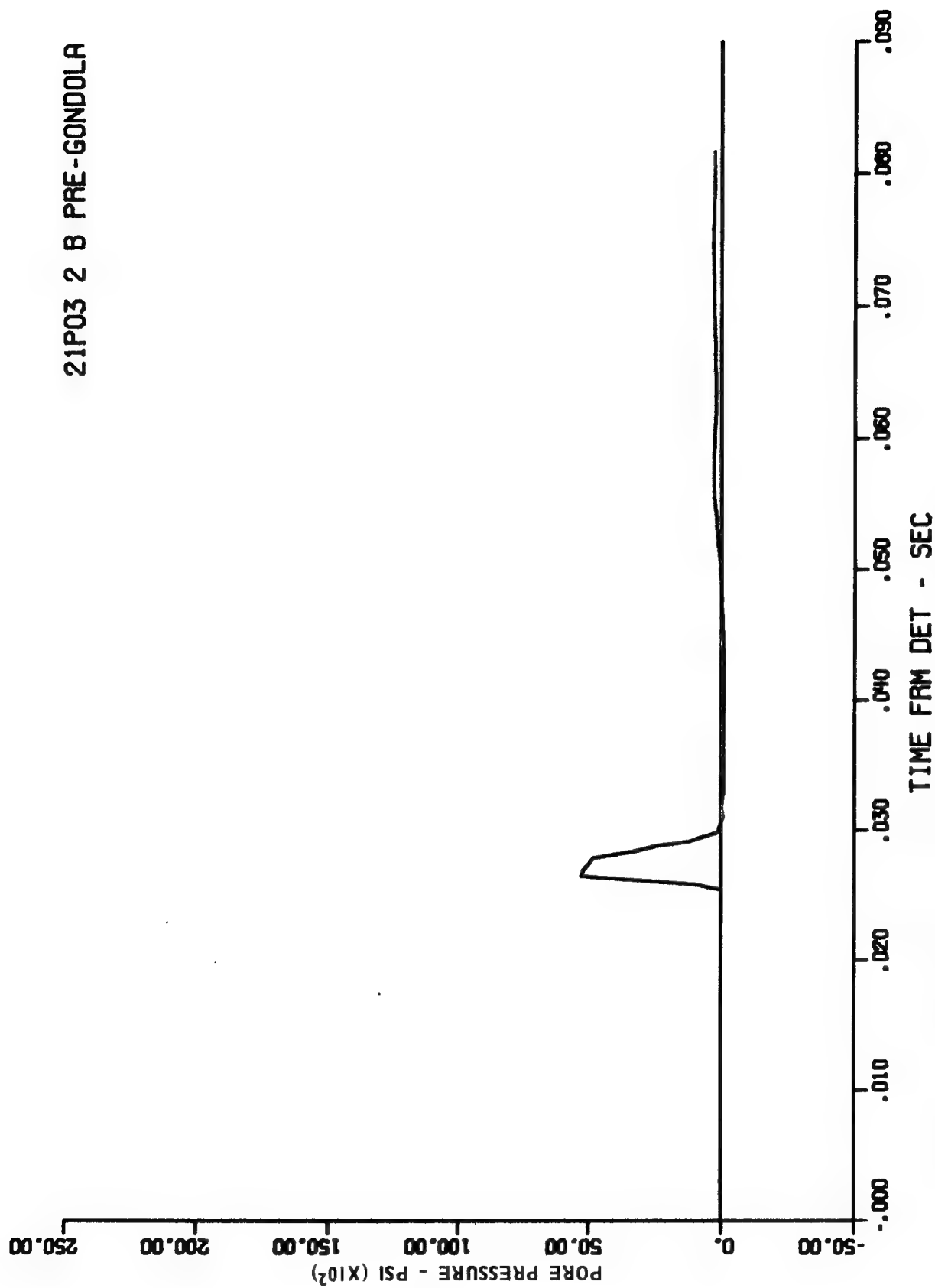
Figure A.14 Gage 21-Pa-3, range 175 ft, depth 46 ft, Event Bravo

65

22509 2 B PRE-GONDOLA
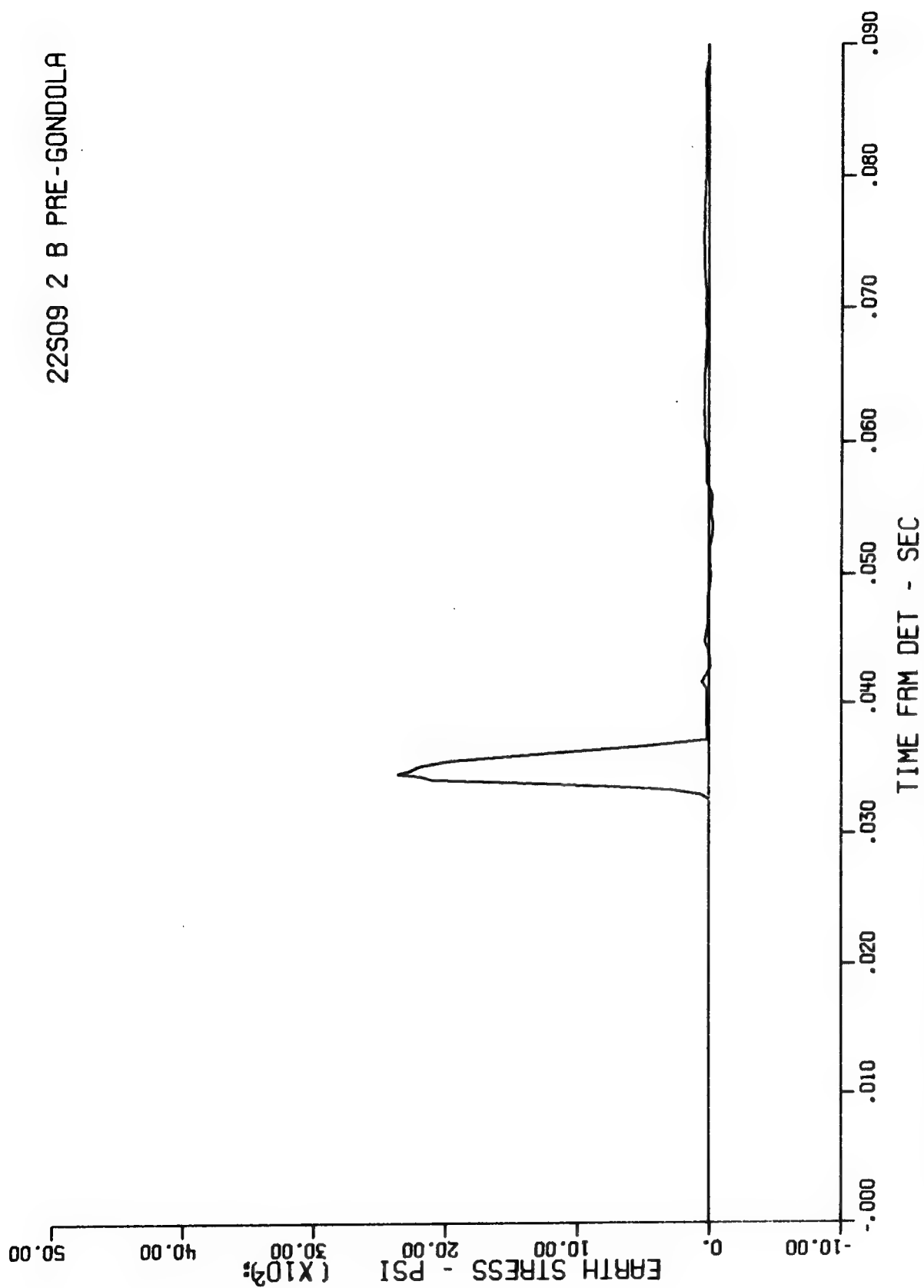
Figure A15 Gage 22-σ-9, range 225 ft, depth 46 ft, Event Bravo
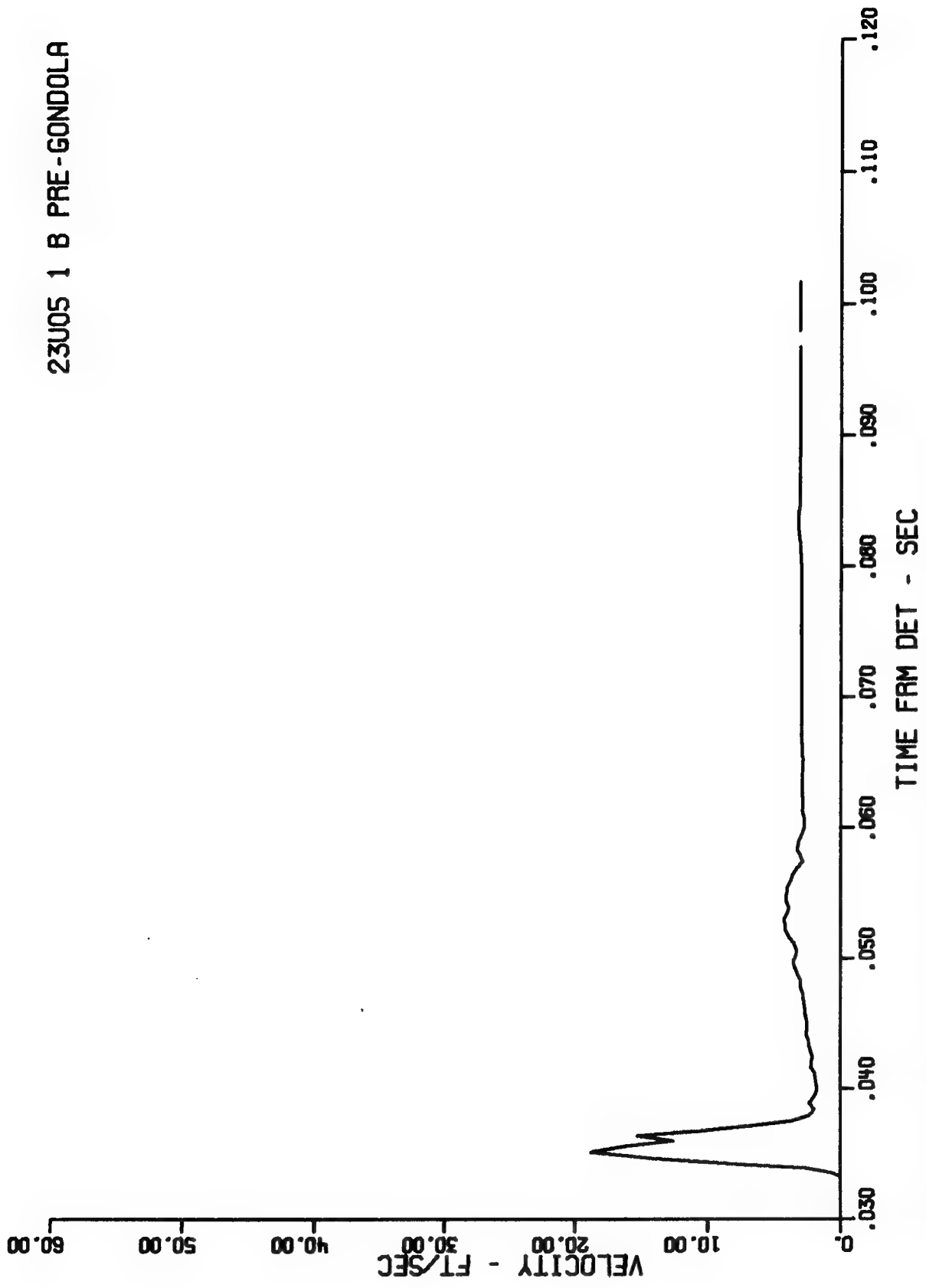
Figure A.16 Gage 23-u-5, range 225 ft, depth 46 ft, Event Bravo
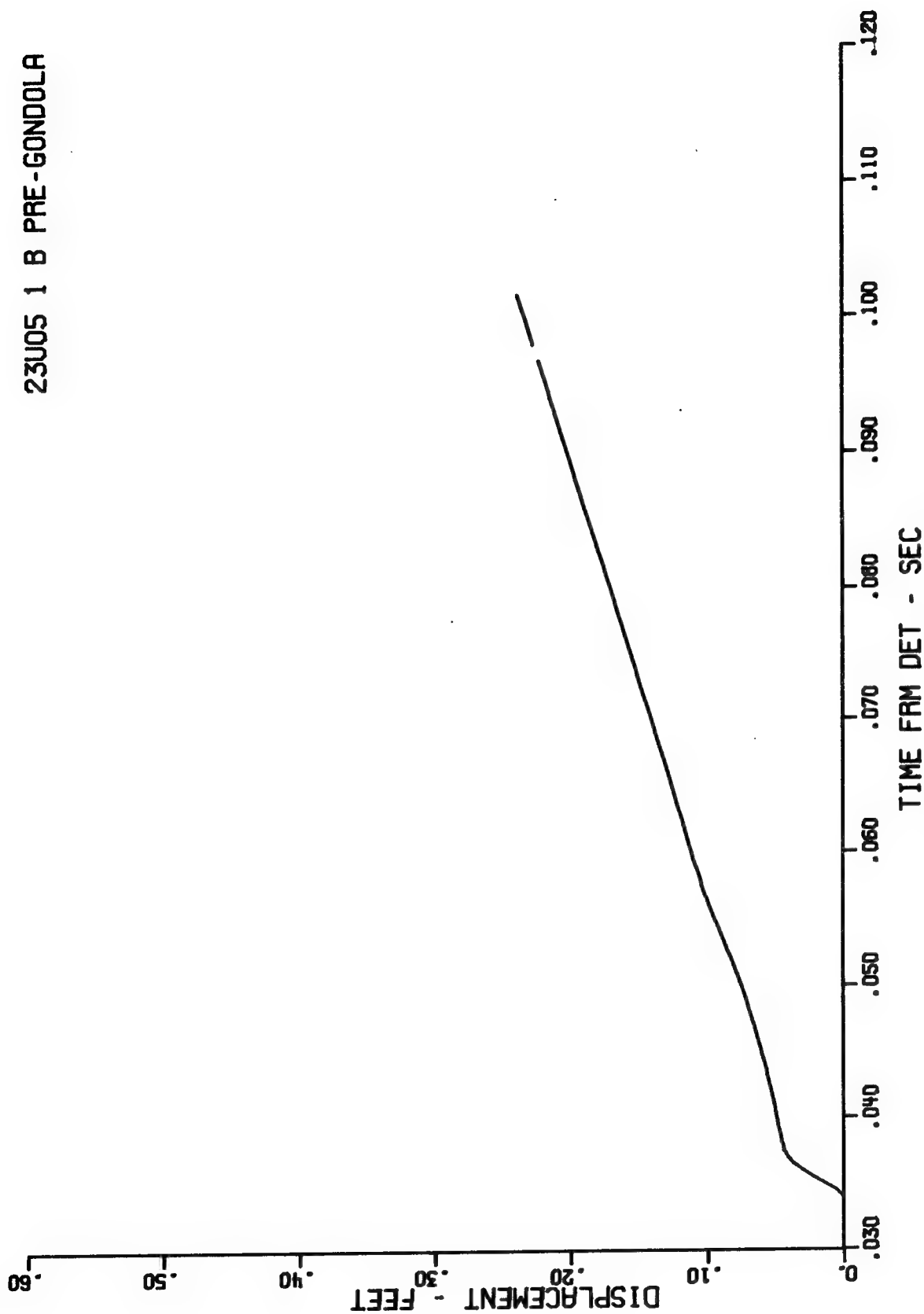
Figure A.17 First integral of Gage 23-u-5, range 225 ft, depth 46 ft, Event Bravo

68
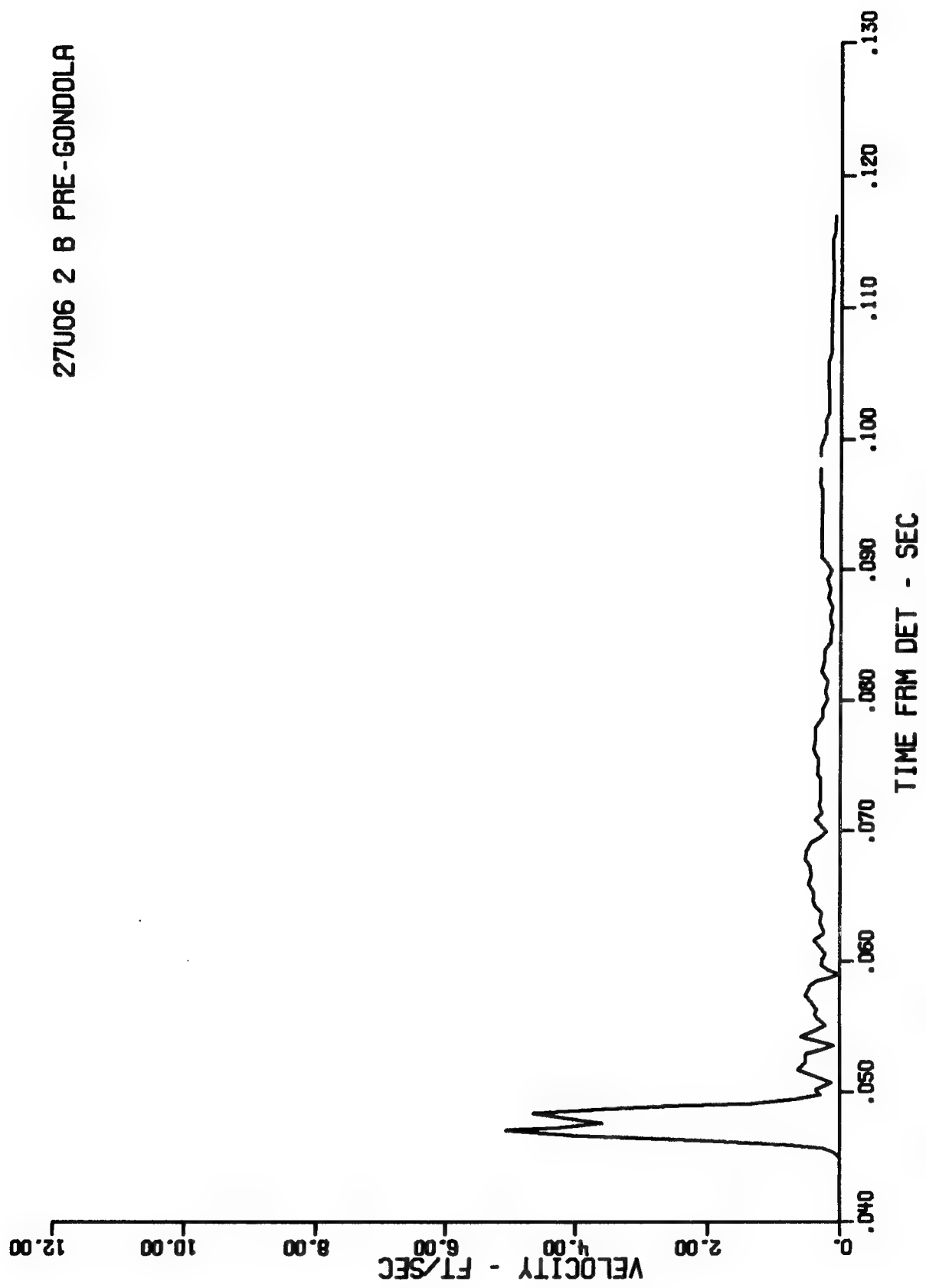
Figure A.18 Gage 27-u-6, range 300 ft, depth 46 ft, Event Bravo

27U06 2 B PRE-GONDOLA

TIME FRM DET - SEC

DISPLACEMENT - FEET
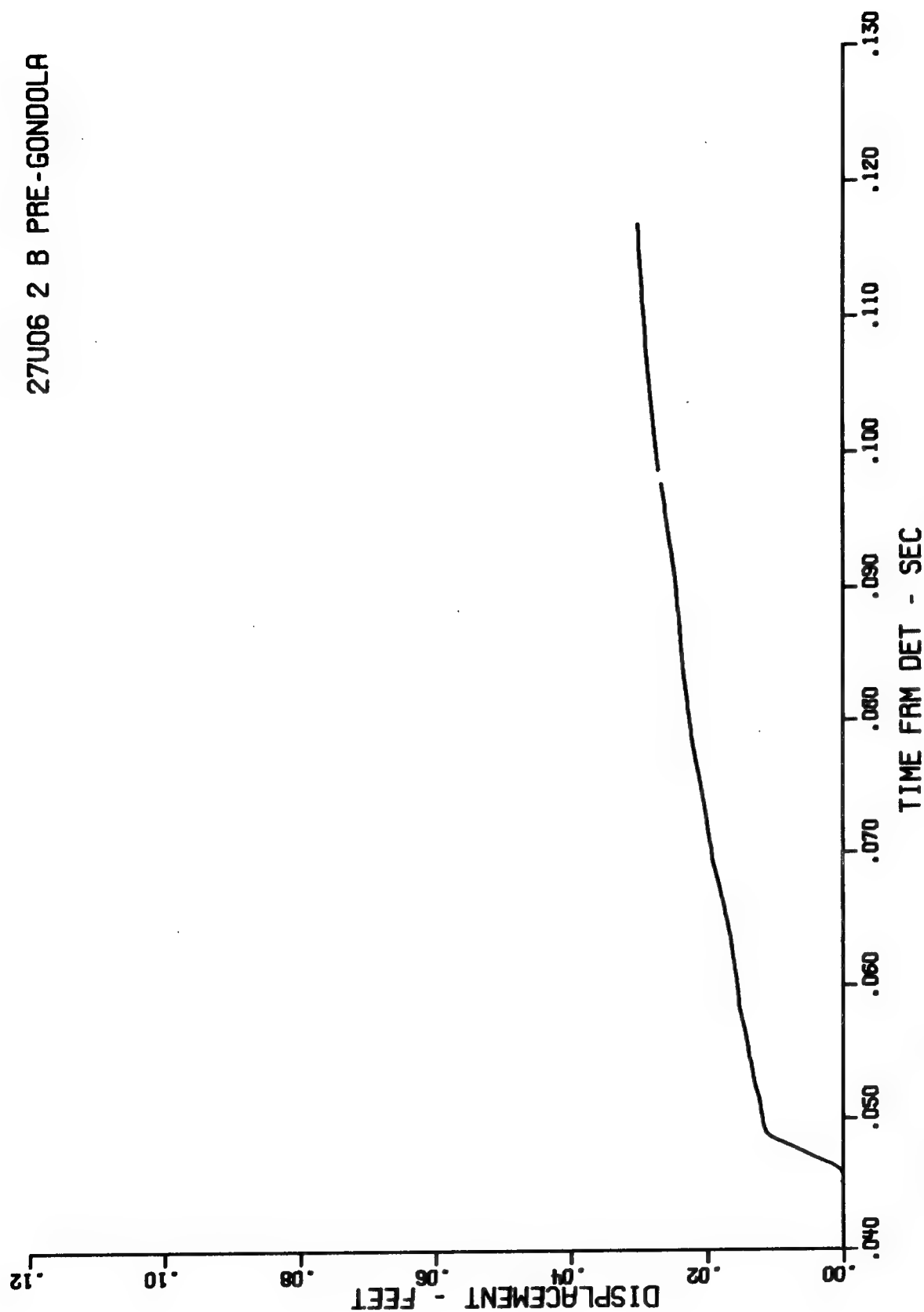
Figure A.19 First integral of Gage 27-u-6, range 300 ft, depth 46 ft, Event Bravo
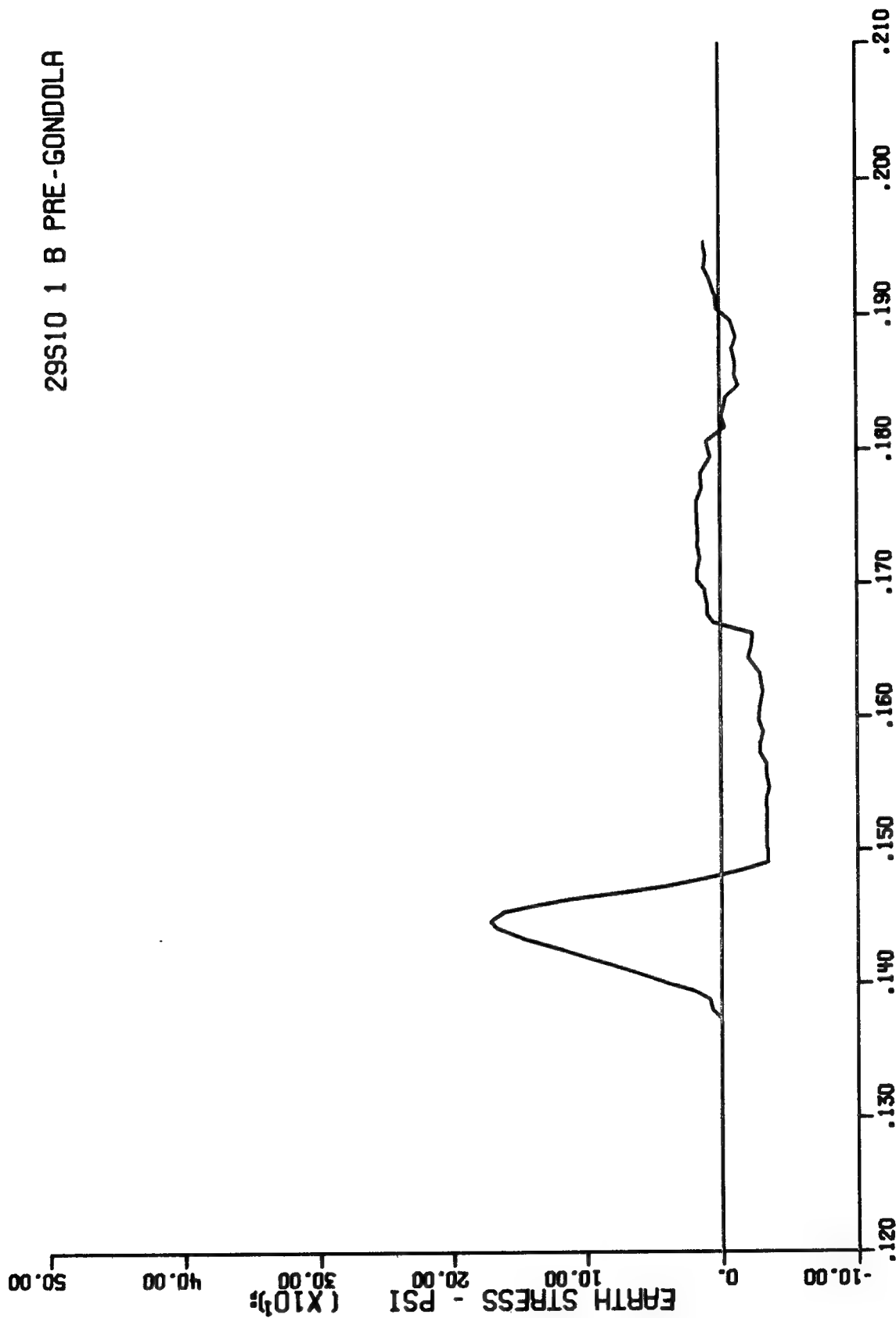
Figure A.20 Gage 29-σ-10, range 930 ft (Delta Site), depth 57 ft, Event Bravo

71
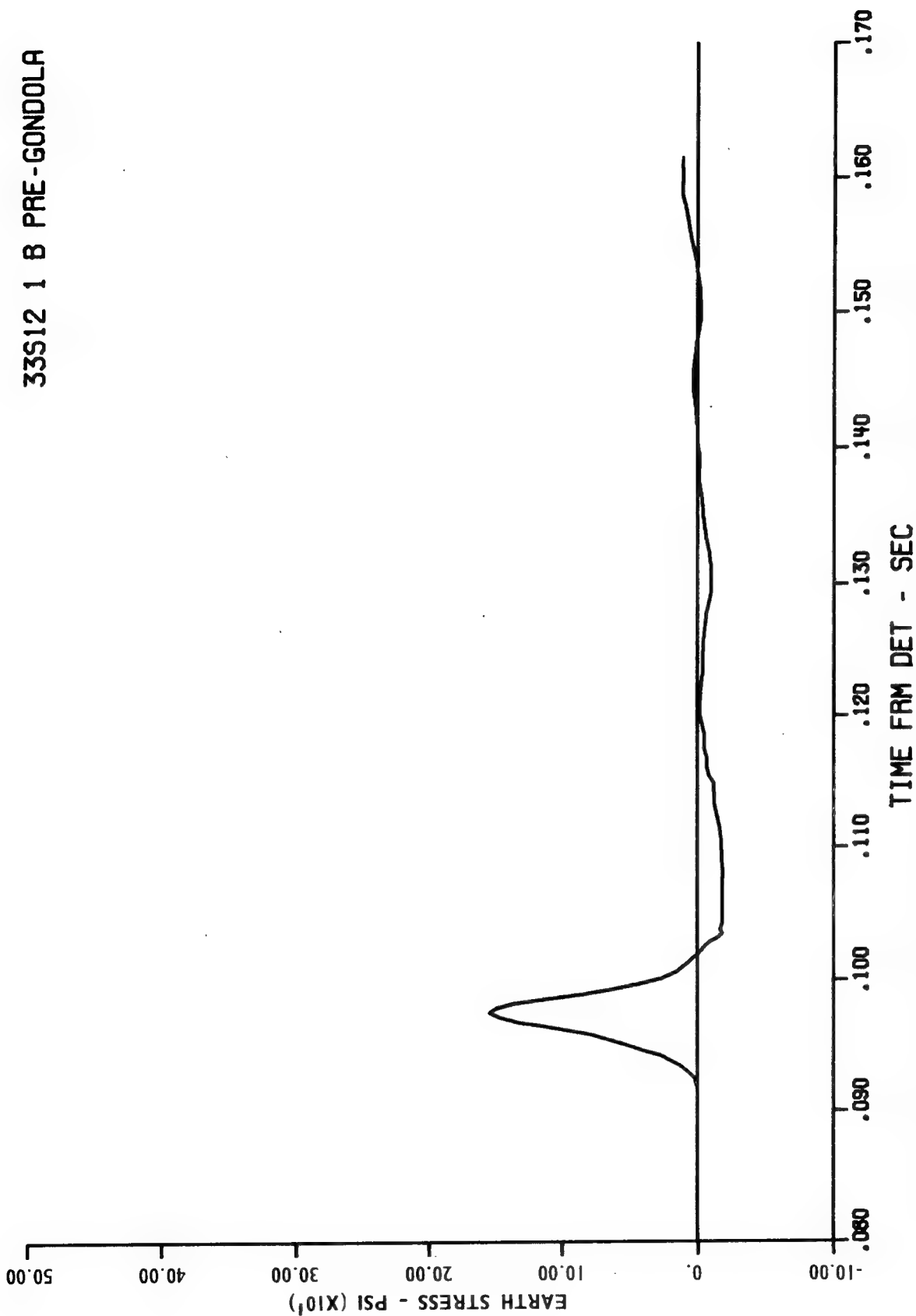
Figure A.21   Gage 33-σ-12, range 660 ft (Alfa Site), depth 52 ft, Event Bravo

34W03 2 B PRE-GONDOLA

WATER PRESSURE - PSI (X10¹)

TIME FRM DET - SEC
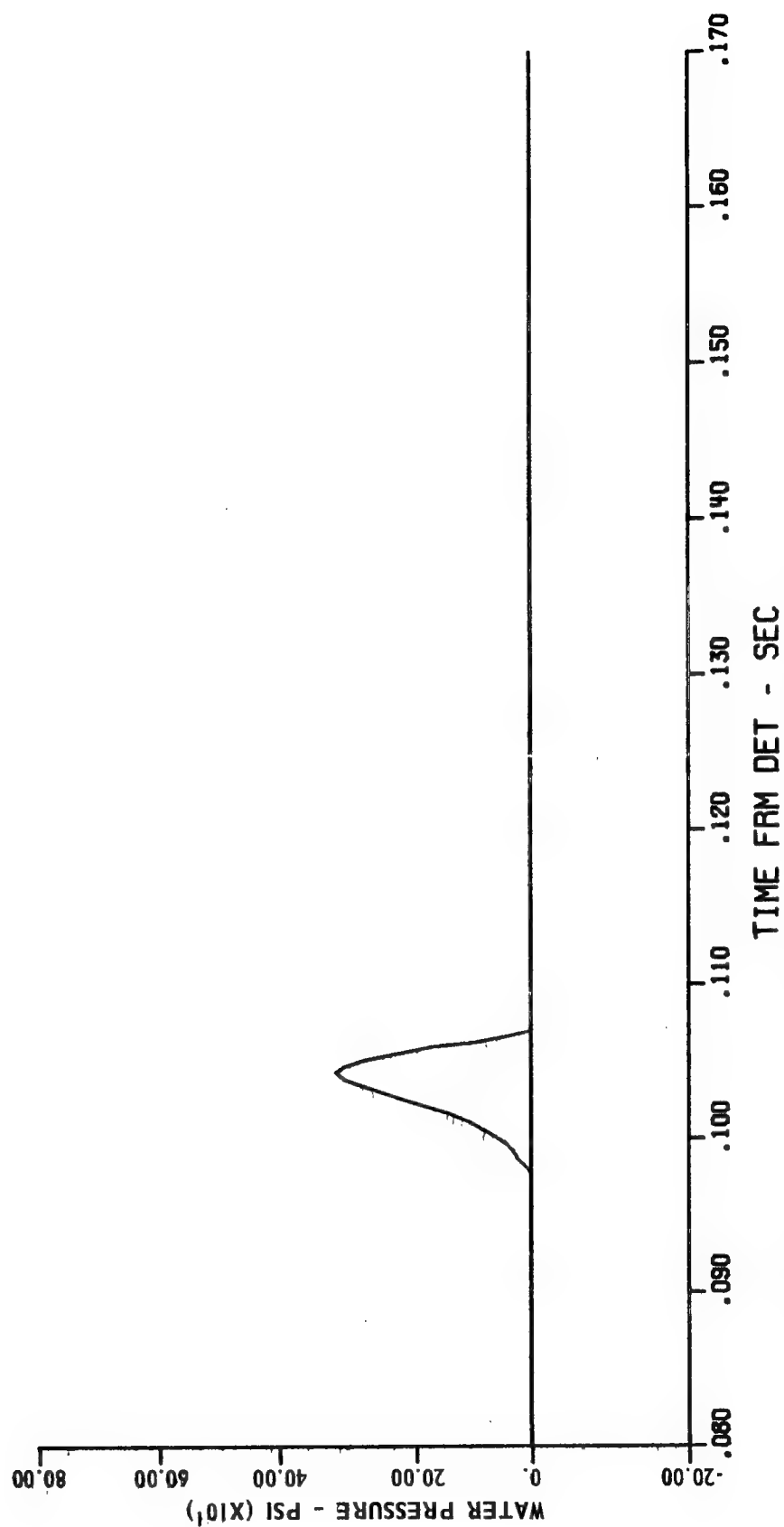
Figure A.22 Gage 34-ω-3, range 660 ft (Alfa Site), depth 52 ft, Event Bravo

73
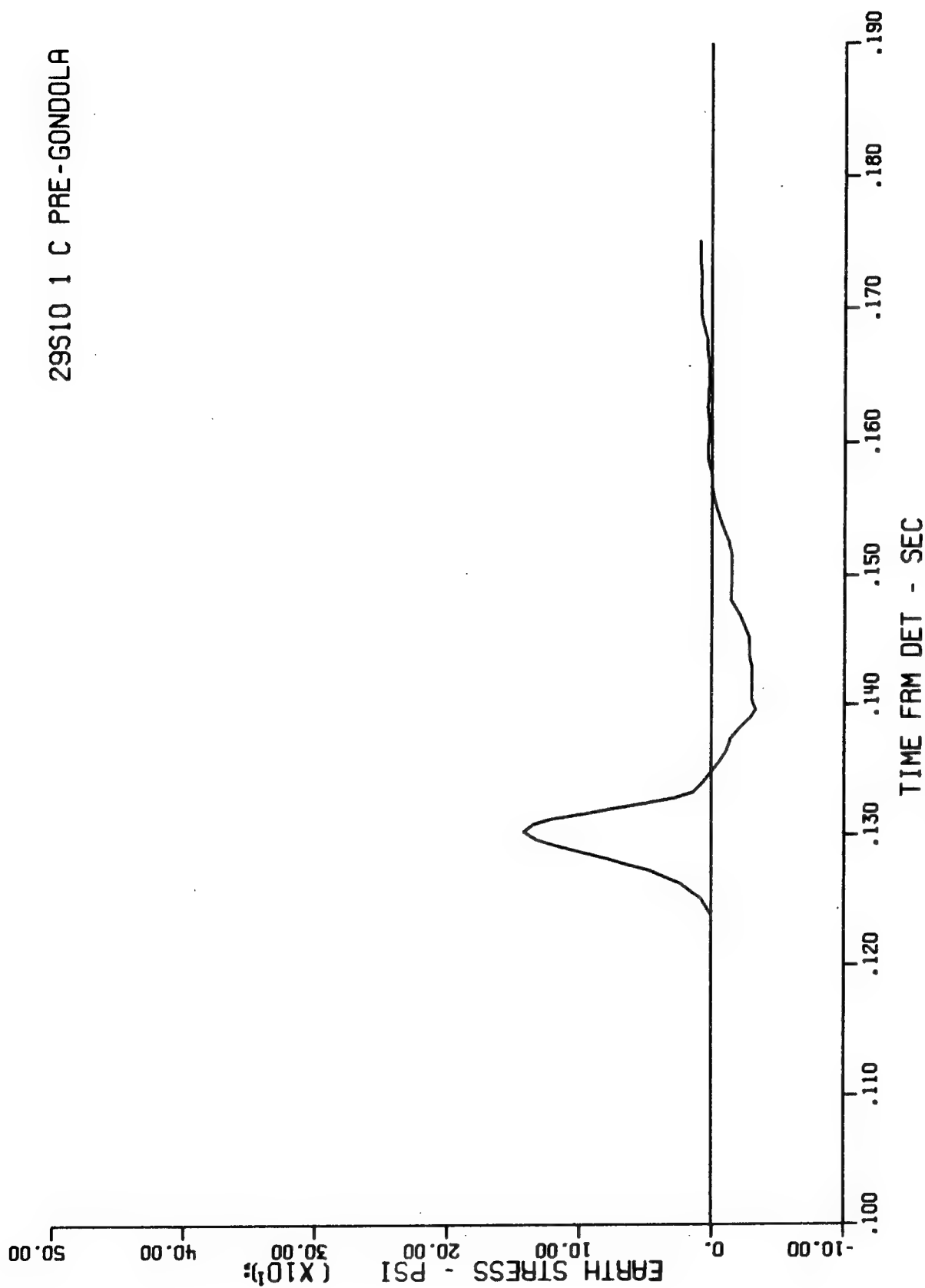
Figure A.23 Gage 2S-σ-10, range 770 ft (Delta Site), depth 57 ft, Event Charlie

74

30W01 1 C PRE-GONDOLA
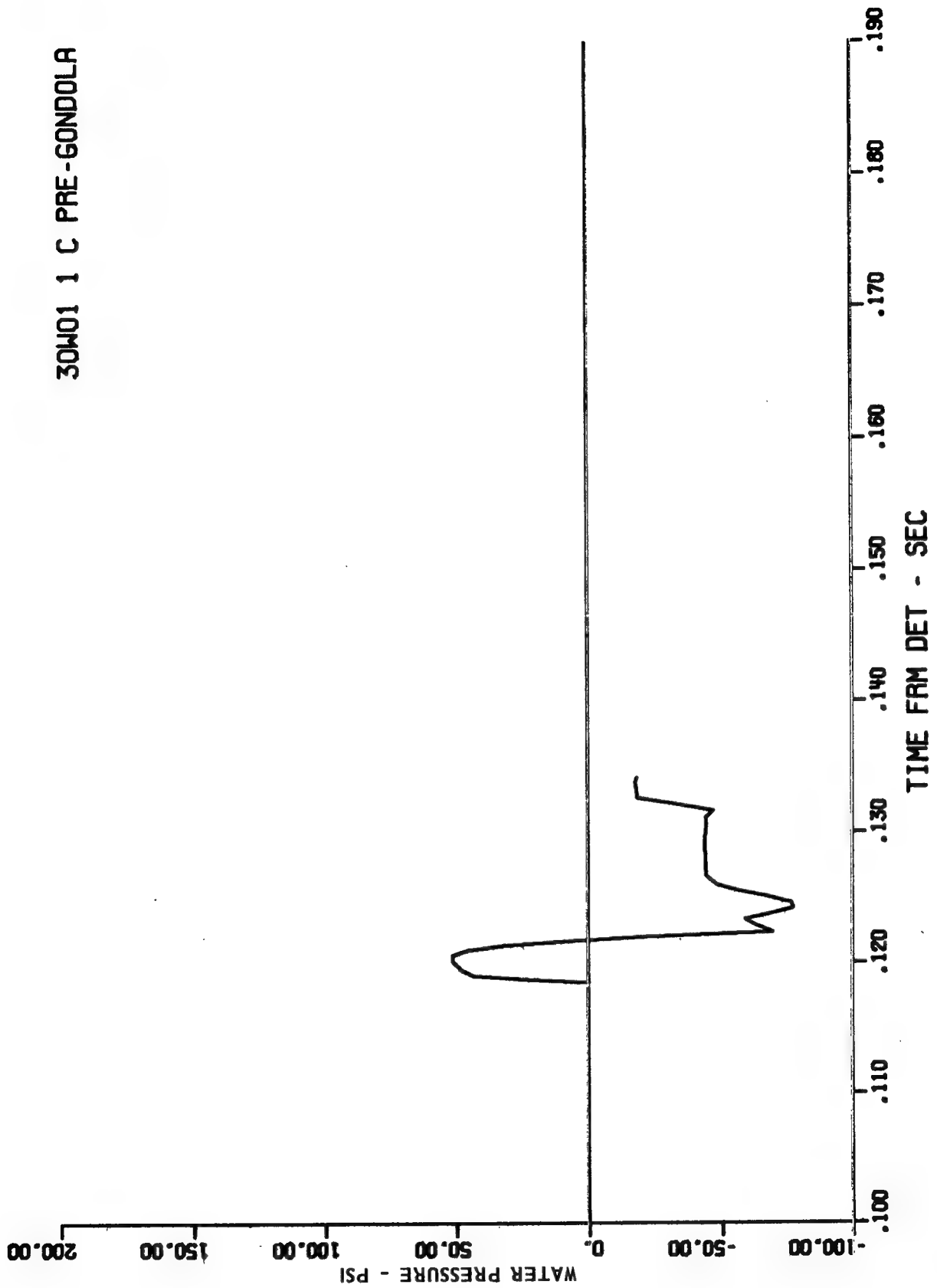
WATER PRESSURE - PSI

TIME FRM DET - SEC

Figure A.24 Gage 30-ω-1, range 770 ft (Delta Site), depth 57 ft, Event Charlie

75
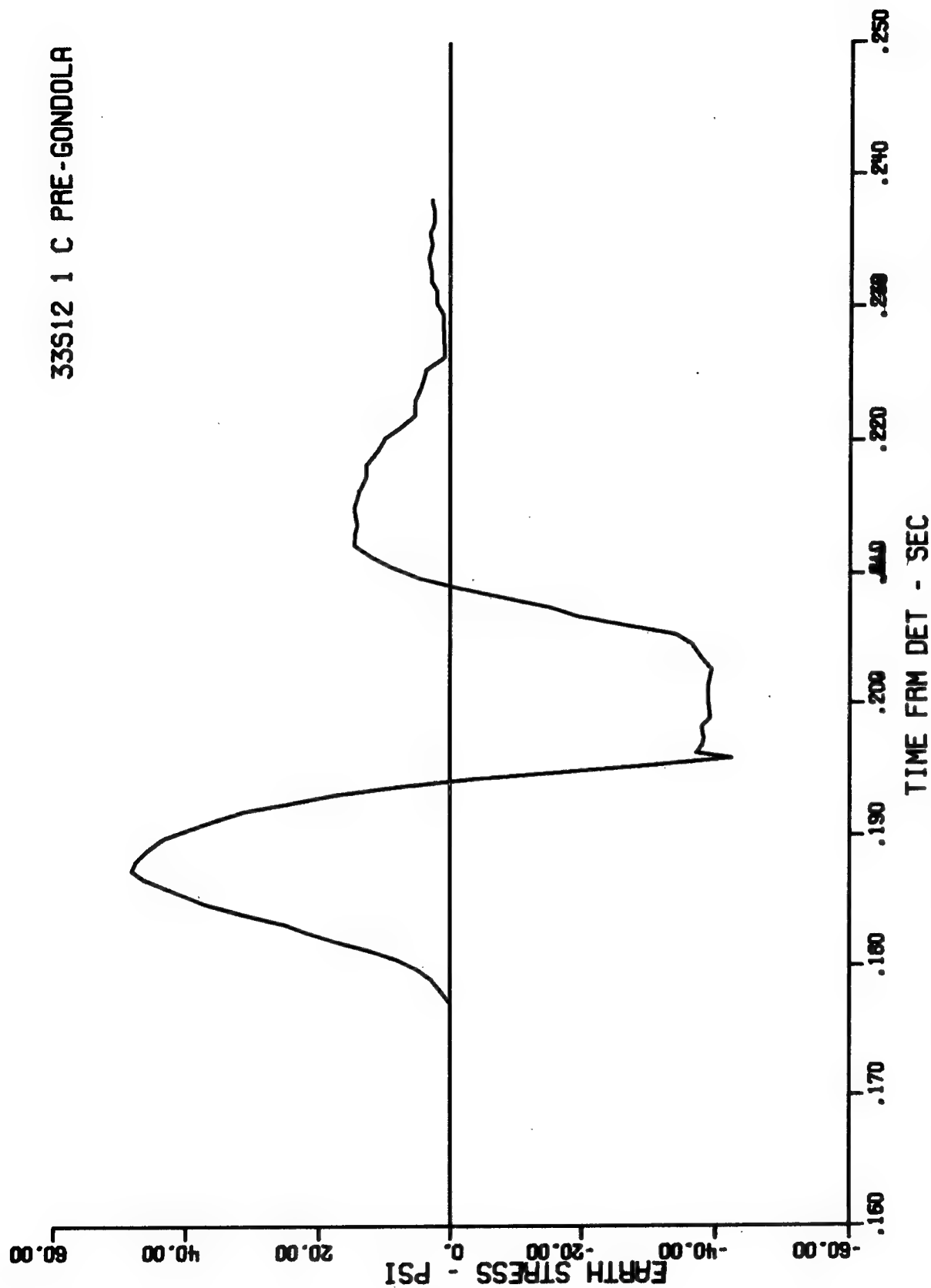
Figure A.25   Gage 33-σ-12, range 1210 ft (Alfa Site), depth 52 ft, Event Charlie
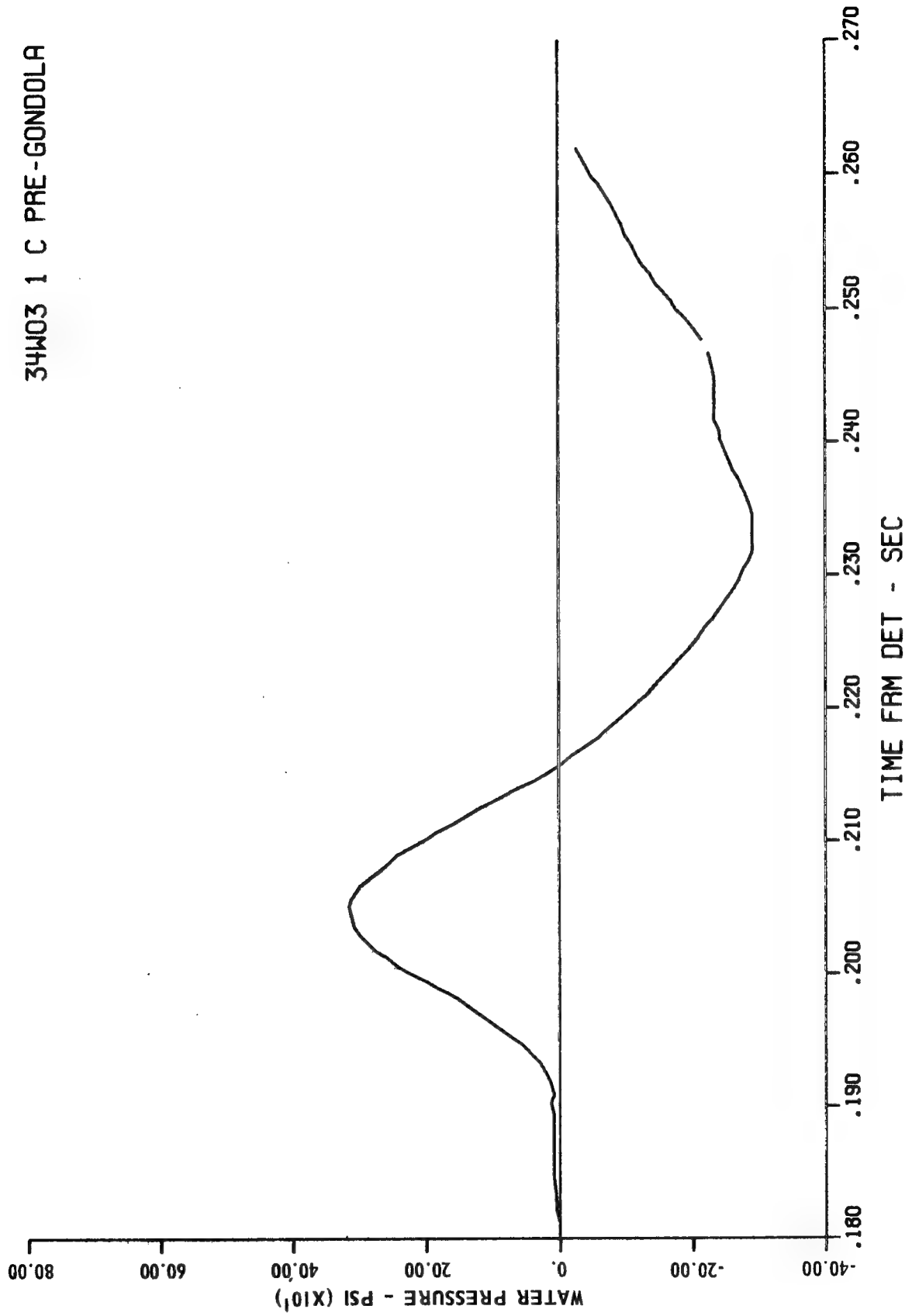
Figure A.26 Gage 34-ω-3, range 1210 ft (Alfa Site), depth 52 ft, Event Charlie

77
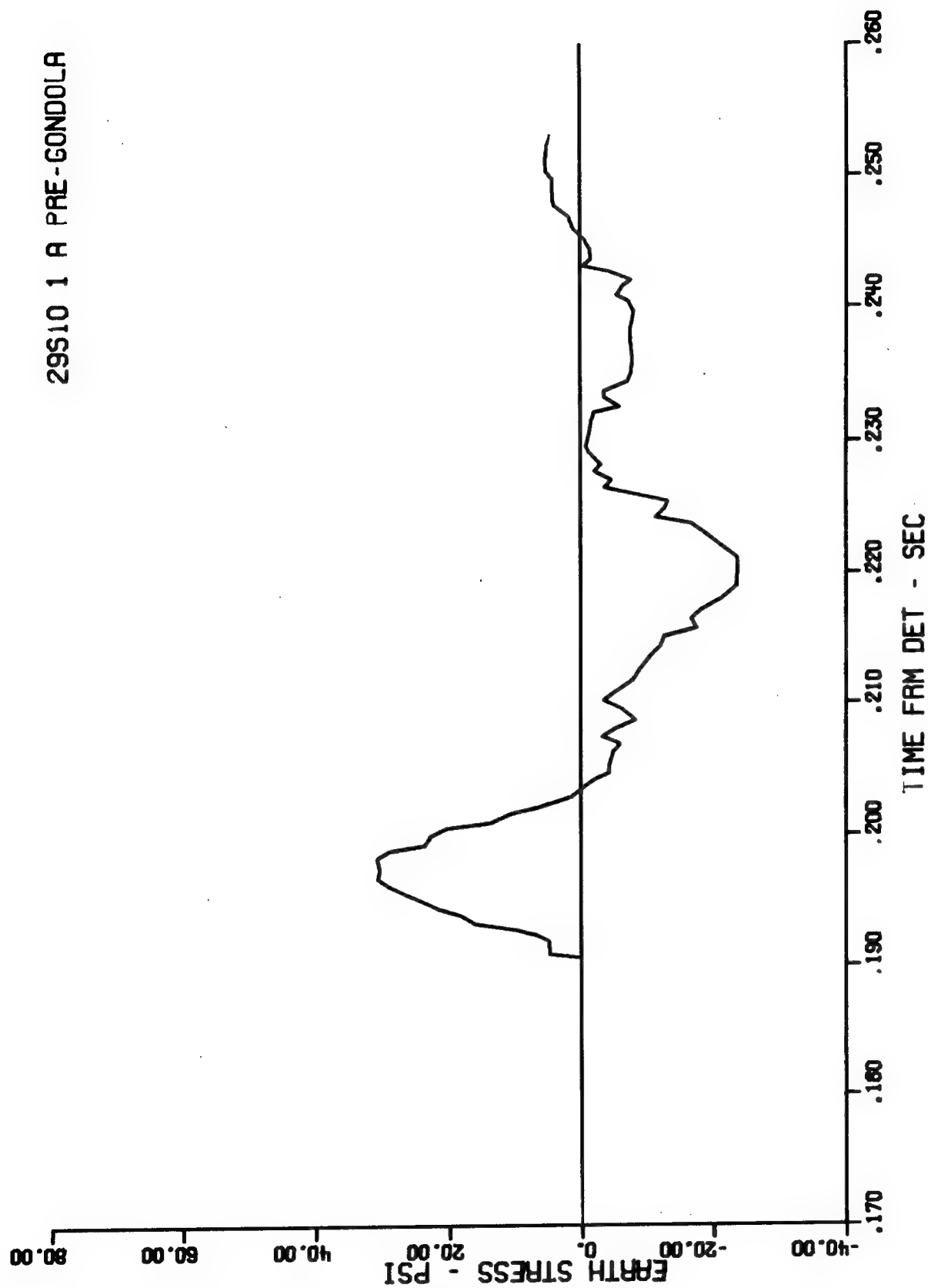
Figure A.27 Gage 29-σ-10, range 1570 ft (Delta Site), depth 57 ft, Event Alfa

78

APPENDIX B

INSTRUMENTATION CALIBRATION FOR GROUND MOTIONS
EARTH STRESS AND PORE PRESSURE MEASUREMENTS

PROJECT PRE-GONDOLA I

SEISMIC SITE CALIBRATION SERIES

L. F. Ingram and J. W. Snyder

U. S. Army Engineer Waterways Experiment Station
Vicksburg, Mississippi 39180

July 1967

ABSTRACT

Measurements were made during Event NCG/SC-2, a 1,000-lb

nitromethane (NM) explosion detonated at a depth of 15.7 ft in

a saturated clay-shale, to test various techniques for measuring

total stresses, pore water pressures, accelerations and velocities

and to predict motions and pressures for planned 20-ton NM shots

in the same material. Although set ranges and, in some cases,

gage capacities were exceeded for part of the measurements,

sufficient data were obtained to meet the test objectives.

In the region instrumented (slant ranges from 30 to 52 ft) a

short duration, intense stress pulse was propagated at a velocity

of 5,750 ft/sec. The amplitudes and durations were approximately

equal to those which would be expected at like distances in a free

water environment.

INTRODUCTION

OBJECTIVES

The objectives of this study were to obtain data with which to predict stresses, motions and pressures for a planned 20-ton shot and to test various instruments for this purpose.

BACKGROUND

The test plan[6] called for detonation of four individual 20-ton charges as well as row-charge and connecting row-charge experiments. The 20-ton tests are discussed in the main body of this report. Prior to these tests it was considered essential to conduct a 1,000-pound test series[7] to calibrate the site seismically and to provide a basis for design of the 20-ton experiments. This appendix describes the portion of the seismic calibration series concerned with measurement of earth stresses, pore pressure and earth motions in the region near the crater.

PROCEDURE

EXPERIMENTAL PLAN

Because of the funding and time limitations, it was decided to instrument only one of the four calibration shots; namely, NCG/SC-2, a 1,000-pound nitromethane sphere detonated at a depth of 15.7 feet in the saturated clay-shale. Reference 7 provides details of the site locations, terrain features, emplacement details, etc.

Figure B.1 shows the instrumentation layout for SC-2. Additional details of the instrumentation and layout are shown in Table B.1.

DESCRIPTION OF INSTRUMENTATION

An assortment of different gages was used in an attempt to make the desired measurements. For the most part, these gages were shelf items at the Waterways Experiment Station (WES) and were adapted for field use with hastily constructed mounts. Figure B.2 is a photograph of several of the measuring devices prior to installation in their mounts.

Total Stress Gage. These gages, which are designated "SE" gages, were designed and made by the WES primarily for use on Defense Atomic Support Agency (DASA)-sponsored weapon effects tests. They are being used extensively at WES for dynamic soil pressure measurements in various laboratory simulation devices as well as on HE field tests.

82

The gage is wafer-shaped, 2 inches in diameter and about 0.25 inch thick. It has two active symmetrical diaphragms 0.75 inch in diameter to which are bonded semiconductor strain gages. Two gages are bonded to each diaphragm such that, when the gage is assembled and the circuit completed, a 4-arm bridge circuit results. The gage is very stiff, has good sensitivity and frequency response, and is sufficiently rugged for field use. Reference 8 provides details of the gage construction as well as results of laboratory evaluation tests.

Pore Pressure Gages. All pore pressure gages consisted of sensors isolated from the solids in the soil and installed in a water-filled borehole. Because considerable uncertainty existed concerning the magnitude of peak and residual pore pressures that would occur, a wide variety of gages with different pressure ranges was utilized. Additional details of installation will be given for the various gages.

Referring to Table B.1 and Figure B.1 the various pore pressure gages are described below.

WES Transducer-Norwood. The Norwood[1] gage, designated NW, is

---

[1] Mention of brand or trade names does not imply endorsement of a particular product.

made by the Advance Technology Laboratory, a subsidiary of American Standard (plumbing fixture maker). The gage (shown on Figure B.2) employs a catenary diaphragm to seal the fluid from the electrical circuit and to apply the load to the end of a thin cylindrical tube. Strain-sensitive wires wrapped around the tube form a bridge circuit. These gages have been proven to be rugged and reliable for measuring blast pressures in the gaseous environments of the WES blast generators as well as in tunnel tests with gaseous explosives. These gages were used because of their wide response bandwidth--from zero frequency (static pressures) to several kiloHertz.

Piezoelectric Gages. The piezoelectric gages consisted of 1/4-inch diameter tourmaline gages made by Crystal Research, Inc., Cambridge, Massachusetts. This type of piezoelectric gage has been in general use for water shock measurements for over 25 years. They are excellent gages for dynamic pressure measurements; there have been no major changes or improvements in basic gage design in many years. These gages were used in this test in order to measure high-frequency, high-amplitude pressure pulses should they exist in the shale.

There are limitations in the use of these (as well as any other) piezoelectric gages for long term measurements. This is brought about by the fact that piezoelectric gages are high impedance, charge generating devices. In order to measure the charge,

an instrument must be connected to the gage (crystal) surfaces. This instrument must have a very high impedance to prevent the charge from leaking off too rapidly. Although very high impedance circuits are available, it is impossible to attain infinite impedance, so the gage can not hold a charge (assumed generated by a static load) indefinitely.

WES Transducer Piezometers. The WES transducer piezometers were designed and fabricated at WES. These devices incorporate CEC pressure transducers placed in a watertight brass housing. A thin porous bronze plate acts as a filter in front of the transducer. The CEC gages, both 250 and 2,000 psi capacity, were made by Consolidated Electrodynamics Corporation, Pasadena, California. These commercial gages use a flush diaphragm attached to an unbonded strain gage transducer. CEC makes a wide assortment of pressure transducers for general purpose usage. If adequately isolated from shock and acceleration, these gages will perform reliably.

U of A Piezometer. The U of A piezometer was designed and fabricated by the University of Alberta, Canada. Arrangements were made to borrow these instruments. Figure B.3 shows details of the instrument which consists of a Dynisco APT 25 pressure transducer isolated from the soil grains by a 1-inch long porous nickel plug. The Dynisco sensor is similar to the Norwood gage in design and performance. The sensor used in this instrument had a capacity of 300 psi.

USBR Piezometer. The USBR piezometer consisted of a standard
U. S. Bureau of Reclamation twin tube hydraulic device (Reference 10).
It includes a porous filter tip connected by two water-filled tubes
to Bourdon pressure gages. A high range (2,000 psi) Bourdon gage
with a check valve was used to record peak pressure. A lesser range
(300 psi) gage was also employed into line to record residual pore
pressures.

MOTION GAGES

The accelerometer, designated "AR1" was a 2,500 grams capacity
instrument made by Endevco Corporation of Pasadena, California. This
accelerometer used piezoresistive strain gages to sense motions of the
seismic mass. The circuit was a conventional 4-arm resistance bridge.

The velocity gages were purchased from Spartan Industries,
Albuquerque, New Mexico. These gages were designed by the Sandia
Laboratory and are designated "Model DX" by Sandia. The gage has an
inductive sensor. The operating principle is that of an overdamped
accelerometer. These instruments have been used routinely on
several explosion-produced ground motion studies. They have per-
formed reliably in environments more severe than encountered in the
Pre-Gondola test.

ELECTRONIC RECORDING EQUIPMENT

All electronic equipment was housed in a small shack located

about 1,000 feet from GZ. Individual 4-conductor Belden cables were used to connect all gages except the piezoelectric gages to the electronic equipment; coaxial cable was used on the PE gages.

Figure B.4 is a schematic diagram of the recording system. The Kistler charge amplifier has a high input impedance and was designed especially for use with piezoelectric gages. The SAM units were designed primarily for use with strain gage (resistance bridge) circuits. The system includes bridge excitation (D. C.) power supplies, range and balance controls, automatic calibration and wide-band amplification. These units have a bandwidth from 0 to 20,000 Hertz. The CEC carrier amplifier system provides 3 kiloHertz power to the transducers and is equipped with range and balance controls, calibration resistors, amplifier and demodulators. The bandwidth is flat from 0 to about 600 Hertz.

The oscillograph used three different types of light beam galvanometers with frequency response characteristics flat from 0 to 600, 0 to 1,000, and 0 to 2,500 Hertz. The record was obtained on 12-inch-wide photosensitive paper which was moving at a nominal speed of 160 in/sec at shot time. The recorder was started manually by the operator; synchronization was by voice countdown. A zero time fiducial pulse was provided from the NCG programmer.

GAGE CALIBRATIONS

All pressure gages were calibrated in the laboratory by

application of pressure to the gages. A pressure equivalent signal was obtained at this particular amplifier gain setting by shunting a calibration resistor across one arm of the bridge circuit. The calibration resistor was used in the field to simulate a known pressure step on the oscillograph record.

Similarly, electrical substitution calibrations were used with the motion gages. Physical calibrations for the accelerometer were applied with a centrifuge. Velocity gages were calibrated by allowing the seismic mass to fall through its stroke under the force of gravity. The slope of the resulting oscillograph trace is 32.2 ft/sec^2, thus a velocity calibration is obtained.

Several of the pore pressure gages were also checked under static conditions immediately after installation. These readings are summarized below:

Pore Pressure Gage No.	Indicated Pore Pressure at Tip, psi		
	20 June	21 June (9:00 A.M.)	21 June (2:00 P.M.)
P5	76.8	72.3	76.8
P6	9.4	9.2	9.4
P7	32.3	32.7	32.4
P8	--	11.3	12.1
P9	--	11.3	11.7

The actual total pore pressure at the piezometer tips due to the groundwater table was approximately 11 psi. Gages P5 and P7

indicated readings considerably in excess of the actual pressure. The excess pressures may have been caused by swelling of the grout seals above the sand filters. The lower temperature of the ground-water may also have affected the readings. On the other hand, readings of closer accuracy should not be expected for instruments with high range capacities.

FIELD OPERATIONS

Installation of the close-in instrumentation in the field was accomplished during the period 15 through 21 June 1966. The instruments were placed in drill holes, approximately 6 inches in diameter, which had been drilled by a crew from the Omaha District prior to the time instrument installation began. A mixture of bentonite and water had been placed in the holes to assist in keeping the walls of the borings from closing in, but this bentonite slurry was not completely successful in maintaining the seven instrument installation drill holes in a completely open condition. Several of the borings had squeezed closed to such an extent that the drill holes had to be reamed out or redrilled before any instruments could be placed in them. The types of instruments placed in each drill hole and the depth of placement are given in Table B.1.

Installation of Pore Pressure Gages. Prior to installing the devices, the drill holes were reamed and flushed with clean water

to insure that all bentonite "mud" was removed from the walls of the drill hole. The pore pressure gages were fastened to a length of 1-1/2-inch steel pipe, and the tip (without the filter disk installed) was placed in water to insure that all air was removed from the diaphragm cavity. Photographs of the WES transducer and U of A piezometers before placement in the drill holes are shown in Figure B.5. All filter disks for the transducer piezometers had been in deaired water for at least 24 hours prior to installation in the piezometer tips. The filter disks were placed in the piezometer housing under water, and the piezometer was placed in the water-filled drill hole, taking care to keep the tip of the piezometer in water at all times, and lowered to the bottom of the hole. Sand was then poured in the drill hole through the water to provide a pocket of 3 to 5 linear feet of filter. A grout mix, consisting of 94 pounds (1 bag) of Type I (high-early strength) Portland cement, 300 pounds sand, 11 pounds bentonite, and 140 pounds water, was then placed by 1-1/2-inch tremie pipe from the top of the sand to approximately 18 feet below ground surface. The remainder of the hole was backfilled with sand.

Installation of Total Stress, Accelerometer and Velocity Gages. The SE gages were lowered on a 1/4-inch-diameter pipe, oriented toward ground zero, and then grouted. The rest of the hole above

the gage was filled with grout, as described above for the pore pressure gages.

The accelerometer (AR1) and the velocity gages were also placed in a similar fashion and grouted in. Figure B.6 shows details of motion gage canisters as well as the Norwood and piezoelectric gage mounts.

Cables and Tubing. The cables and plastic tubing from the USBR gages were placed in a 1-foot deep trench. A 4-foot deep trench had been planned but time and equipment limitations precluded this depth. Part of the trench was backfilled with sand, the remainder with native soil. The cables as previously noted were brought to the recording equipment about 1,000 feet from SGZ. The plastic tubing from the USBR gages was run to a gage board and valve control center located in a pit 4- by 4- by 2-1/2-feet deep located approximately 100 feet from SGZ.

RESULTS

INSTRUMENT PERFORMANCE

All gages survived the installation and were operative at shot time. All cables were broken by a large chunk of debris which impacted the cable trench a few seconds postshot about 150 feet from GZ. Further checking from the break showed all instruments except VR2 and P7 inoperative. It was not possible to determine whether these were gage or cable failures; however, it was learned later from recovered pore pressure gages P5 and P6 that these gage diaphragms had failed from overload (see Figures B.7 and B.8).

No readings could be made of the USBR pore pressure gages inasmuch as a large piece of ejecta fell adjacent to the pit containing the gage board, completely rupturing the plastic tubing (see Figure B.8b).

Figure B.9 is a reproduction of the oscillogram with superposed scale factors. It is immediately obvious that there were intense short pulses, overranged gages and relatively early cable failures. However, considerable information can be gleaned from the record.

Table B.2 presents a tabulation of arrival times and peak values scaled from the traces. From the arrival times, which are plotted in Figure B.10, it is seen that the wave velocity through

92

the blast line was 5,750 ft/sec and, as can best be determined within the scatter of data points, the velocity was constant over this distance. The average wave velocities (computed from slant distance divided by arrival time) are much higher than the 5,750 ft/sec velocity through the gaged zone shown in Figure A.10. This indicates that a much higher propagation velocity existed close-in to the point of detonation.

Of the peak values presented in Table B.2, four values (P1, VR2, SE2, and P7) were read from well-defined peaks. The peak from VR1 only slightly overshot the paper and was estimated with fair confidence. The remaining values were estimated by judgment and extrapolation of slopes of the traces that were discernible. Although admittedly crude, the values thus obtained are of value for prediction purposes.

All the pressure points except those from P7 were plotted on Figure B.11 in order to arrive at a prediction curve. Although P5 failed to produce a time history, a point at 4,000 psi was plotted for this location based upon the manufacturer's information that the gage would be damaged at twice its rated pressure. It is reasonable that this gage was subjected to at least 3,000 psi as manifested by the dished-in diaphragm. The measurement from P7 was omitted because of its obviously low value; this is attributed to the filtering action of the porous tip of the piezometer.

In addition to the measured pressure points, Figure B.11 shows two pressure points computed from the velocity peak values using the relation $\sigma = \rho u c$ where:

σ = stress

ρ = mass density

u = particle velocity

c = wave propagation velocity

The accelerometer trace excursion far exceeded set range (1,000 grams) and no measurement was obtained other than arrival time. A crude approximation of peak accelerations was obtained by differentiation of the initial rise of the velocity traces. This procedure is fraught with uncertainty and error and was done merely to get a ballpark estimate of the accelerations. Based upon this method it is estimated that the peak horizontal acceleration exceeded 3,000 grams. The accelerometer was rated at 2,500 grams.

The velocity measurements are considered to be fairly reliable. The traces from VR1 and VR2 were integrated numerically to produce displacement time plots. These results are shown in Figures B.12 and B.13, respectively.

DISCUSSION OF RESULTS

Early Motions and Stresses. Early motions and stresses are those measured within the first few seconds of the blast. Large

amplitudes of motions, pressures and stresses during this time indicate good coupling to the wet material. The pressure (and stress) histories closely resemble water shock waves both in amplitude and duration. Because of the paucity of the data and the small space interval instrumented, it is not possible to infer the rate of attenuation of peak pressures with distance. The grouping of points (in Figure B.11) at slant ranges between 30 and 50 feet suggest that peaks were nearly equal to water shock values to be expected at the same distance in an unbounded mass of water.

Stress and particle velocity attenuate with distance R as R^{-2} to R^{-3} in typical earth materials ranging from desert alluvium to basalt and halite. Theoretical attenuation for elastic materials (which would include water) would be as R^{-1} ; empirically, at close ranges the exponent is slightly greater than unity. Thus, in drier earth materials the attenuation of stress with distance is much faster than in water.

If the saturated clay-shale is in fact capable of transmitting shocks (as seems to be the case for this test) there is another effect which would tend to reduce the pressure, distance and impulse as the range increases. This is the "surface cutoff" effect which is explained as follows. The first perturbation to reach a gage located in an isotropic medium takes the straight line path from the source. For gages located at distances relatively remote from

the source (compared to depth of burial or immersion) a second perturbation arrives later (having taken the ray path with equal angles of incidence and reflection at the surface) as a rarefaction wave. This tensile wave results from reflection of the compression wave at the ground-air or water-air interface. Depending on the geometry, the material properties and the pulse duration (related to weapon yield), there will be locations at which the surface rarefaction will tend to cancel or "cutoff" the positive impulse of the primary compression wave.

The significance of the above discussion is the inference that the surface effect might provide an attenuation mechanism which we cannot evaluate with our meager results.

The apparent predominance of the shock transmission accounts for the extreme particle acceleration sensed by our lone accelerometer. Accelerations are extremely sensitive to rise time of the stress pulse; for a discontinuity the acceleration is infinite. In reality, the gage inertia and finite time for the wave to engulf the gage make measurement of infinite acceleration impossible. Fortunately, velocities are not dependent upon acceleration amplitudes alone but the time integral of acceleration.

With regard to "pore pressures" it is suspected that the peak pressure should be equal or very close to the peak total stress (fluid plus mineral phases) in a saturated media. The observational

96

data did not permit a direct comparison of peak total stress and peak pore pressure.

Gage P7 survived for a relatively long time. The trace from P7 has been replotted in Figure B.14 with a compressed time scale. The trace shows a decrease in pressure over that registered prior to the explosion following the buildup at the time of the explosion. The low amplitudes measured by the P7 gage are attributed to the effectiveness of the porous tip in filtering the high amplitude peak. It is suspected that the oscillations and low amplitudes were caused by air which might have been entrapped in the filter.

Both total stress gages (SE1 and SE2) indicated a net positive residual stress on the order of 250 psi following the initial pulse. These levels held relatively constant for roughly 35 msec until the cables failed. All evidence indicates that the apparent residual pressures were not real in that the gage diaphragms likely yielded and suffered some plastic deformation. This statement is based on results of computations of yield stress for the diaphragm and on subsequent laboratory tests of a gage under static load.

The fact that the only two downhole cables to survive were 50 feet from SGZ might be of some value in the estimation of the limits of the rupture zone.

Residual Pore Pressures. It had been planned to take static postshot readings of the residual, total and pore water stresses

97

with a strain indicator; however, this could not be accomplished because of the cable breaks except in the case of pore pressure gage P7. This gage indicated a total pressure at the tip of 3.0 psi 6.5 hours after the shot; 25 hours after the shot the observed pressure had increased to 3.9 psi. These readings indicate a substantial reduction from the preshot pressure of 32.4 psi and indicates the development of a negative pore pressure as a result of the blast. Negative pore pressures reflect a tendency for the soils adjacent to the crater to dilate as a result of shearing forces. Although sufficient data are not available to predict accurately the time at which equalization of pore pressures will occur, it is estimated to be in the order of several months.

Participation in the SC-2 Event provided data which were extremely valuable for planning similar measurements on Shot Bravo. Although all instruments did not produce usable data, the test objectives were met in that we now have considerable experience and knowledge in making future measurements on Bravo.

CONCLUSIONS

An intense, short duration pressure pulse was transmitted through the saturated clay-shale at slant ranges from 30 to 50 feet from the explosion of 1,000 pounds of nitromethane. The propagation velocity of this disturbance was 5,750 ft/sec and constant over the distance interval. This velocity corresponds closely with the value of 5,700 ft/sec determined by seismic refraction survey[9] performed by R. Ballard of WES.

Although several pressure transducers were overranged and recording channel set ranges were exceeded, sufficient observations were made to estimate peak values for purposes of predicting response on planned Shot Bravo of Pre-Gondola I. The sole surviving pore pressure gage indicated a reduction in the pore pressure level existing prior to the event.

The intensity and steepness of the pressure front caused high accelerations. Particle velocities are also much higher than would be expected in other earth materials.

In retrospect, it is apparent that predictions were too low and in some instances the instrumentation limited the results. The requirements to make measurements in this environment are stringent. The gages are required to survive the intense accelerations and pressures in order to obtain residual measurements in the potential

zone of slope failures. This region, which is just outside the true crater, undergoes large motions as well as fractures. The protection of downhole cables in this region is critical, especially if long term measurements are needed. There are no certain ways of assuring instrument survival in this environment.

RECOMMENDATIONS

The following recommendations are made as a result of this experiment:

1. Total stress and peak pore pressures for Shot Bravo should be predicted using the free water values shown in Figure B.11. Although it is suspected that these peak parameters will attenuate (with distance) at a faster rate than indicated (see estimated curve), the prudent approach is to use the free water values to set instrument ranges. This is especially true at the same scaled distances as were instrumented on SC-2. There is no reason to believe that cube root scaling will not apply for prediction of stresses, pressures and velocities.

2. Figure B.15 should be used to range the velocity instruments.

3. Horizontal cable runs should be placed in a 4-foot deep covered trench to protect against debris. This is a requirement for postshot, relatively long term observations; such precautions are not needed solely for transient measurements.

4. Downhole cables should be protected by placing them inside pipes or rigid plastic tubing. This will lessen shear type failures in the grouted boreholes and will increase the chances of survival in the heavily fractured zone near the true crater limit.

5. The maximum pressure at which the WES SE gages should be used is at least 1,800 psi. If stress measurements are required at closer ranges (than at this stress level) it will be necessary to use different instruments; piezoelectric gages are recommended for these transient measurements. If residual stresses at these levels are required it will be necessary to locate or design a new gage. Gage survivability in this region tends to discourage attempting these measurements.

6. Gages used to measure residual pore pressure should be rugged enough to withstand the initial shock and yet sensitive enough to measure the low level residual pressures (assumed to be a small fraction of the transient peak). If a gage sufficiently stiff to survive the transient pulse were used it would be neces- sary to provide variable, high gain amplification to record the residual pressure. Another approach, which is recommended, is to use a relatively sensitive pressure transducer in conjunction with a porous filter capable of rejecting the transient. Sensors capable of measuring negative pore pressures should be employed.

7. Hydraulic pore pressure devices for measuring residual pore pressures should be employed no closer than 3 crater radii from SGZ with the gages and control panels provided with suitable protection against falling debris.

8. All transient measurements should be recorded on magnetic

tape as the primary system with backup on light beam galvanometers. For the Bravo shot the pulse durations should be about three times as long as for the 1,000-pound shots. Wide-band FM with a flat bandwidth from 0 to 20 kiloHertz should be adequate. It is also recommended that parallel recording of at least one channel (preferably one of the piezoelectric gages located in a water-filled charge container) be monitored on a cathode-ray oscilloscope equipped with sweep delay capability.

TABLE B.1 GAGE TYPE AND LOCATION

Gage No.	Type	Sensor	Nominal Capacity	Hole No. SC-2	Distance from W.P. Horizontal feet	Distance from W.P. Slant feet	Tip Elevation ft-msl	Depth Below Surface feet	Depth Below GWL[a] feet
Accelerometers:									
AR1	Endevco	--	2,500 g	a	30.0	30.0	2,226.7	15.7	12.3
Velocity Gages:									
VR1	Sandia DX	--	200 fps	b	35.0	35.0	2,226.7	15.7	12.3
VR2	Sandia DX	--	200 fps	e	50.0	50.0	2,226.9	15.7	12.1
Total Stress Gages:									
SE1	WES SE	--	1,800 psi	b	35.0	35.3	2,222.4	20.0	16.6
SE2	WES SE	--	1,800 psi	d	45.0	45.5	2,221.4	21.3	17.6
Pore Pressure Gages:									
P1	Piezoelectric	Tourmaline	30,000 psi	a	30.0	33.2	2,212.4	30.0	26.6
P2	WES transducer	Norwood	1,000 psi	a	30.0	33.2	2,212.4	30.0	26.6
P3	Piezoelectric	Tourmaline	30,000 psi	c	40.0	42.6	2,212.4	30.0	26.6
P4	WES transducer	Norwood	1,000 psi	c	40.0	42.6	2,212.4	30.0	26.6
P5	WES transducer	CEC	2,000 psi	f	40.0	42.6	2,214.9	27.5	24.1
P6	WES transducer	CEC	250 psi	d	45.0	47.2	2,215.2	27.5	23.8
P7	U of A transducer	Dynisco	300 psi	g	50.0	52.1	2,212.2	30.2	26.8
P8	USBR hydraulic	Bourdon tube	2,000 psi	e	40.0	42.6	2,213.0	29.6	26.0
P9	USBR hydraulic	Bourdon tube	2,000 psi	f	50.0	52.1	2,213.1	29.5	25.9

a Based on GWL at elevation 2,239.0.

TABLE B.2 RESULTS

Hole	Gage Designation	Slant Range	Arrival Time	Duration of First Peak	Peak Value	Remarks
		feet	msec	msec		
a	AR1	30.0	4.10	--	None	Off-scale
a	P2	33.2	4.78	--	None	Off-scale
a	P1	33.2	4.78	2.0	4,750 psi	--
b	VR1	35.0	5.09	--	21.8 ft/sec	Cable broke at 41.5 msec
b	SE1	35.3	4.97	2.0	3,600 psi	Estimated
c	P4	42.6	6.14	--	--	Overranged
c	P3	42.6	6.14	2.1	3,120 psi	Peak estimated
d	SE2	45.5	6.37	2.0	3,700 psi	Probably overranged
d	P6	47.2	7.05	--	--	Overranged gage
e	VR2	50.0	7.66	--	10.2 ft/sec	--
f	P5	42.6	6.31	--	--	Overranged gage
g	P7	52.1	7.97	--	39 psi	Highly filtered

HOLE NOS.

PLAN
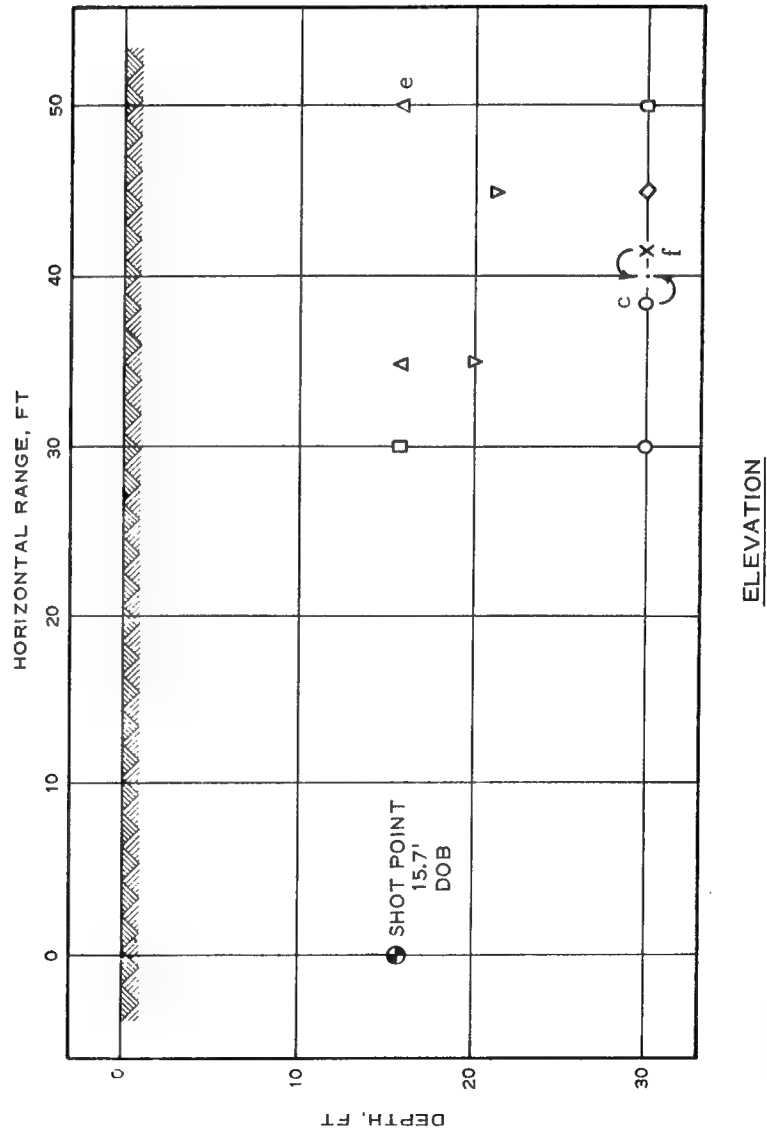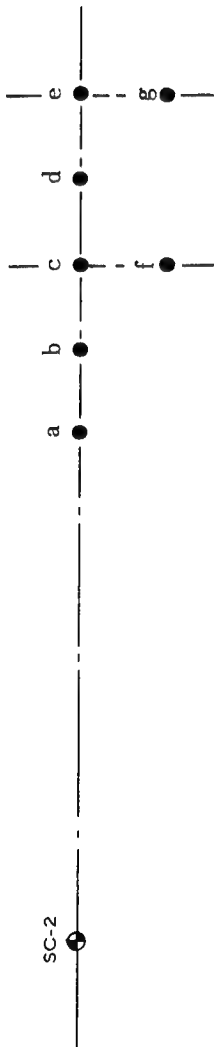
LEGEND

□ ACCELERATION AND PORE PRESSURE
○ PE AND NORWOOD GAGE
✕ CEC AND USBR
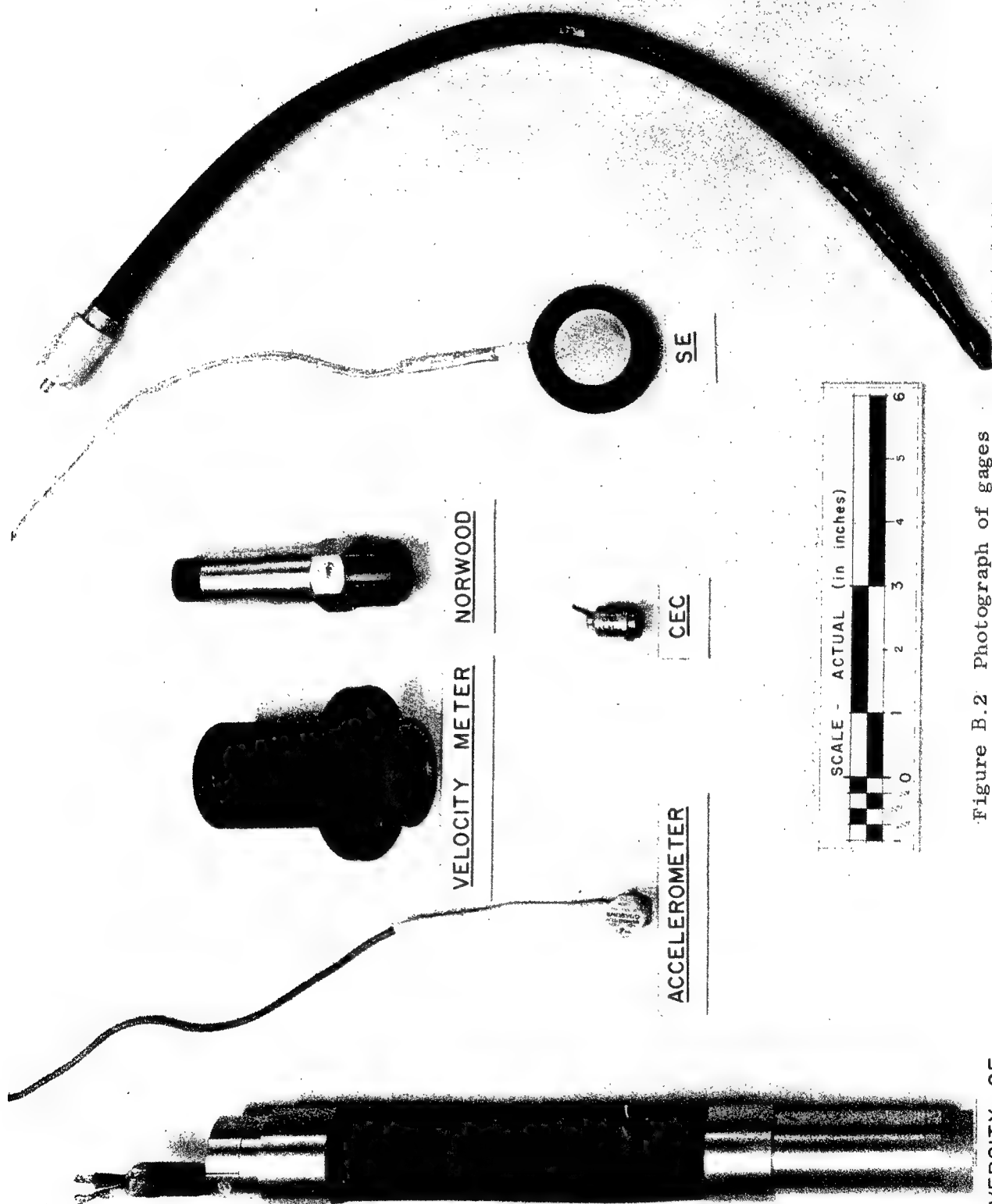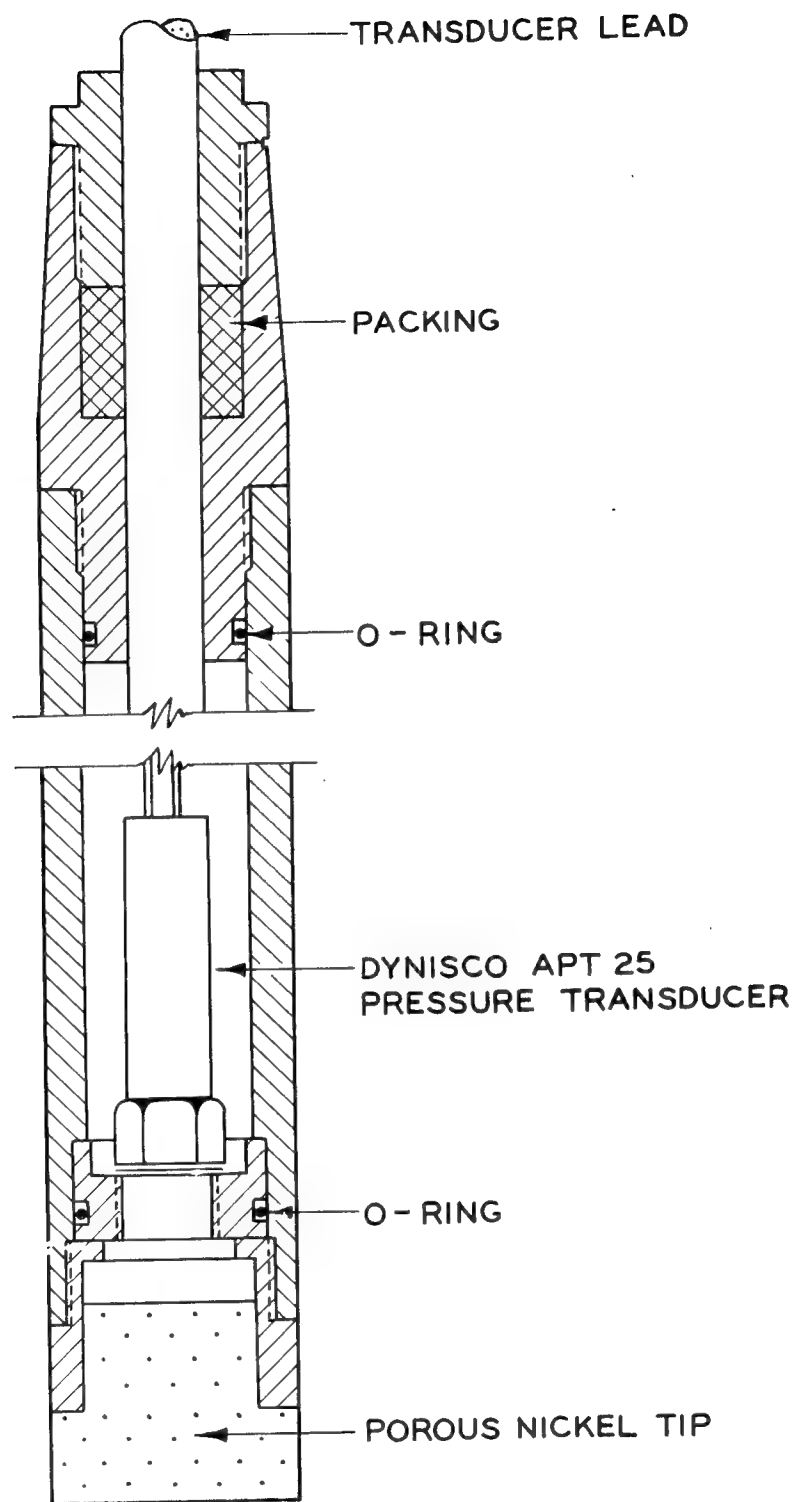◇ CEC
◲ U OF A USBR
△ PARTICLE VELOCITY
▽ TOTAL STRESS

HORIZONTAL RANGE, FT

SHOT POINT
15.7'
DOB

DEPTH, FT

ELEVATION

Figure B.1 Gage layout

Figure B.2 Photograph of gages

WATER SHOCK

SE

NORWOOD

CEC

VELOCITY METER

ACCELEROMETER

SCALE - ACTUAL (in inches)

UNIVERSITY OF
ALBERTA

107

TRANSDUCER LEAD

PACKING

O – RING

DYNISCO APT 25
PRESSURE TRANSDUCER

O – RING

POROUS NICKEL TIP

UNIVERSITY OF
ALBERTA PIEZOMETER

NOT TO SCALE

Figure B.3   Drawing of U of A piezometer

Gages	Cable	Amplifier	Recorder

Gages	Cable	Amplifier	Recorder
P1 P3	2 Coax →	Kistler Charge Amplifier	→ CEC Light Beam O'graph
AR1 P2 P4 SE1 SE2	5 Belden →	Allegheny Instr. Co. Sensor Analog Module (SAM)	→ 12" wide paper paper speed: 160 ips
VR1 VR2 P6 P5 P7	5 Belden →	CEC 3KHz Carrier Amplifier System Type 1-118	time → Zero time pulse provided by NCG from their programmer
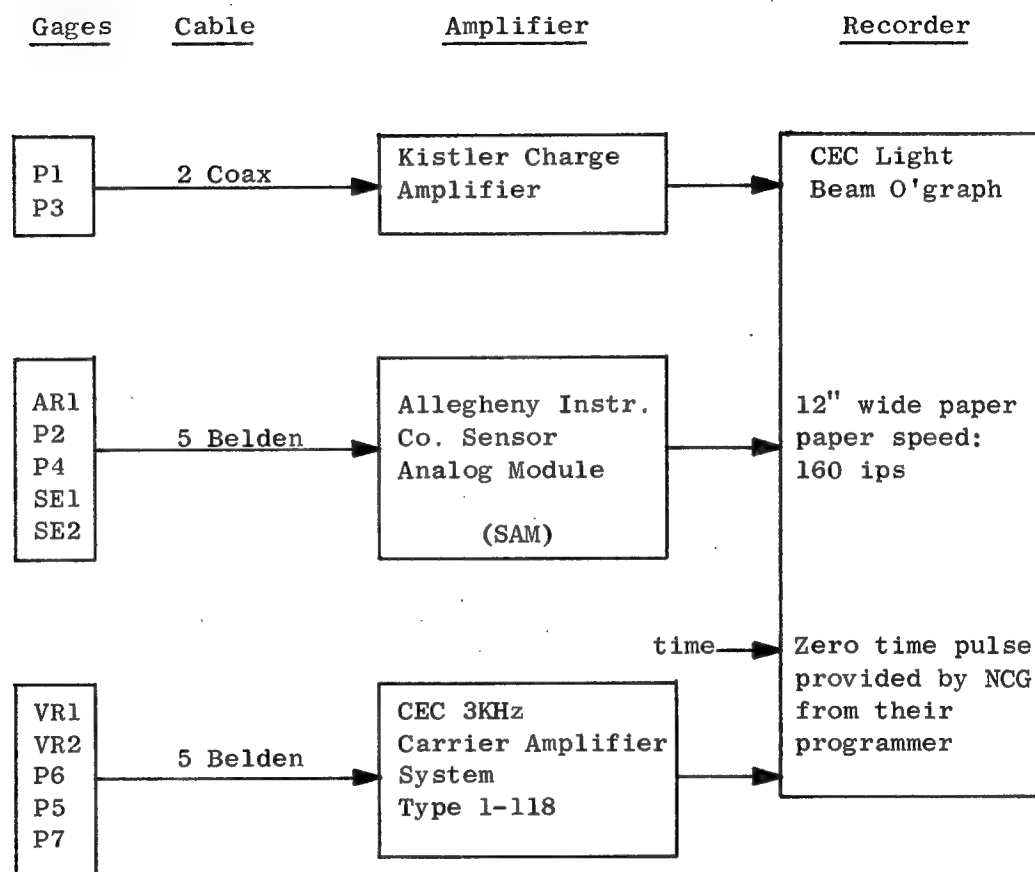
Figure B.4   Schematic diagram of recording system
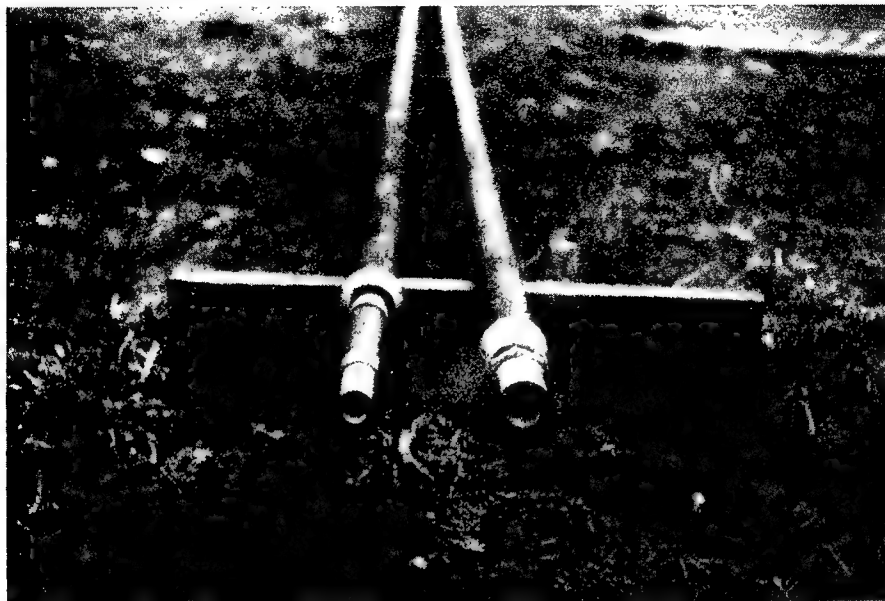
a. UA piezometer (left) and WES transducer piezom-
eter (right) before filter disks were attached
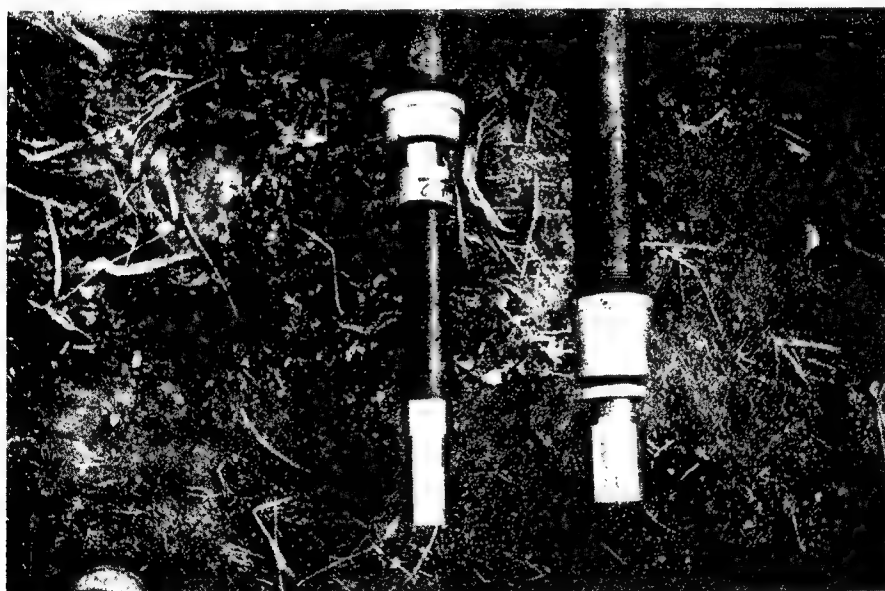
b. UA piezometer (left) and WES transducer piezom-
eter (right) attached to 1-1/2-in. pipe
for insertion in drill holes

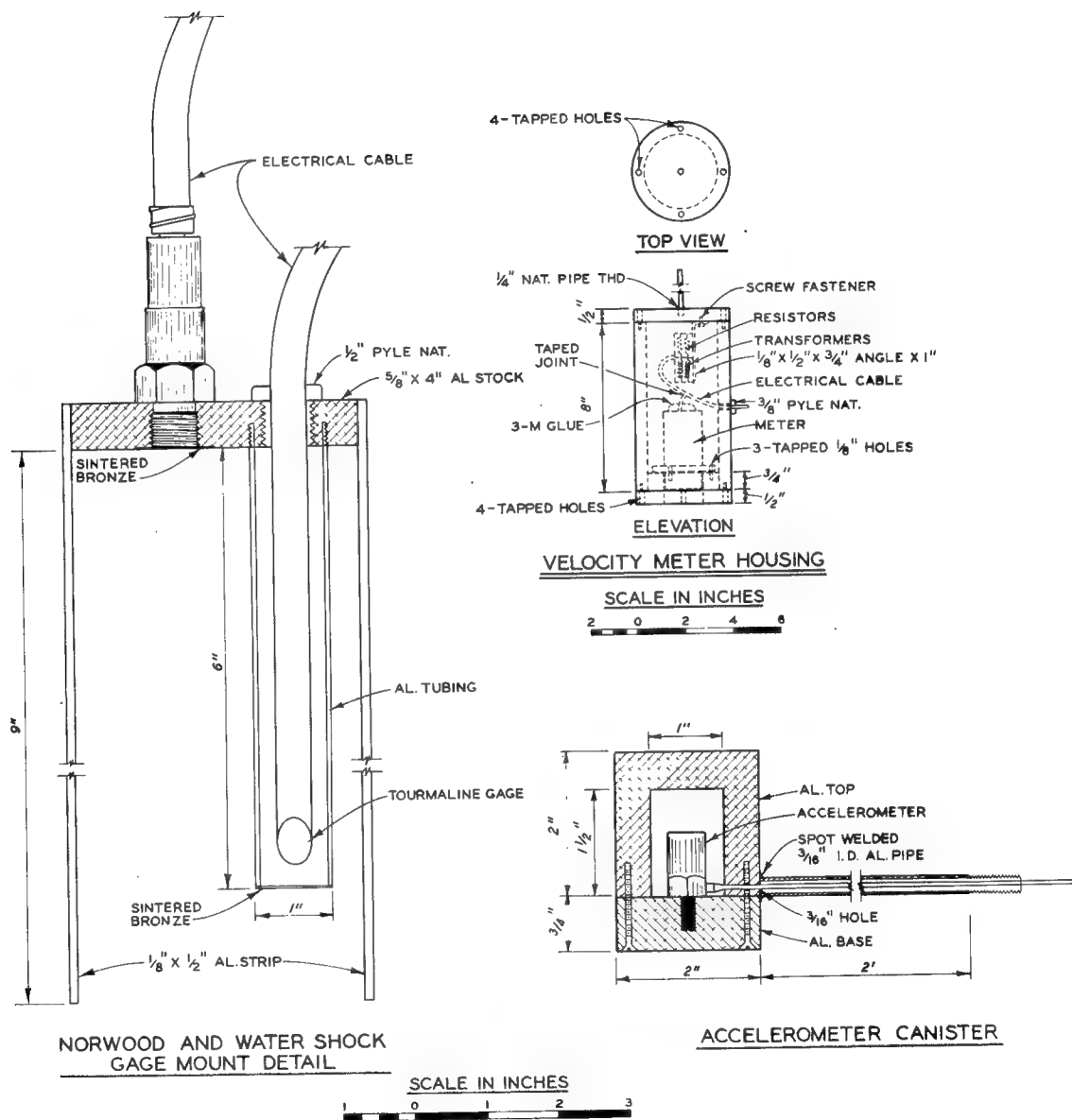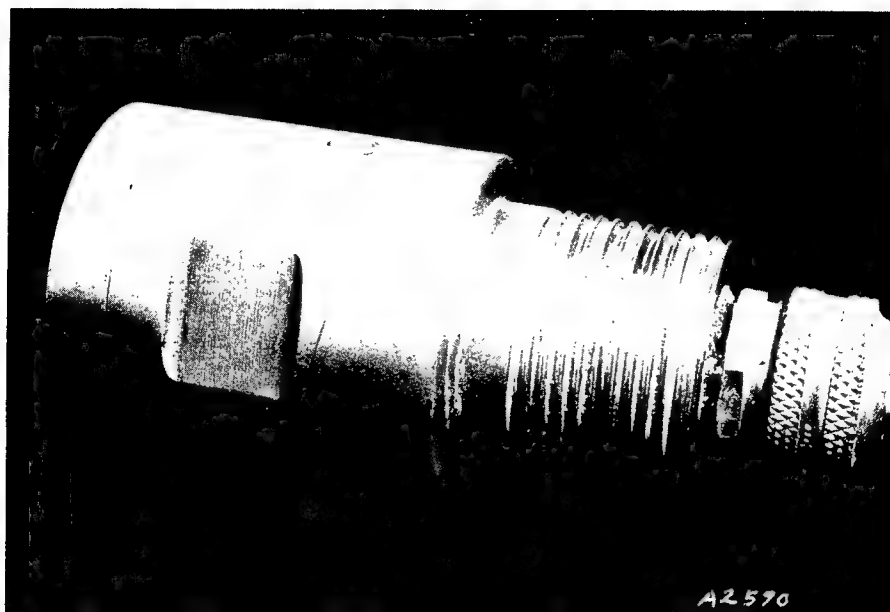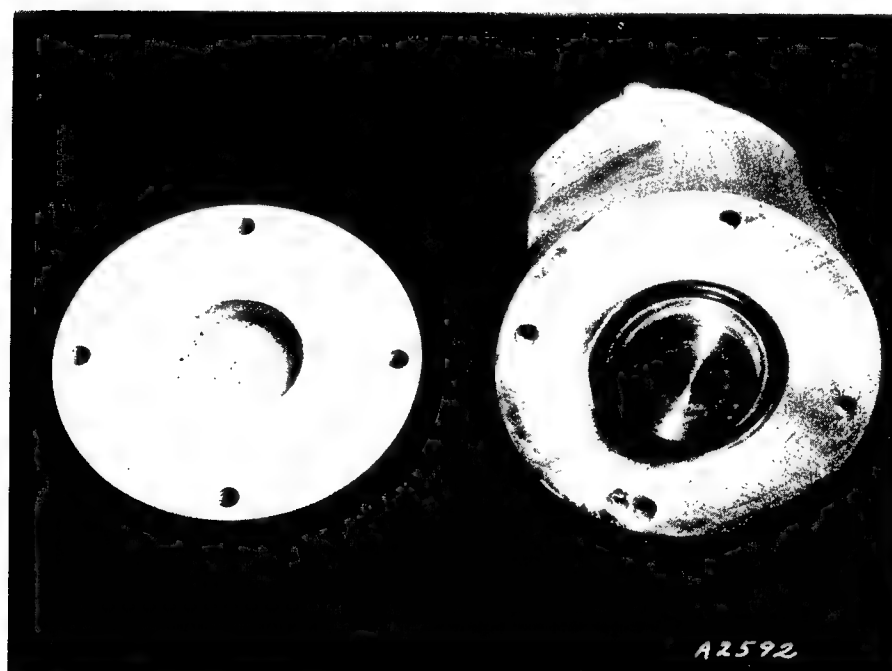Figure B.5   Photographs of pore pressure gages

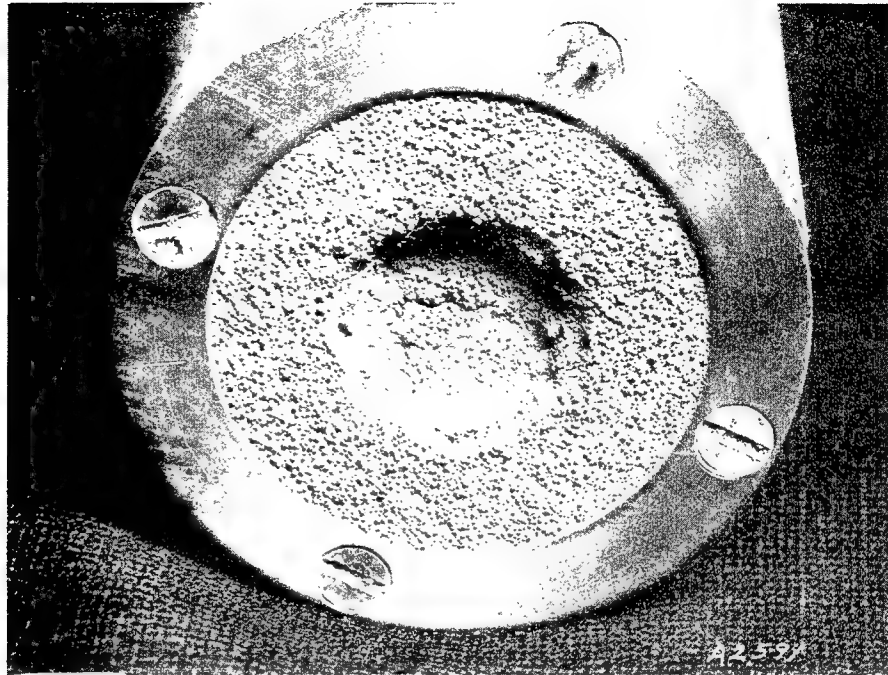Figure B.6 Mounting details of motion and pore pressure gages

111

a. Side view of piezometer housing for WES-built
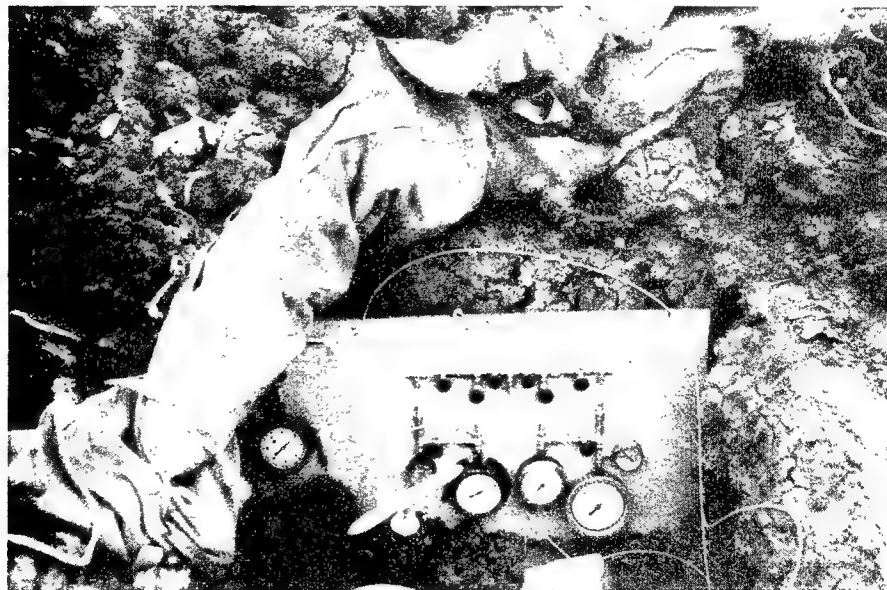CEC transducer piezometer (OD = ±1-3/4 in.)

b. End view of piezometer with filter ring removed.
Note diaphragm end of transducer fits into cavity on
back side of filter ring

Figure B.7 Postshot photographs of P5

Front view showing filter (porous bronze) disk
which was forced back into diaphragm cavity on
2000 psi transducer piezometer by force of
blast from SC-2

USBR piezometer gage pit after shot. Note soil
clods just below left-hand gage and broken
tubing resting against the left-hand gage

Figure B.8   a. Damage to P5
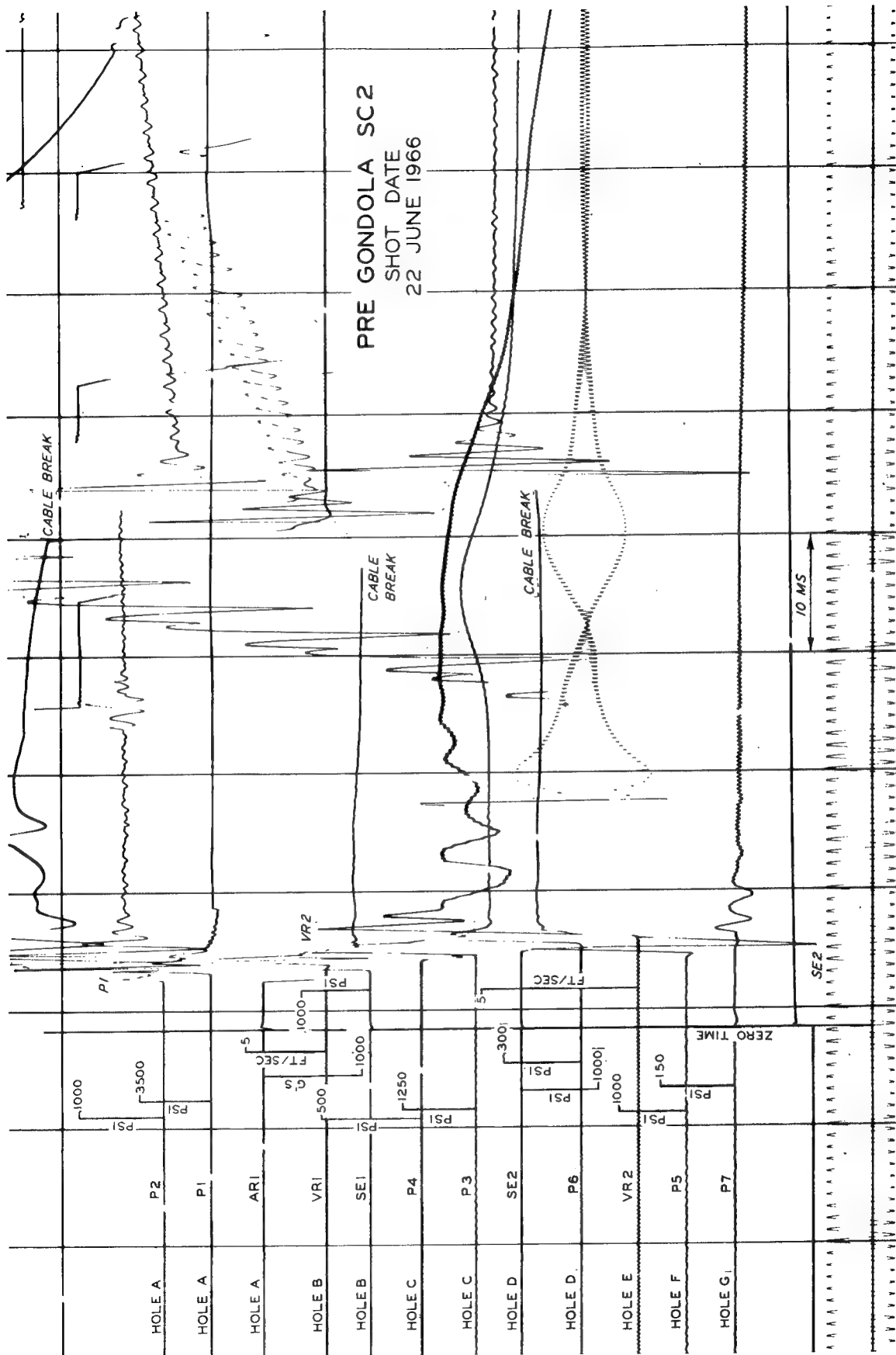   b. Postshot view of USBR gage pit

113
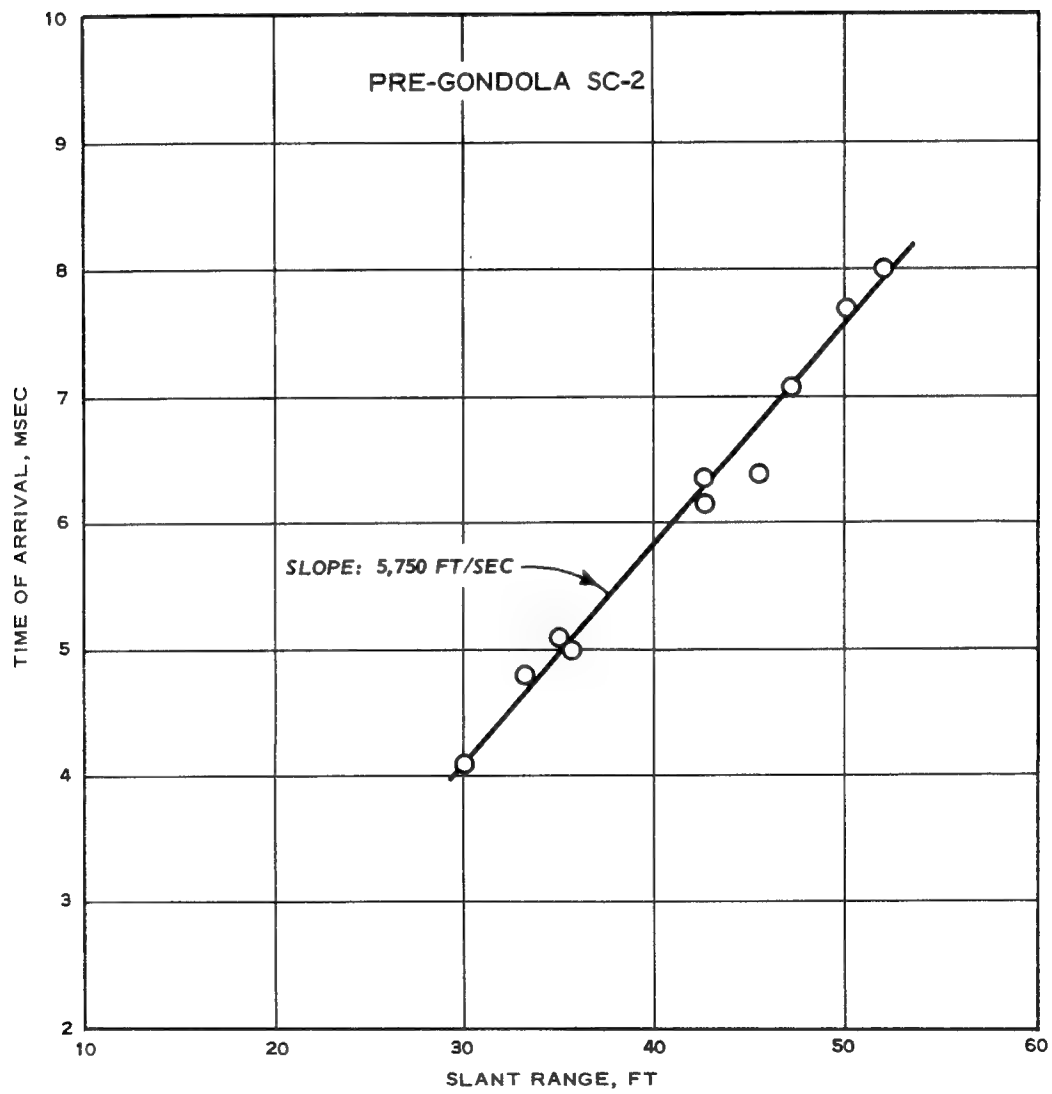
Figure B.9 Reproduction of oscillogram

114

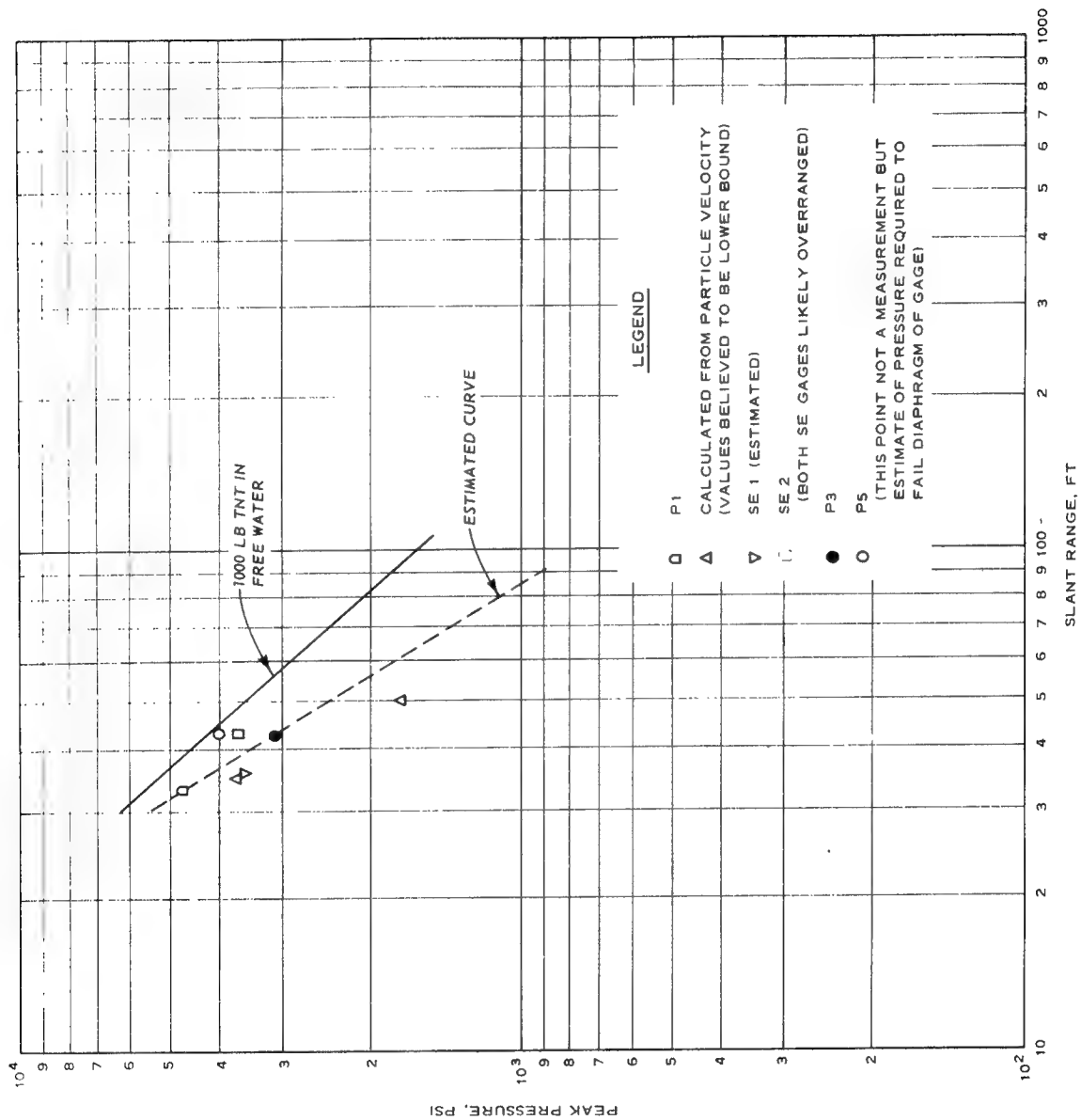Figure B.10   Arrival time of first disturbance

115

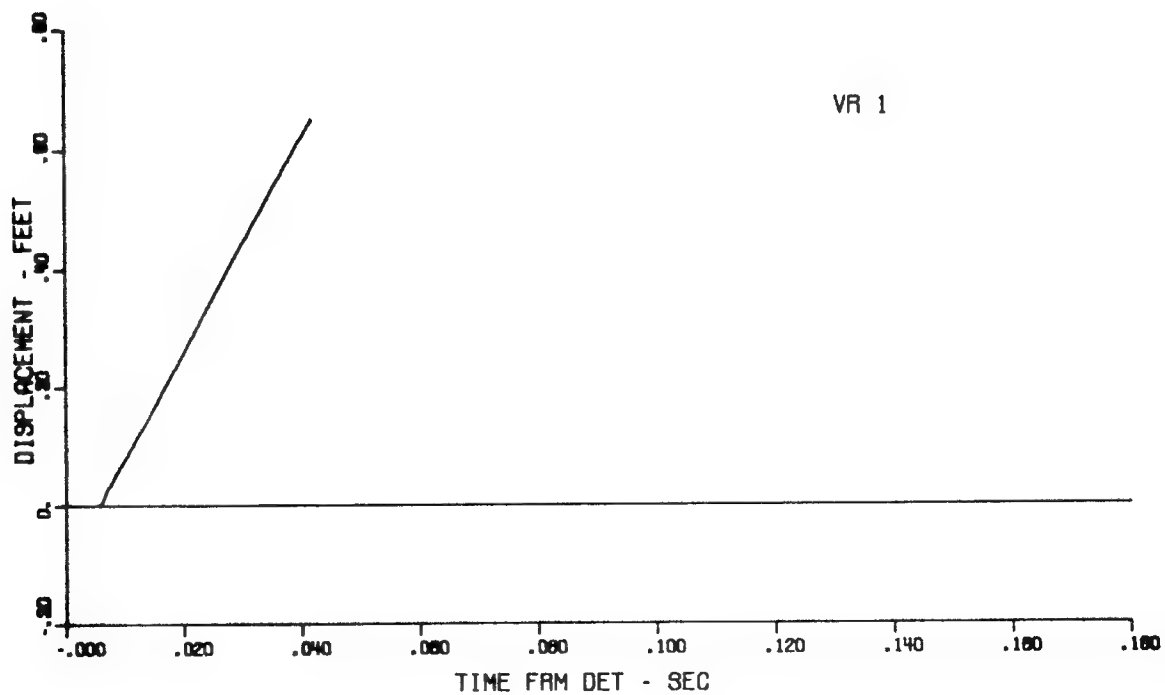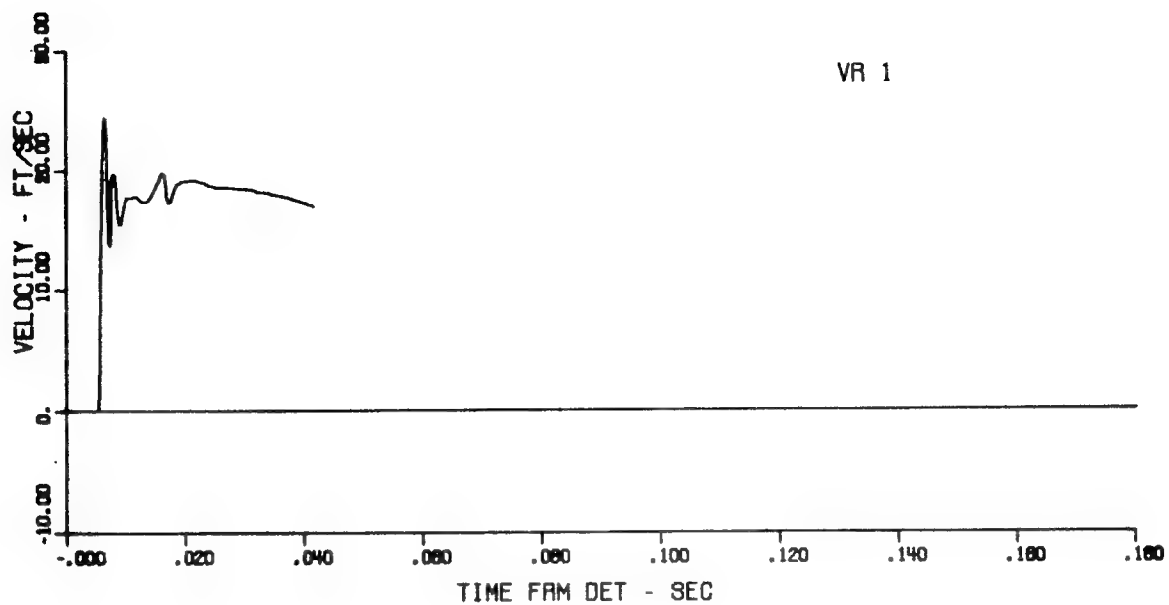Figure B.11 Pressure-distance plot

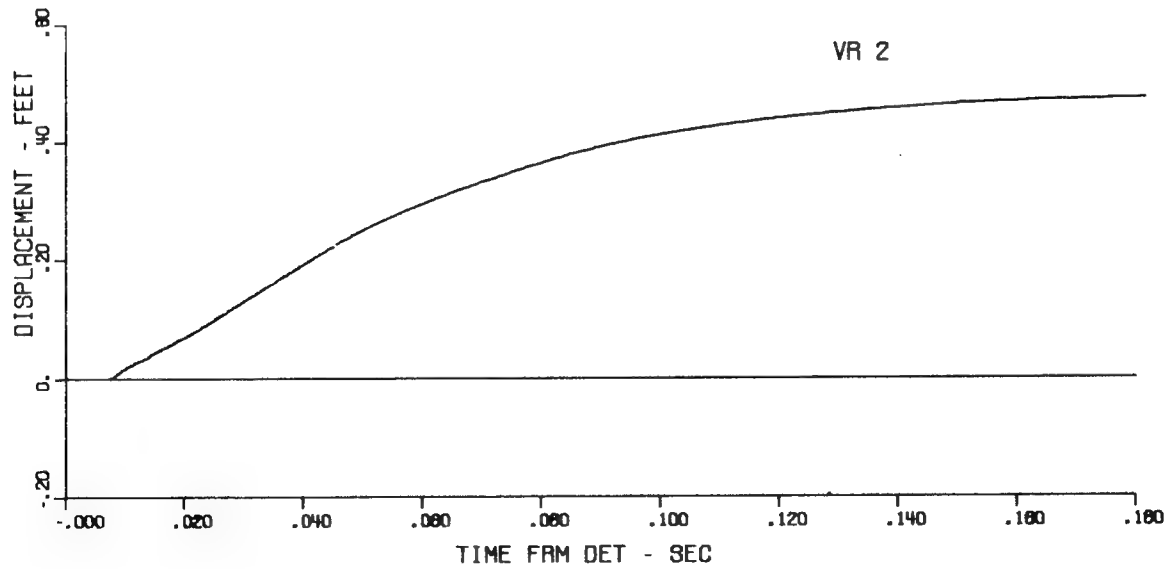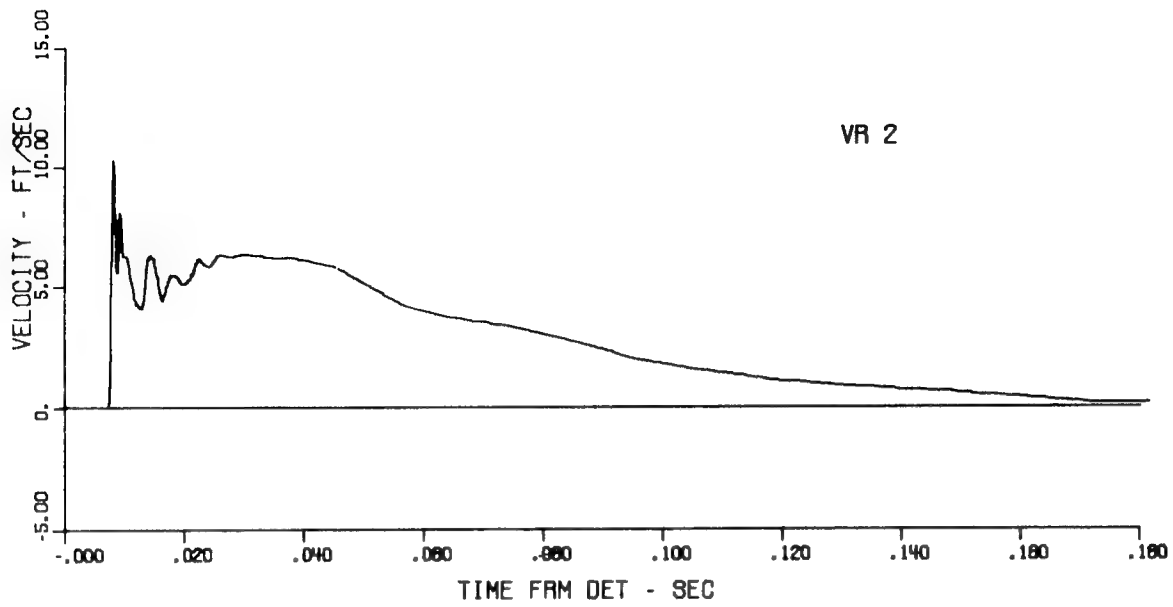Figure B.12 Velocity and displacement from VR 1

117

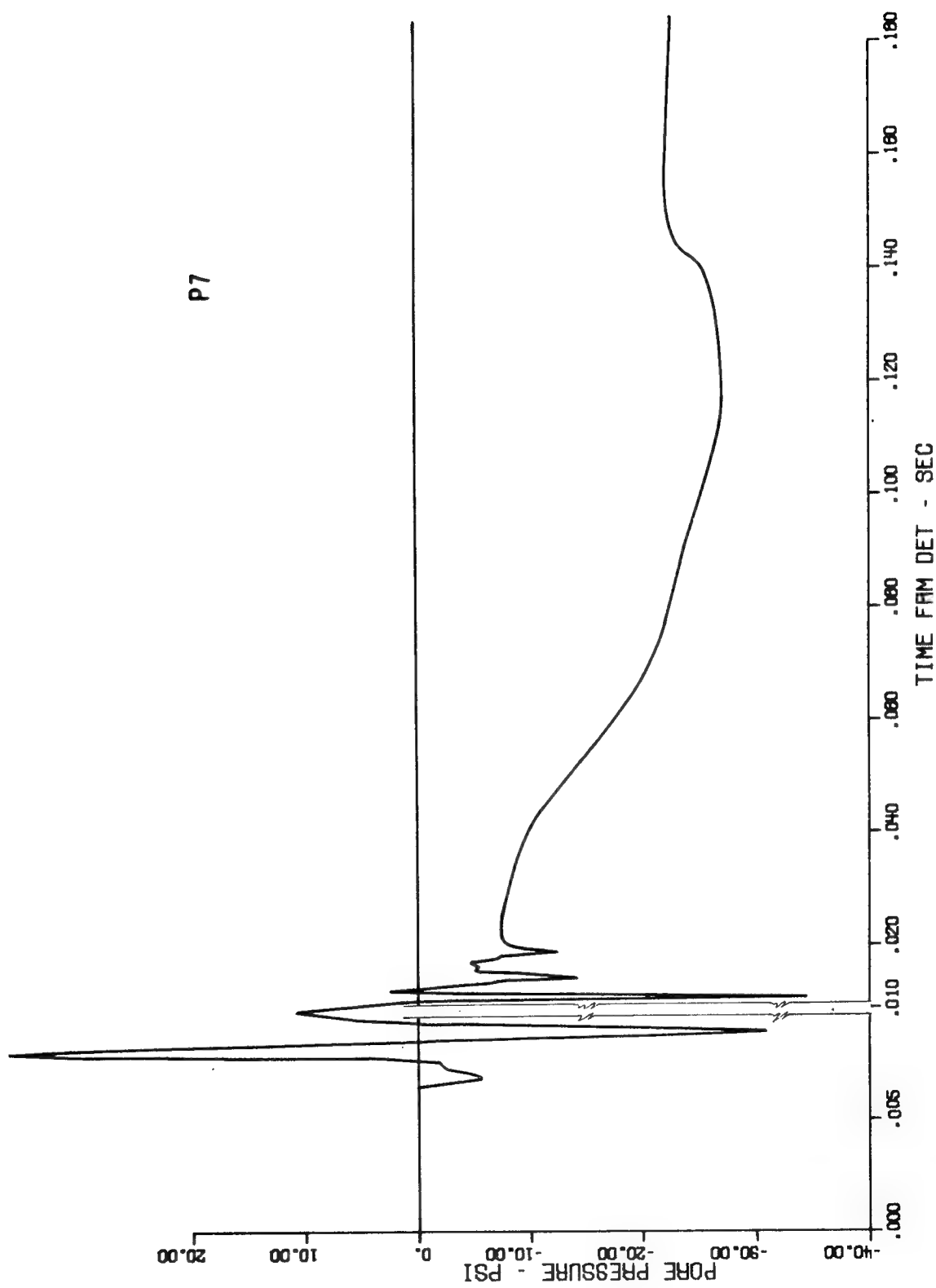Figure B.13   Velocity and displacement from VR 2

118

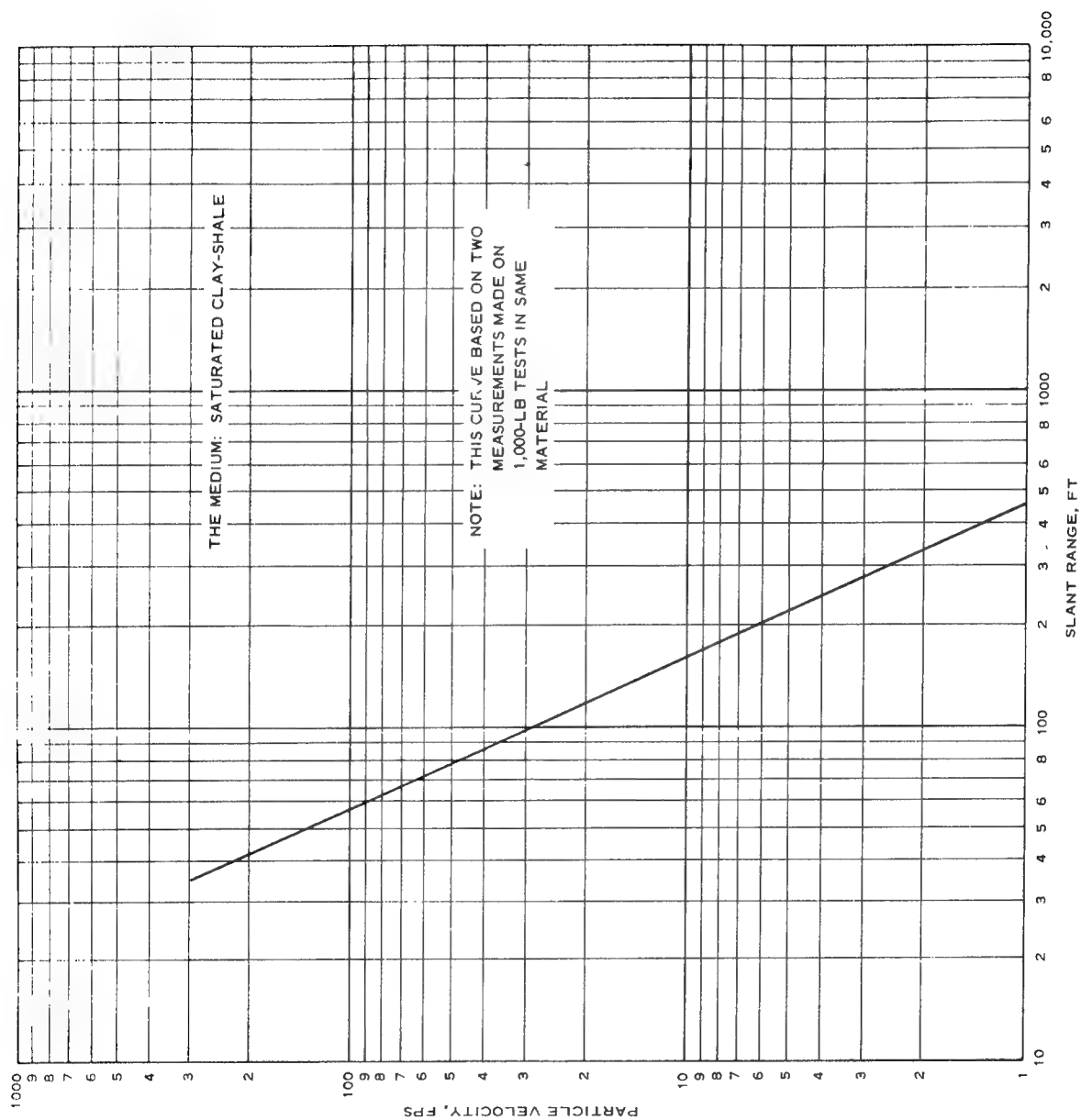Figure B.14   Replot of record from P7

119

Figure B.15 Particle velocity prediction curve for BRAVO

120

REFERENCES

1. F. M. Sauer and others; "Nuclear Geoplosics"; DASA 1285, May 1964; Unclassified.

2. William R. Perret; "Free-Field Ground Motion Studies in Granite"; Operation Nougat, Shot Hard Hat, DASA POR-1803, April 1963; Sandia Corporation, Albuquerque, New Mexico;

3. Wendell D. Weart; "Free-Field Earth Motion and Spalling Measurements in Granite"; Vela Uniform Project Shoal, VUF-2001, February 1965; Sandia Corporation, Albuquerque, New Mexico;

4. T. E. Kennedy and N. Palacios; "The Dynamic Response of Buried Concrete Arches"; U. S. Army Engineer Waterways Experiment Station, Vicksburg, Mississippi; (to be published); Unclassified.

5. O. Kummeneje and O. Eide; "Investigation of Loose Sand Deposits by Blasting"; Publication No. 45, 1961; Norwegian Geotechnical Institute, Oslo, Norway; Unclassified.

6. Project Pre-Gondola, Wet Medium Cratering Experiments, Project Planning Concept; USAENCG; 21 April 1966; Unclassified.

7. Technical Director's Operation Plan for Seismic Site Calibration Series, Project Pre-Gondola; USAENCG; 1 June 1967; Unclassified.

8. J. K. Ingram; "The Development of a Free-Field Soil Stress Gage for Static and Dynamic Measurements"; Instruments and Apparatus for Soil and Rock Mechanics, ASTM STP 392 (presented at symposium in Lafayette, Indiana, 13 June 1965); Unclassified.

9. R. L. Ballard; "Pre-Gondola, Seismic Site Calibration, Structure Response Measurements"; Unclassified.

10. U. S. Bureau of Reclamation; "Earth Manual"; First Edition, Revised, 1963; Unclassified.

PRE-GONDOLA TECHNICAL REPORTS

Title of Report	Agency	Author and/or Technical Program Officer	Report Number
Pre-GONDOLA			
Seismic Site Calibration	NCG	M. K. Kurtz B. B. Redpath	PNE 1100
Site Selection Investigations	NCG/Omaha	H. A. Jack W. W. Dudley	PNE 1101
Pre-GONDOLA I			
Technical Director's Summary Report	NCG	M. K. Kurtz et al	PNE 1102
Geologic and Engineering Properties Investigations	NCG/Omaha	P. R. Fisher et al	PNE 1103
Close-in Ground Motion, Earth Stress, and Pore Pressure Measurements	WES	J. D. Day et al	PNE 1104
Intermediate Range Ground Motion	LRL	D. V. Power	PNE 1105
Structures Instrumentation	WES	R. F. Ballard	PNE 1106

Crater Studies:
  Crater Measurements
  Surface Motion Studies
	
	NCG
	NCG
		
		R. W. Harlan
		W. G. Christopher
			
			PNE 1107 Part I
			PNE 1107 Part II

Cloud Development Studies	NCG/LRL	W. C. Day R. F. Rohrer	PNE 1108
Close-in Displacement Studies	AFWL	C. J. Lemont	PNE 1109
Lidar Observations of Pre-GONDOLA I Clouds	SRI	J. W. Oblanas R. T. H. Collis	PNE 1110
Preshot Geophysical Measurements	LRL-N	R. T. Stearns J. T. Rambo	PNE 1111

DISTRIBUTION

LRL Internal Distribution	No. of Copies
Director's Office	
Information Department	10
R. Batzel	
J. Bell	
J. Carothers	
W. Decker	
S. Fernbach	
R. Goeckermann	
J. Gofman	
E. Goldberg	
J. Hadley	
W. Harford	
C. Haussman	
R. Herbst	
G. Higgins	
A. Holzer	2
E. Hulse	
J. Kane	
J. Knox	2
J. Kury	
C. McDonald	
M. Nordyke	2
J. Rosengren	
R. Rohrer	
B. Rubin	
D. Sewell	
P. Stevenson	2
H. Tewes	2
J. Toman	
C. VanAtta	
G. Werth	

LRL Berkeley

    R. K. Wakerling

    D. M. Wilkes

    E. Teller

LRL Mercury

    L. Crooks

External Distribution

    John W. Oblanas and R. T. H. Collis
    Stanford Research Institute
    Menlo Park, California

    TID-4500, UC-35, Nuclear Explosions -   277
    Peaceful Applications

    Department of Mines and Technical Surveys
    Canada
       D. J. Convey

    Oil and Gas Conservation Board
    Canada
       G. W. Govier

    U. S. Army Engineer Division, Lower Mississippi Valley
    Vicksburg, Mississippi

       U. S. Army Engineer District, Memphis
       Memphis, Texas

       U. S. Army Engineer District, New Orleans
       New Orleans, Louisiana

    U. S. Army Engineer Waterways Experiment Station   75
    Vicksburg, Mississippi

       U. S. Army Engineer District, St. Louis
       St. Louis, Missouri

       U. S. Army Engineer District, Vicksburg
       Vicksburg, Mississippi

    U. S. Army Engineer Division, Mediterranean
    APO, New York

       U. S. Army Liaison Detachment
       New York, New York

       U. S. Army Engineer District, GULF
       APO, New York

U. S. Army Engineer Division, Missouri River   2
Omaha, Nebraska

    U. S. Army Engineer District, Kansas City
    Kansas City, Missouri

    U. S. Army Engineer District, Omaha   2
    Omaha, Nebraska

U. S. Army Engineer Division, New England
Waltham, Massachusetts

U. S. Army Engineer Division, North Atlantic
New York, New York

    U. S. Army Engineer District, Baltimore
    Baltimore, Maryland

    U. S. Army Engineer District, New York
    New York, New York

    U. S. Army Engineer District, Norfolk
    Norfolk, Virginia

    U. S. Army Engineer District, Philadelphia
    Philadelphia, Pennsylvania

U. S. Army Engineer Division, North Central
Chicago, Illinois

    U. S. Army Engineer District, Buffalo
    Buffalo, New York

    U. S. Army Engineer District, Chicago
    Chicago, Illinois

    U. S. Army Engineer District, Detroit
    Detroit, Michigan

    U. S. Army Engineer District, Rock Island
    Rock Island, Illinois

    U. S. Army Engineer District, St. Paul
    St. Paul, Minnesota

    U. S. Army Engineer District, Lake Survey
    Detroit, Michigan

U. S. Army Engineer Division, North Pacific
Portland, Oregon

    U. S. Army Engineer District, Portland
    Portland, Oregon

U. S. Army Engineer District, Alaska
Anchorage, Alaska

U. S. Army Engineer District, Seattle
Seattle, Washington

U. S. Army Engineer District, Walla Walla
Walla Walla, Washington

U. S. Army Engineer Division, Ohio River
Cincinnati, Ohio

U. S. Army Engineer District, Huntington
Huntington, West Virginia

U. S. Army Engineer District, Louisville
Louisville, Kentucky

U. S. Army Engineer District, Nashville
Nashville, Tennessee

U. S. Army Engineer District, Pittsburgh
Pittsburgh, Pennsylvania

U. S. Army Engineer Division, Pacific Ocean
Honolulu, Hawaii

U. S. Army Engineer District, Far East
APO, San Francisco, California

U. S. Army Engineer District, Honolulu
Honolulu, Hawaii

U. S. Army Engineer District, Okinawa
APO, San Francisco, California

U. S. Army Engineer Division, South Atlantic
Atlanta, Georgia

U. S. Army Engineer District, Canaveral
Merritt Island, Florida

U. S. Army Engineer District, Charleston
Charleston, South Carolina

U. S. Army Engineer District, Jacksonville
Jacksonville, Florida

U. S. Army Engineer District, Mobile
Mobile, Alabama

U. S. Army Engineer District, Savannah
Savannah, Georgia

U. S. Army Engineer District, Wilmington
Wilmington, North Carolina

U. S. Army Engineer Division, South Pacific
San Francisco, California

U. S. Army Engineer District, Los Angeles
Los Angeles, California

U. S. Army Engineer District, Sacramento
Sacramento, California

U. S. Army Engineer District, San Francisco
San Francisco, California

U. S. Army Engineer Division, Southwestern
Dallas, Texas

U. S. Army Engineer District, Albuquerque
Albuquerque, New Mexico

U. S. Army Engineer District, Fort Worth
Fort Worth, Texas

U. S. Army Engineer District, Galveston
Galveston, Texas

U. S. Army Engineer District, Little Rock
Little Rock, Arkansas

U. S. Army Engineer District, Tulsa
Tulsa, Oklahoma

U. S. Army Coastal Engineering Research Board
Washington, D. C.

Mississippi River Commission
Vicksburg, Mississippi

Rivers and Harbors, Board of Engineers
Washington, D. C.

Corps of Engineers Ballistic Missile Construction Office
Norton Air Force Base, California

U. S. Army Engineer Center
Ft. Belvoir, Virginia

U. S. Army Engineer Reactors Group
Ft. Belvoir, Virginia

U. S. Army Engineer Training Center
Ft. Leonard Wood, Missouri

U. S. Army Engineer School
Ft. Belvoir, Virginia

U. S. Army Engineer Nuclear Cratering Group   74
Livermore, California